CTEQ

Some Aspects of Higgs Physics, after July 2012

C.-P. Yuan
Michigan State University

July 16-19, 2013 @
IPMU School on the Future of Collider Physics,
U. of Tokyo

Outline

- A New Boson
- Parton Model and QCD
- Hard part calculations
- Parton Distribution Functions
- Higgs boson cross sections and distributions
- Jets in QCD
- Use jet energy profile to discriminate Higgs boson production mechanisms
- The Big Question (as requested by Nojiri)

July 4, 2012

- Scientists at CERN say they've found a new particle consistent with the Standard Model Higgs boson with 5-sigma certainty — a false positive probability of about 1 in 9 trillion.
- This is hardly the end of the road for Higgs study, though. It’s only the beginning.
- So a Higgs-like boson has been discovered. What’s next?

What do we know about this New Boson

- Its mass is between 124 GeV and126 GeV
- Its production rates in various decay channels have been found to be in good agreement with the Standard Model (SM) predictions.
- The Higgs boson couplings to any SM particles are found to generally agree with SM predictions within 20%.

A New Boson

ATLAS

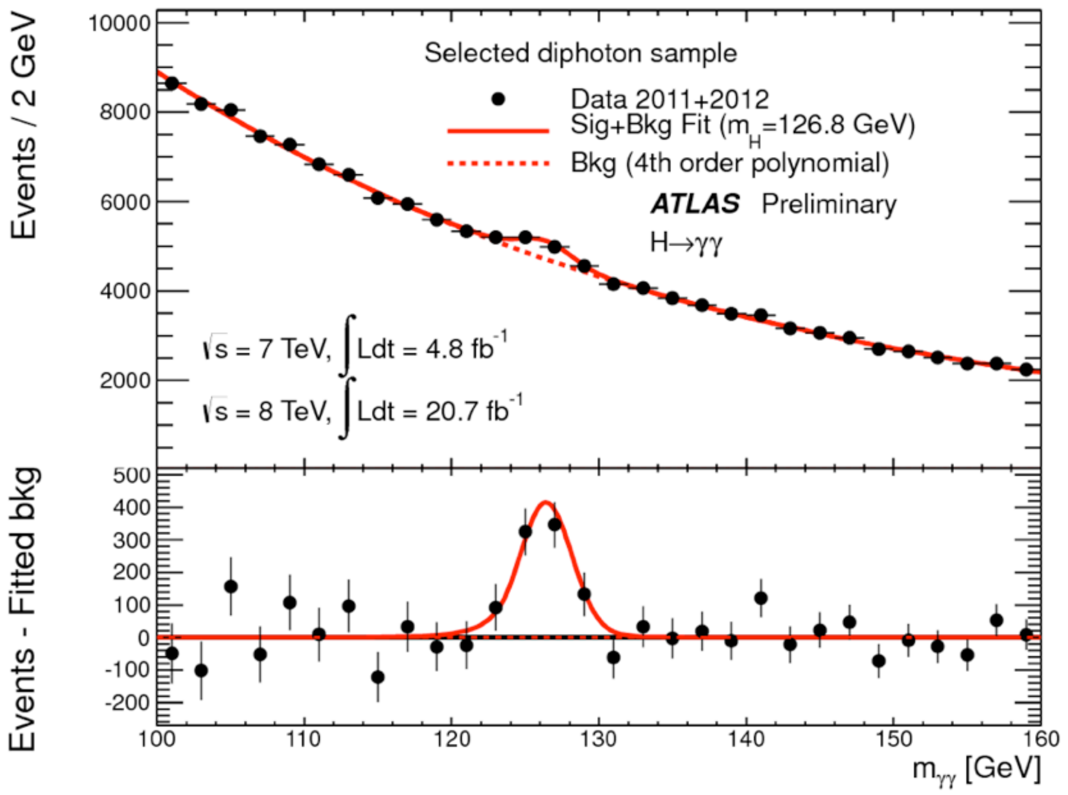

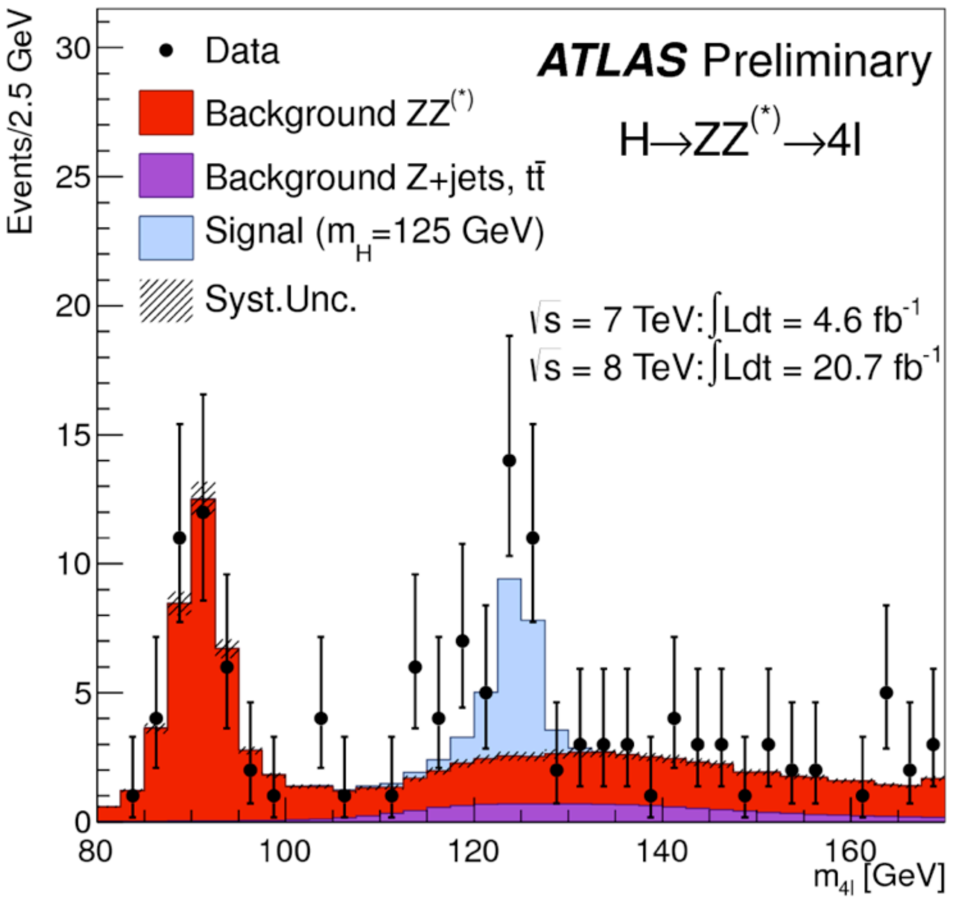

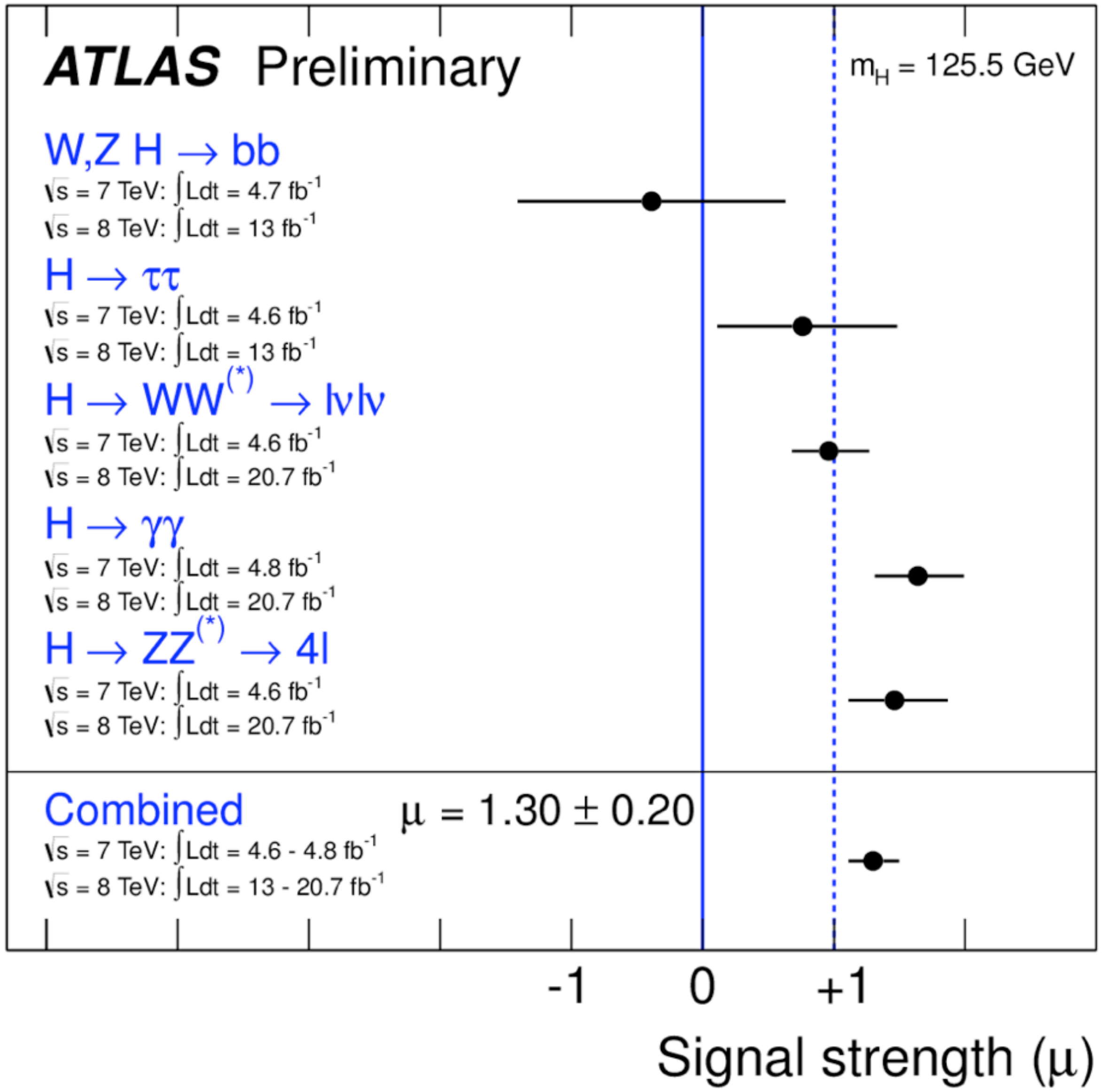

Moriond EW 2013
ATLAS-CONF-2013-034,012,013

CMS

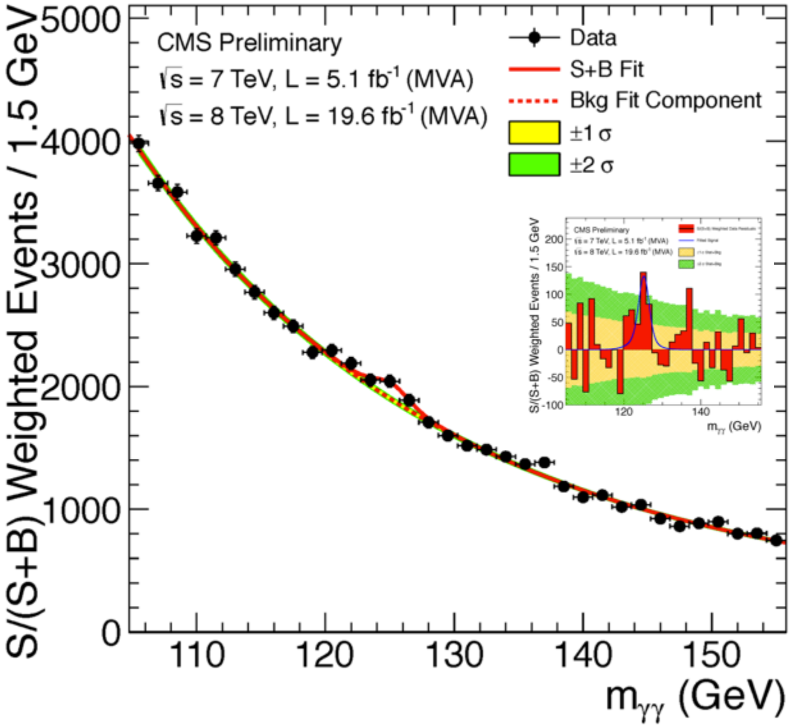

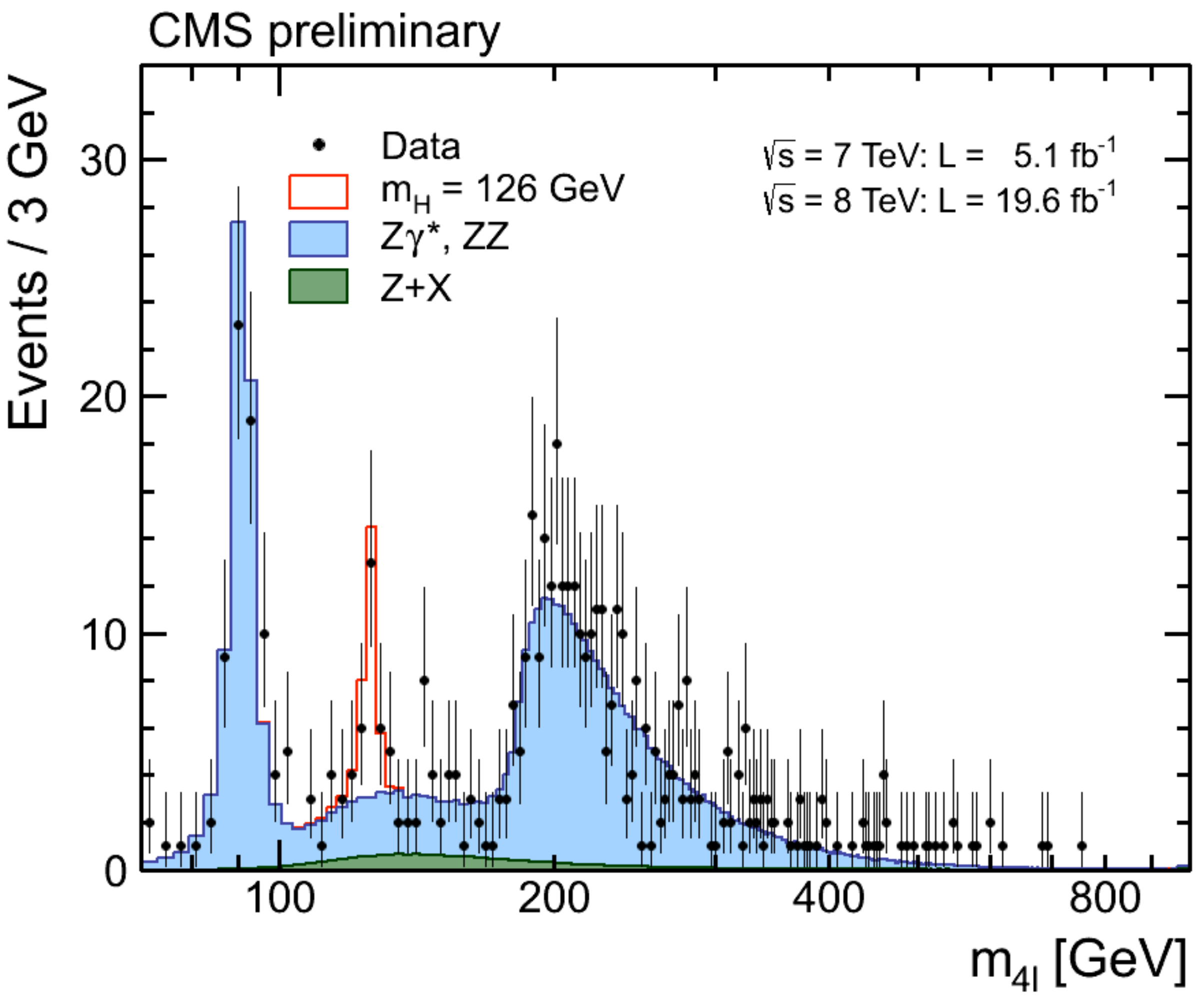

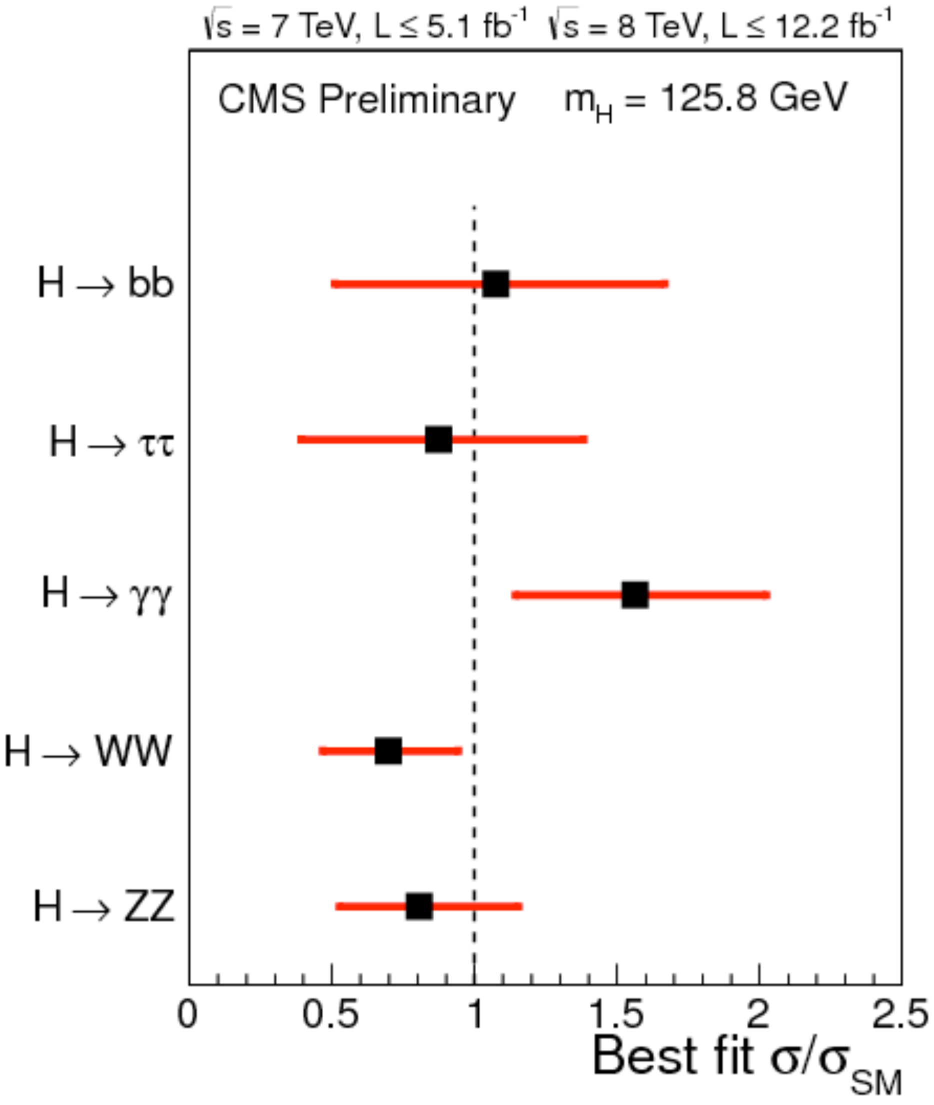

Moriond EW 2013
CMS-PAS-HIG-13-001,2
CMS-PAS-HIG-12-045

Data and Theory

The observed Higgs event number

is proportional to the product of

Higgs Production cross section

and

Higgs decay branching ratio

into a specific decay channel (i.e. detection mode).

arXiv: 1101.0593

SM Higgs @ 14 TeV LHC

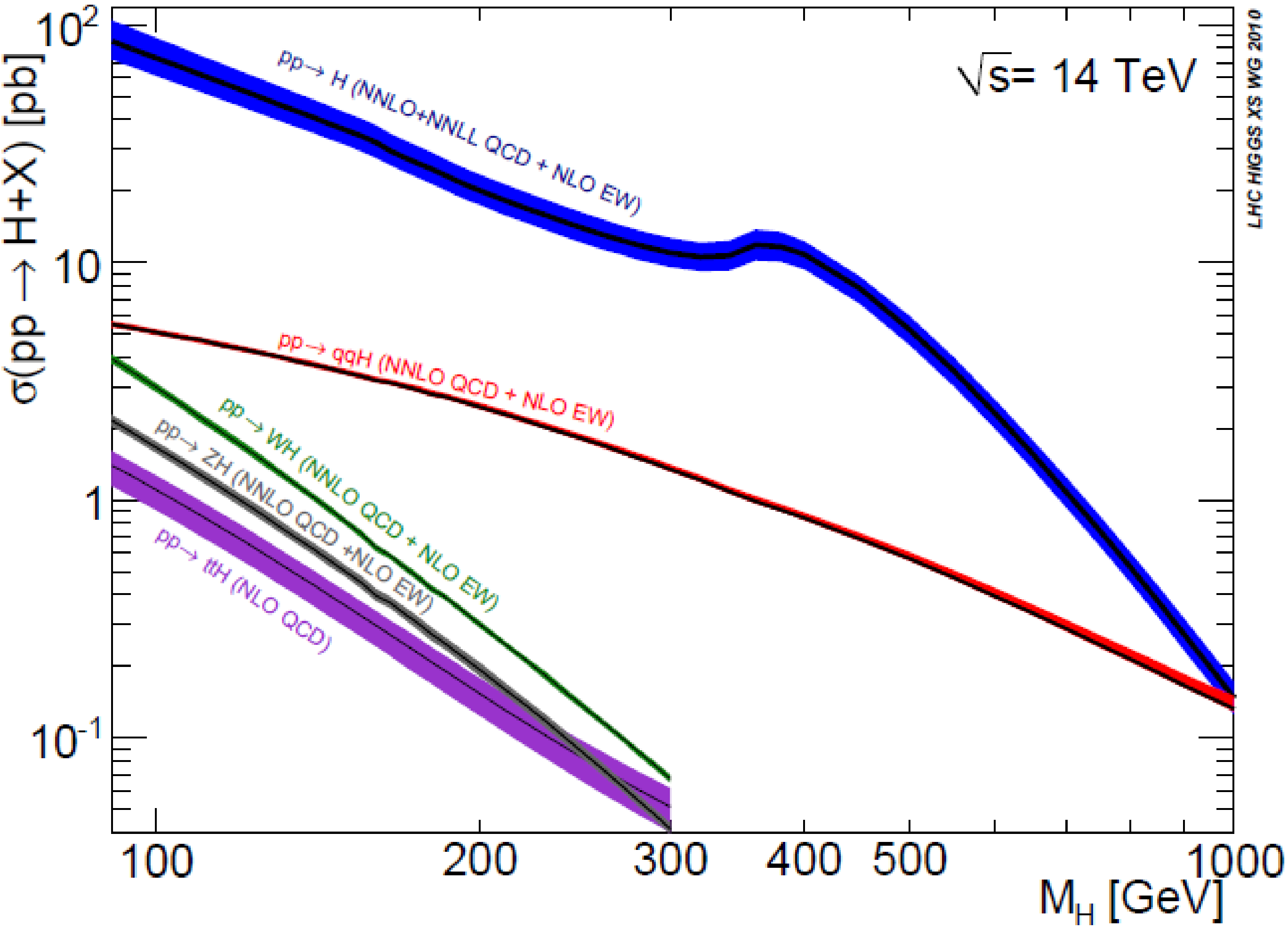

Higgs decay branching ratios

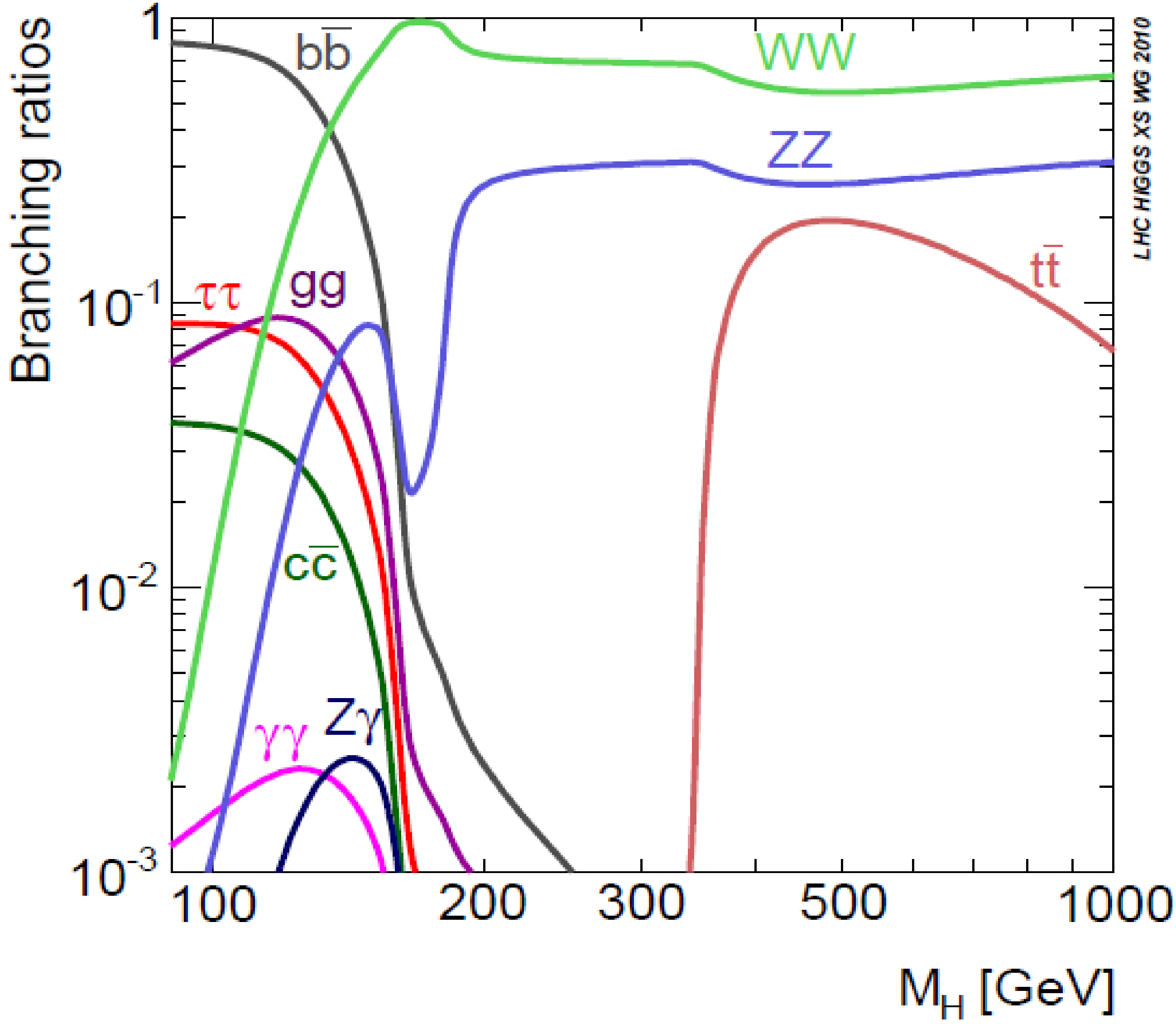

For 125 GeV Higgs, Total decay width is 4.03 MeV.

$$Br(\bar{b}b) = 0.58$$
$$Br(WW) = 0.22$$
$$Br(gg) = 0.086$$
$$Br(\tau\tau) = 0.06$$
$$Br(cc) = 0.028$$
$$Br(ZZ) = 0.027$$
$$Br(\gamma\gamma) = 0.0023$$
$$Br(Z\gamma) = 0.0016$$

What's this New Boson?

Theory	Hierarchy Problem	Precision EW	Λ_{UV}	$\delta g_H/g_H$	LHC
Fundamental Higgs	YES!	✔	< 10^9 GeV	0%	😃
SUSY	No	✔	M_{GUT}?	<10%	🤔
Composite Higgs	No	f > few TeV	50 TeV	O(10%)	🤔
Dilaton	No	✔?	1-10 TeV	O(100%)	😟
Higgsless/ TC	No	Ideal fermions	1-10 TeV	no narrow scalar?	😟

Sekhar Chivukula, 2013

Precision Tests are needed

- New Physics effects (from heavy particles) could contribute in loops.
- Hence, precision tests of Higgs production cross sections and decay branching ratios are needed.

Parton Model and QCD

- Naïve Parton Model
- QCD Theory
- QCD improved Parton Model
- Factorization Theorem

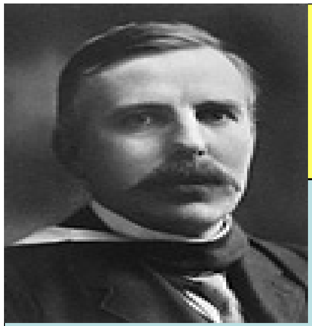

Rutherford Scattering

Rutherford taught us the most important lesson:
use a scattering process to learn about the structure of matter

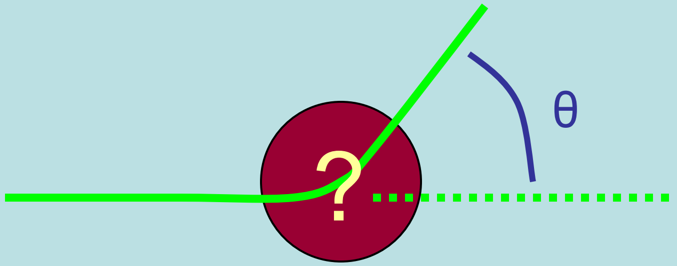

This story is well known:

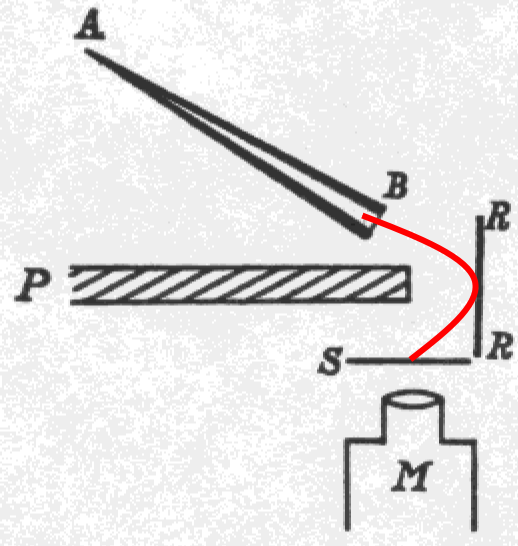

FIG. 1.

H. Geiger and E. Marsden observed that α-particles were sometimes scattered through very large angles.

Rutherford interpreted these results as due to the coulomb scattering of the α-particles with the atomic nucleus:

$$\sigma(\theta) = \frac{z^2 Z^2 e^4}{16E^2} \frac{1}{\sin^4 \frac{1}{2}\theta}$$

The SLAC-MIT Experiment

1990 Nobel Prize

Under the leadership of Taylor, Friedman, Kendall

~ 1969

Electron scattered by
liquid hydrogen or deuterium

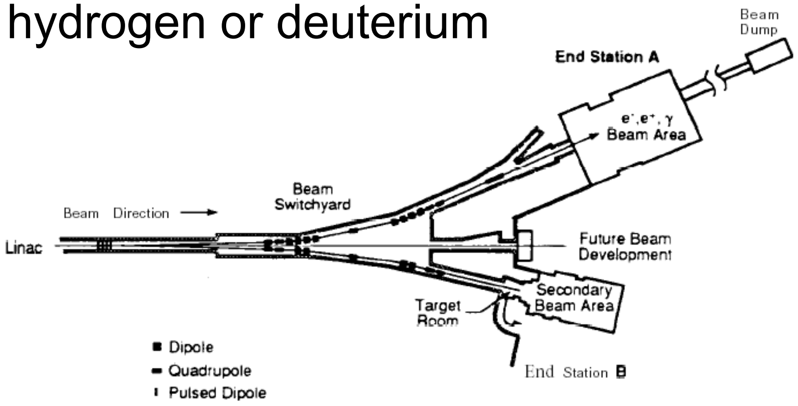

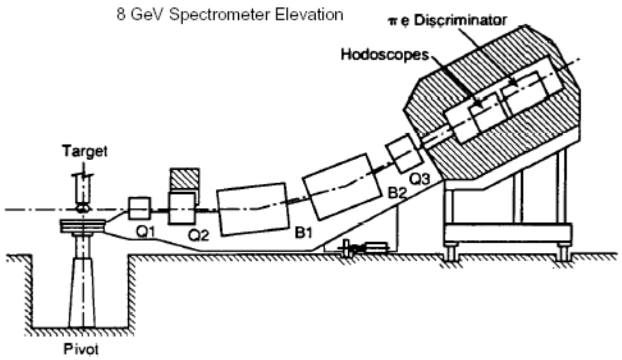

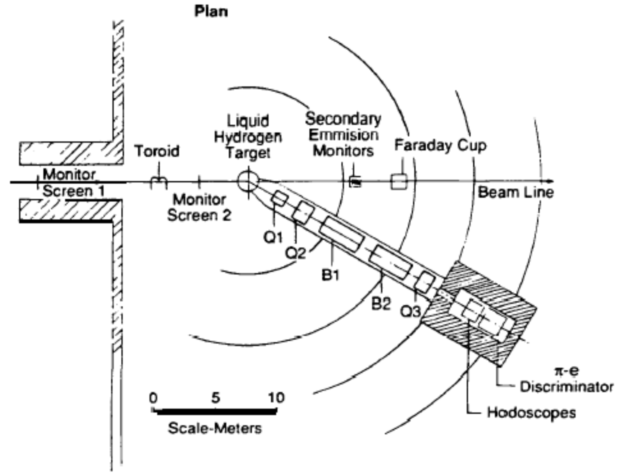

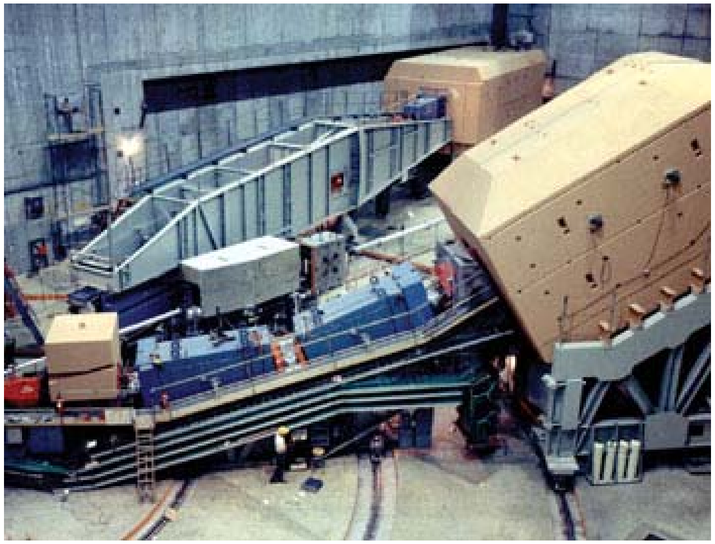

First SLAC-MIT results

Two unexpected results…

Deep-inelastic scattering (DIS)

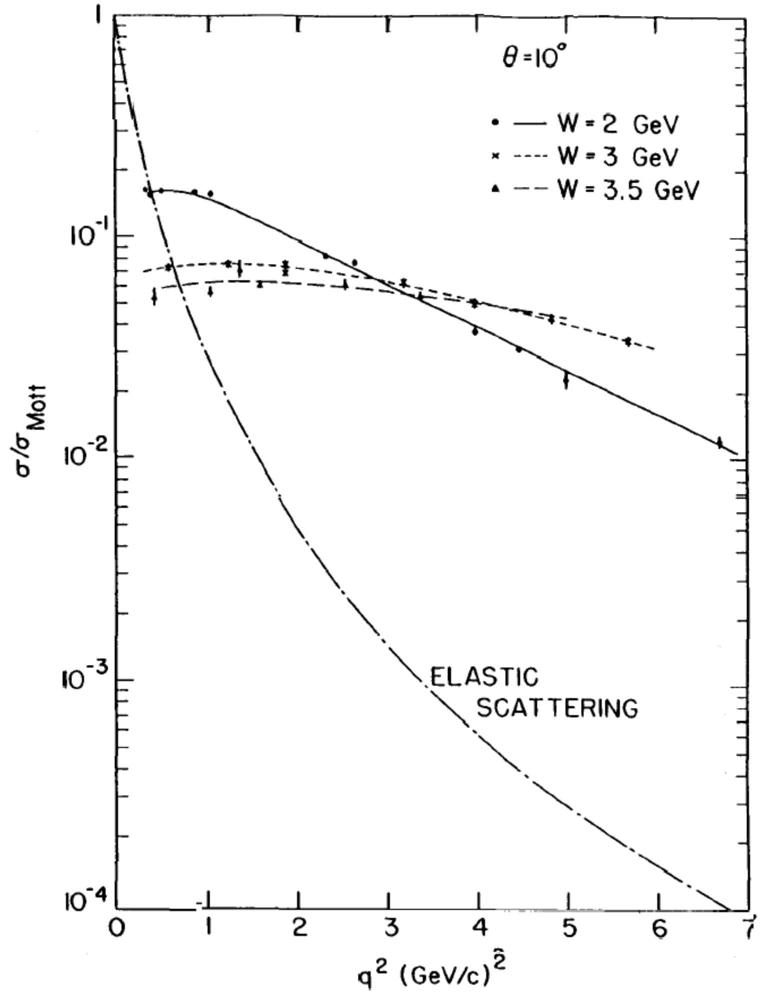

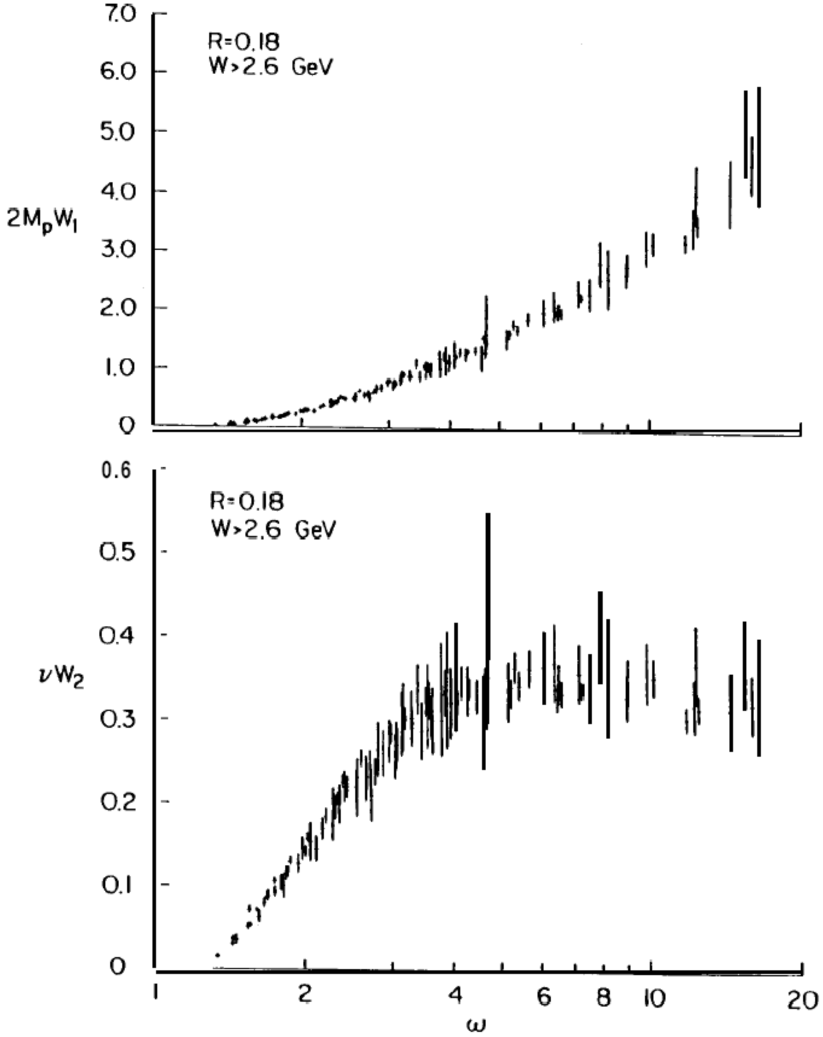

First SLAC-MIT results

Two unexpected results…

Deep-inelastic scattering (DIS)

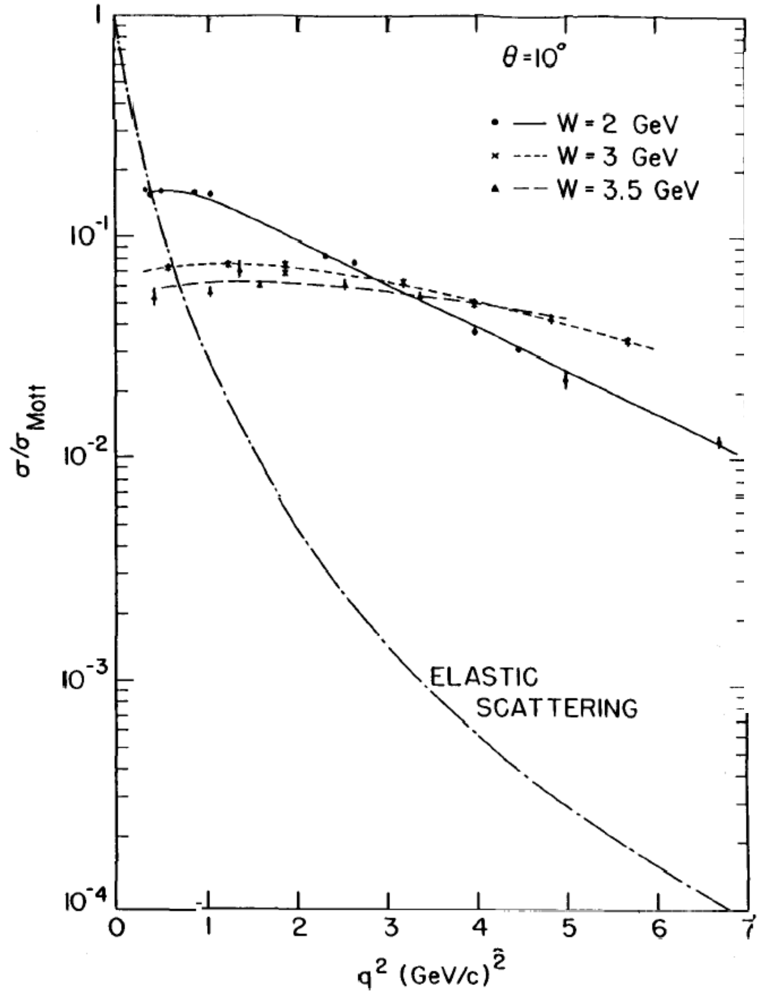

Scaling behavior

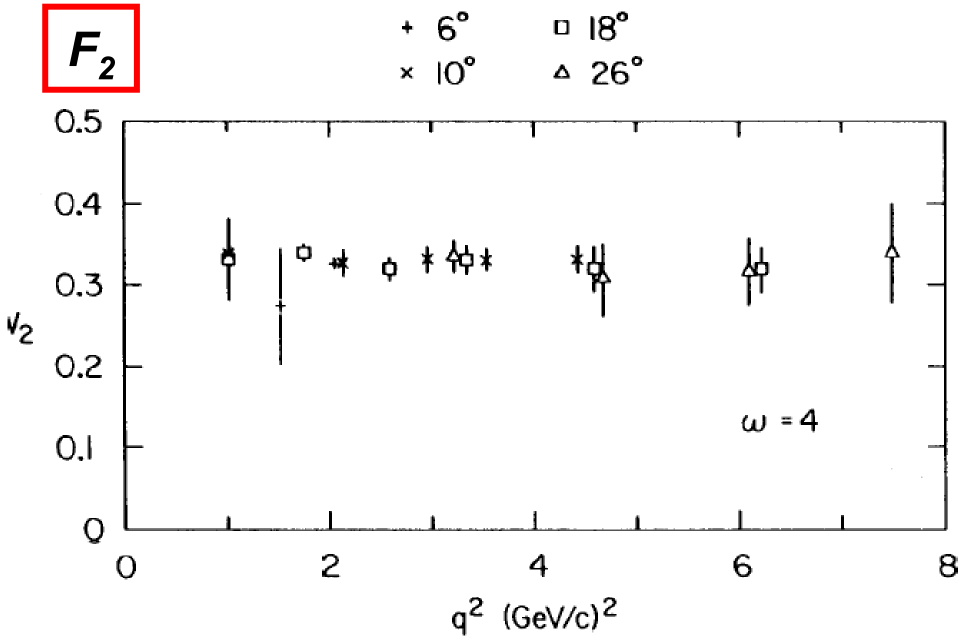

$\boxed{\omega=1/x}$

Physical Interpretations of DIS Structure Function measurements

- The Parton Model (Feynman-Bjorken)
- Theoretical basis of the parton picture and the QCD improved parton model

High energy (Bjorken) limit:
(large Q^2 and ν, for a fixed x value)

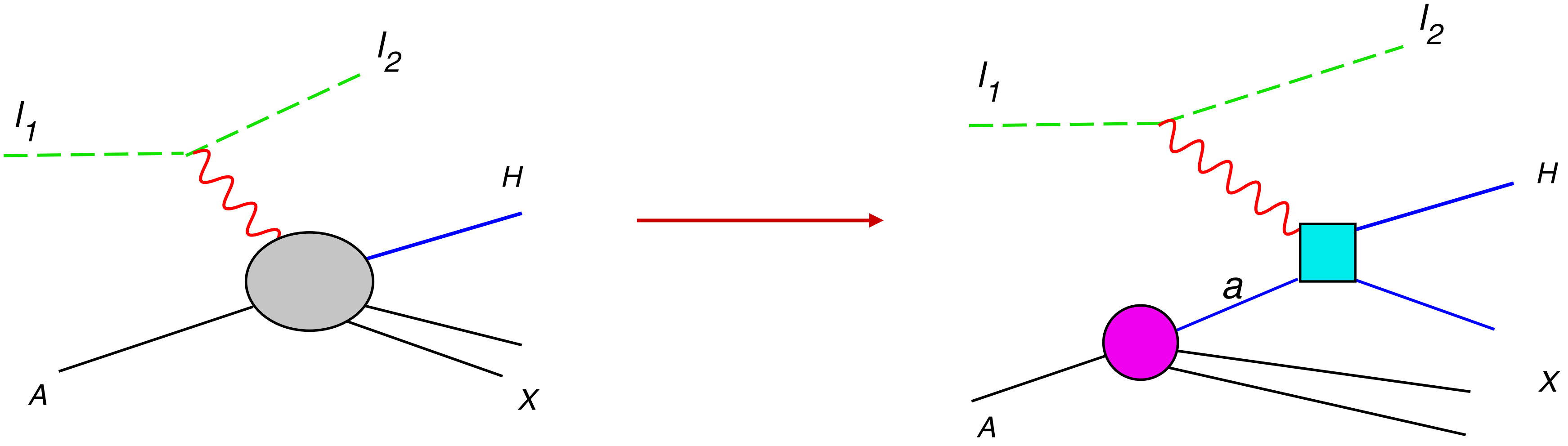

Quantum Chromodynamics

Fields: Quarks ψ^{color}_{flavor} and Gluon $G^{color}(A{\cdot}T, g)$.

Basic Lagrangian:

$$\mathcal{L} = \bar{\psi}(i \not\partial - g \not A \cdot t - m)\psi - \frac{1}{4} G(A \cdot T, g) \cdot G(A \cdot T, g)$$

- g: gauge Coupling Strength
- m_i: quark masses
- t & T: color SU(3) matrices in the fundamental and adjoint representations.

  Group factors: $C_F = \frac{4}{3}$; $T_F = \frac{1}{2}$; $C_A = 3$

Interaction Vertices:

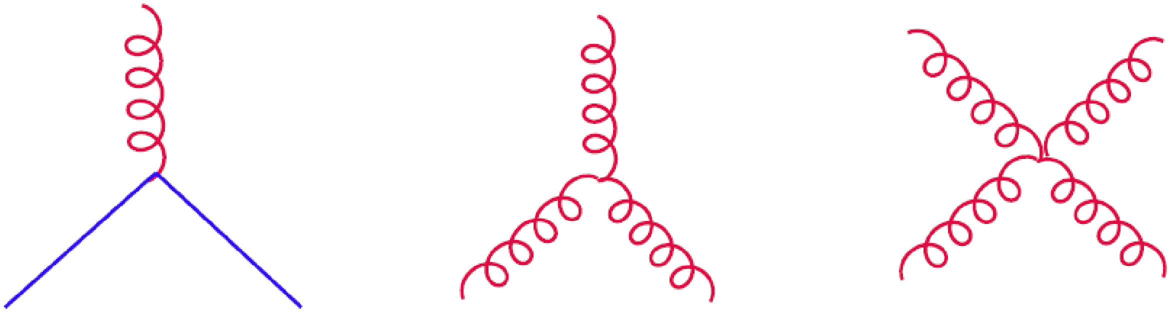

Lepton-hadron Sc.

Master Equation for QCD Parton Model
– the Factorization Theorem

$$F_A^\lambda(x,\frac{m}{Q},\frac{M}{Q}) = \sum_a f_A^a(x,\frac{m}{\mu}) \otimes \hat{F}_a^\lambda(x,\frac{Q}{\mu},\frac{M}{Q}) + \mathcal{O}((\frac{\Lambda}{Q})^2)$$

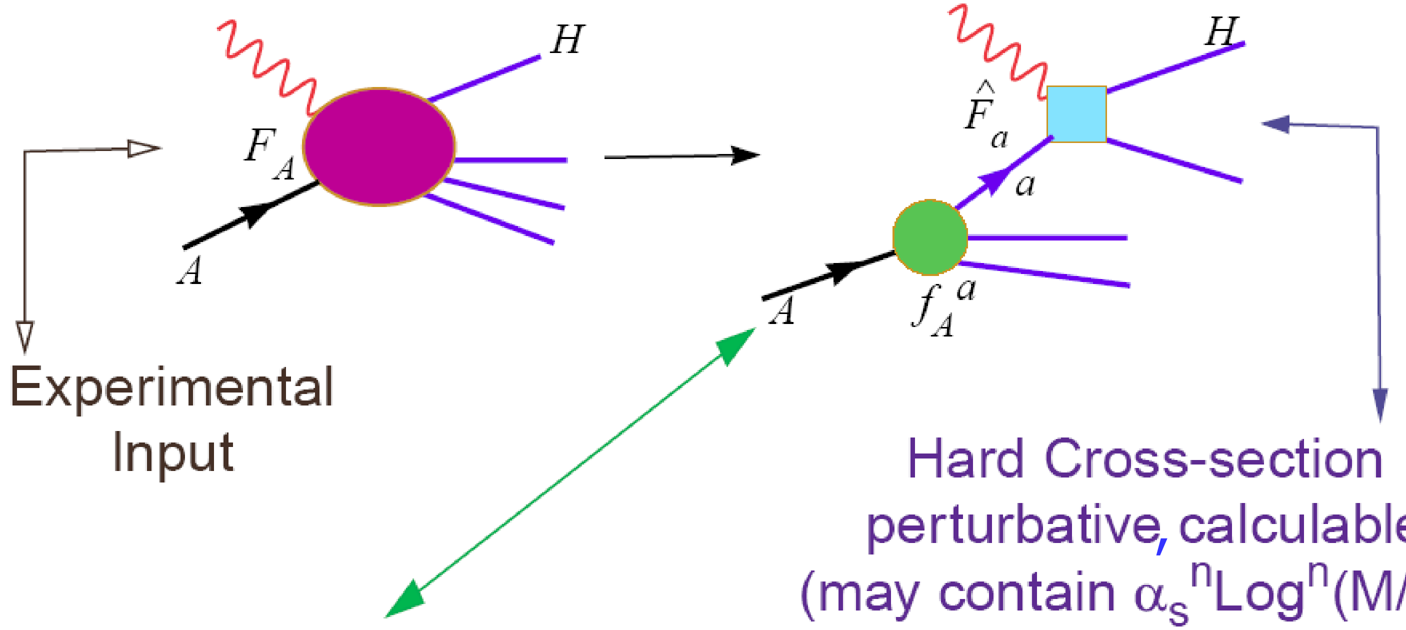

Experimental
Input

Theory
Input

Hard Cross-section
perturbative, calculable
(may contain $\alpha_s^n \mathrm{Log}^n(M/Q)$)

universal Parton Dist. Fn.
Non-Perturbative Parametrization at *Q_0*
GLAP Evolution to *Q*
extracted by global analysis

F_2 : "Scaling violation"
— Q-dependence inherent in QCD

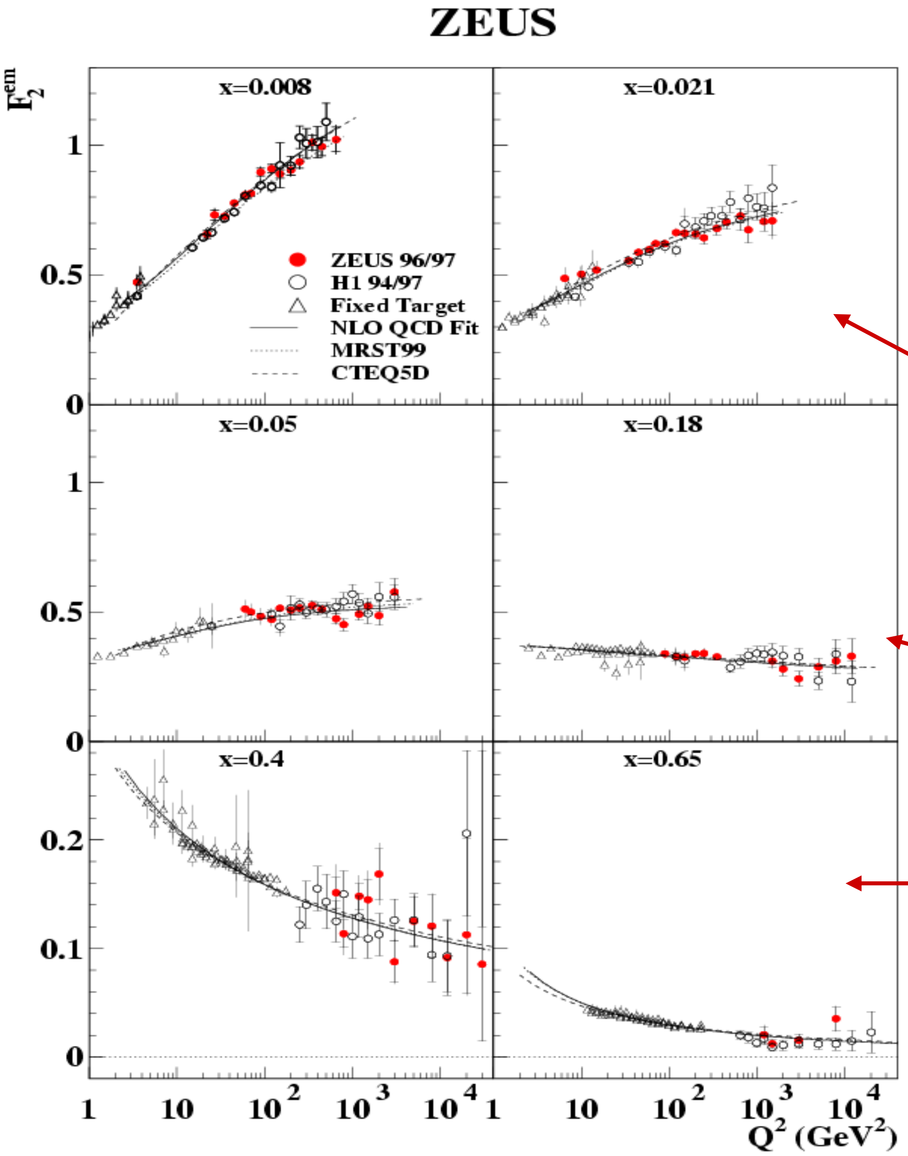

Renormalization group equation governs the scale dependence of parton distributions and hard cross sections. (DGLAP)

Rise with increasing Q at small-x

Flat behavior at medium x

decrease with increasing Q at high x

CT10 PDF plots

Low Scale

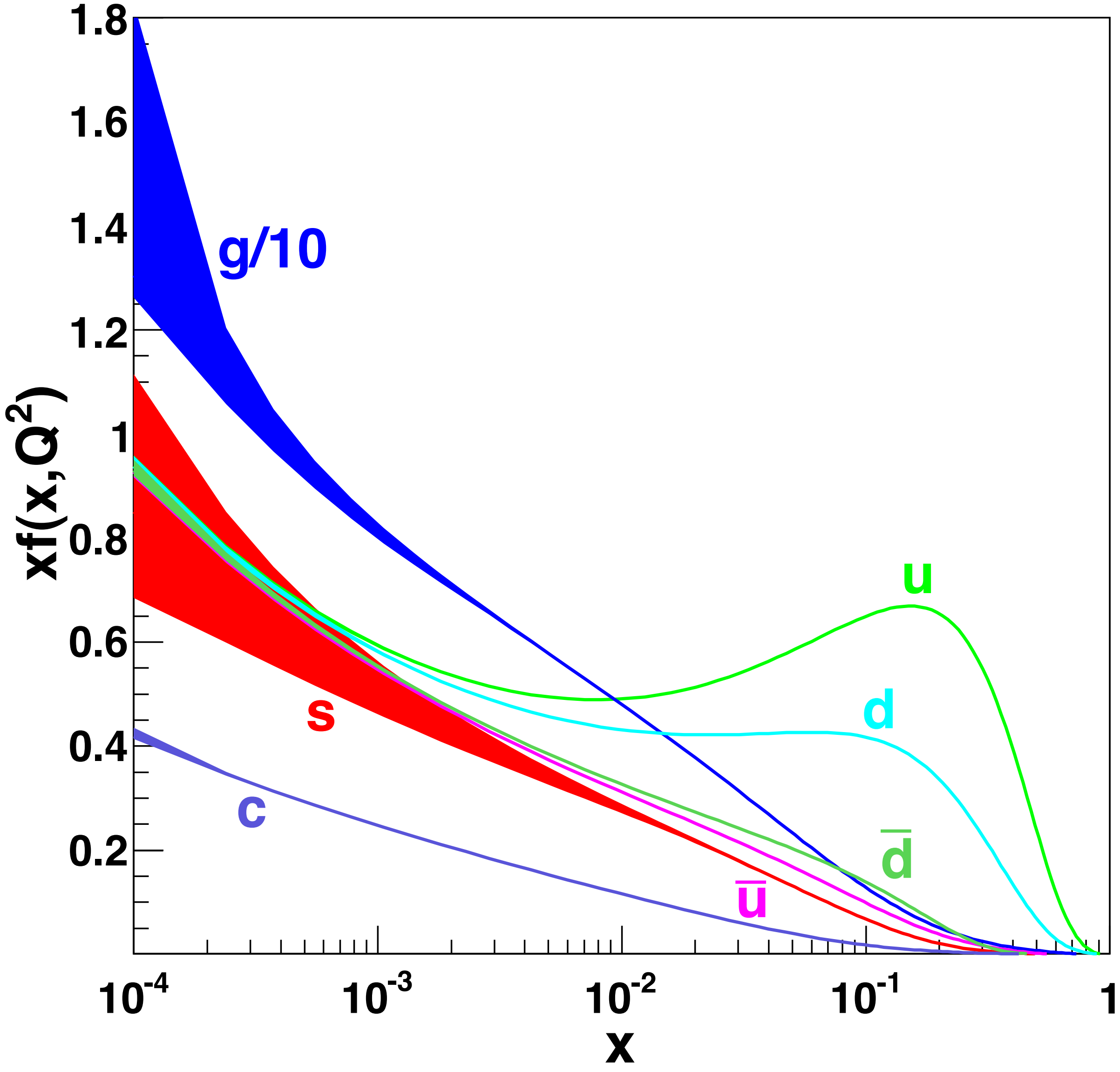

High Scale

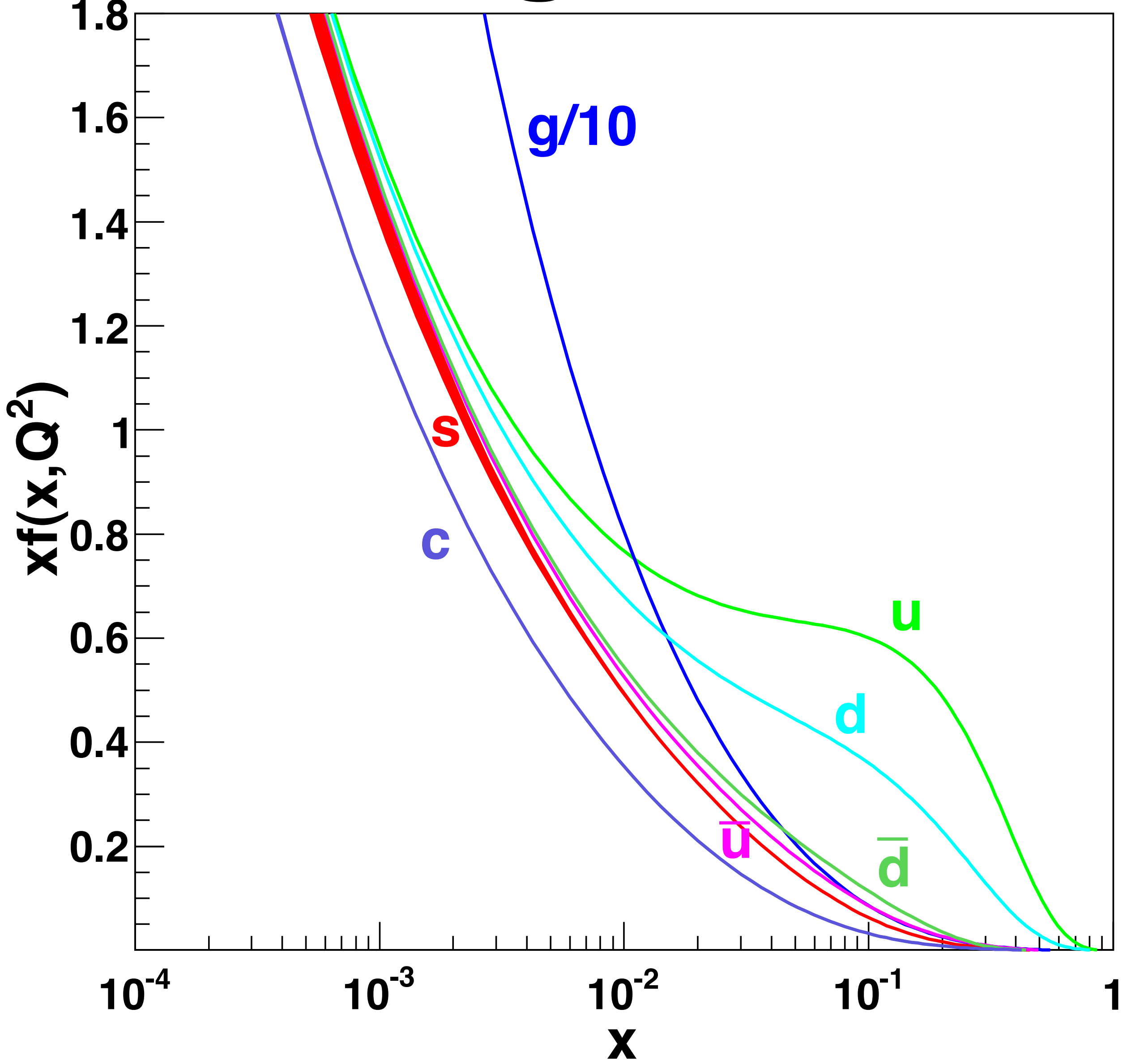

The QCD-Parton Picture of High Energy

(At least one large momentum scale (Q)
short-distance interaction; asymptotic)

lepton-lepton

$e^+ e^-$

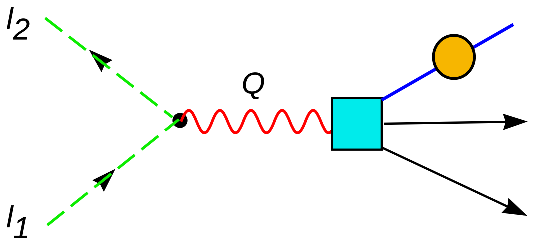

PEP,
PETRA,
Cornell,
LEP,
SLD,
NLC

lepton-hadron

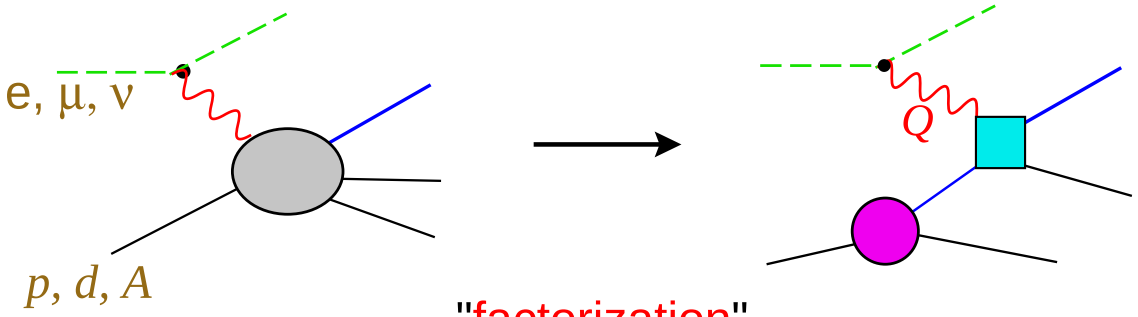

"factorization"

SLAC,
FNAL,
CERN,
HERA

hadron-hadron

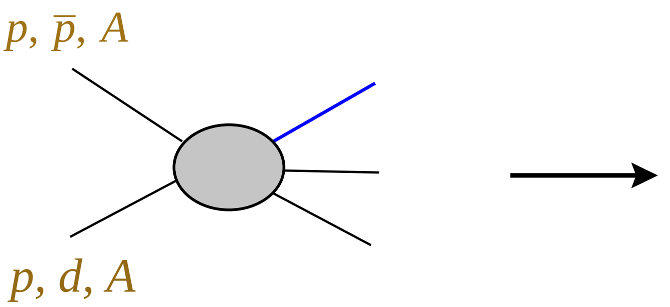

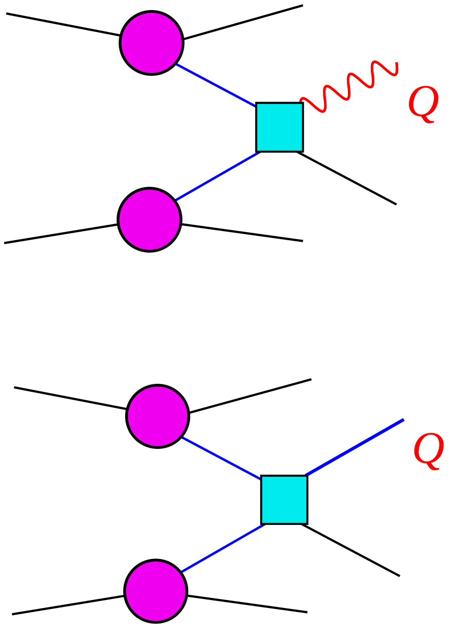

FNAL,
CERN,
Tevatron,
RHIC,
LHC

■ short } distance
● ● long } distance

Why does QCD play such a crucial role in High Energy Phenomenology?

- The parton picture language provides the foundation on which all modern particle theories are formulated, and all experimental results are interpreted.
- The validity of the parton picture is based empirically on an overwhelming amount of experimental evidence collected in the last 30-40 years, and theoretically on the Factorization Theorems of PQCD.

How could the *simple* (almost non-interacting) *parton picture* possibly hold in QCD — a strongly interacting quantum gauge field theory?

Answer: 3 unique features of QCD:

1. Asymptotic Freedom:
   A strongly interacting theory at long-distance can become weakly interacting at short-distance.
2. Infra-red Safety:
   There are classes of *infra-red safe* quantities which are independent of long-distance physics, hence are calculable in PQCD.
3. Factorization:
   There are an even wider class of physical quantities which can be *factorized* into a long-distance piece (not calculable, but *universal*) and short-distance piece (process-dependent, but infra-red safe, hence *calculable*).

Key concepts: Ultra-violet divergences, bare Green fns, renormalization, RGE, anomalous dimensions, renormalized G.Fs ; … etc.

Asymptotic Freedom

Universal (running) coupling:

$$\alpha_s(Q) = \frac{g^2}{4\pi} = \frac{b}{\ln(Q/\Lambda)}(1 + \ldots)$$

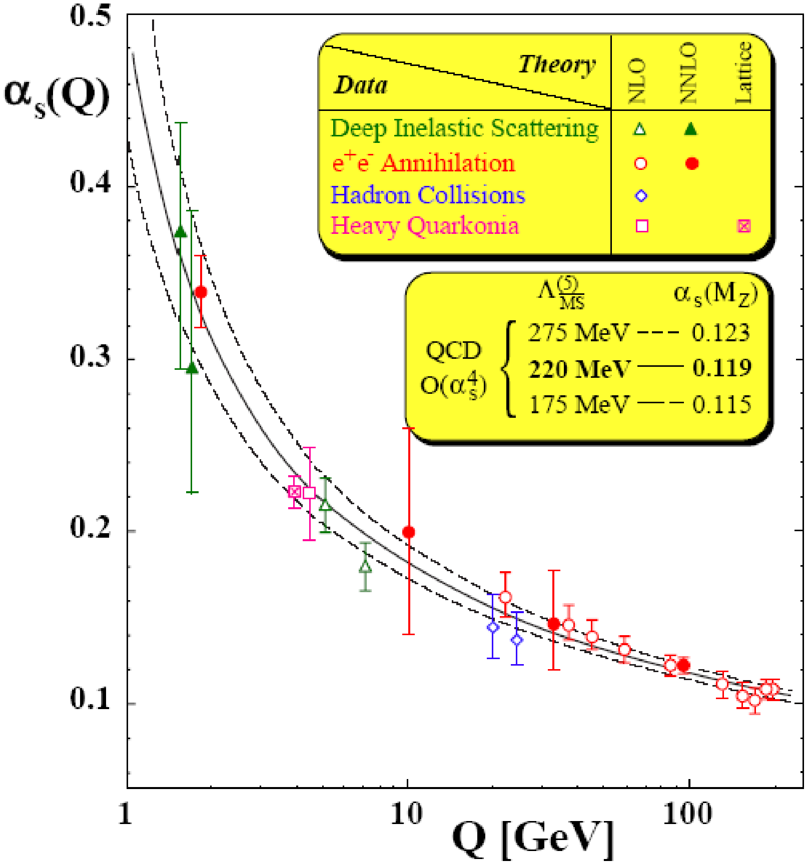

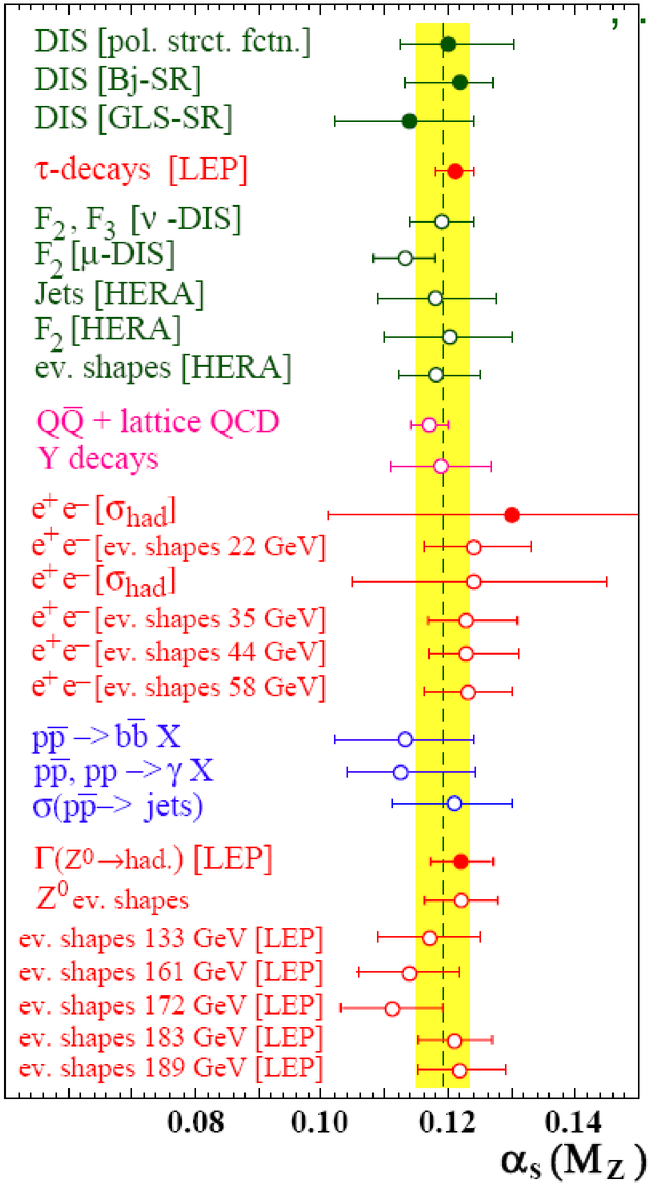

QCD and DIS

Master Equation for QCD Parton Model
– the Factorization Theorem

$$F_A^{\lambda}(x,\frac{m}{Q},\frac{M}{Q}) = \sum_a f_A^a(x,\frac{m}{\mu}) \otimes \hat{F}_a^{\lambda}(x,\frac{Q}{\mu},\frac{M}{Q}) + \mathcal{O}((\frac{\Lambda}{Q})^2)$$

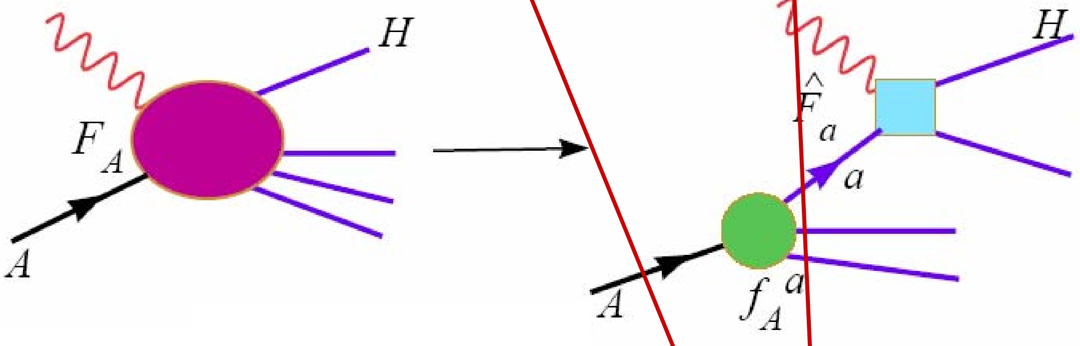

A physical observable is independent of μ,
i.e., renormalization group invariant.

μ is the factorization scale.
Usually choose μ = *Q*: that is how *f(x,Q)* acquires *Q*-dep.

“Renormalization” and “Factorization”

UV renormalization			Collinear/soft factorization		
A:	Bare Green Func.	$G_0(\alpha_0, m_0, ..)$	Partonic X-sect		F_a
B:	Ren. constants	$Z_i(\mu)$	Pert. parton dist.		$f_a^b(\mu)$
C:	Ren. Green Fun.	$G_R = G_0/Z$	Hard X-sect		$\widehat{F} = F \,/\, f$
D:	Anomalous dim.	$\gamma = \frac{\mu}{Z}\frac{d}{d\mu}Z$	Splitting fun.		$P = \frac{\mu}{f}\frac{d}{d\mu}f$
E:	Phys. para. α, m	$\alpha_0 Z_i \ldots$	Had. parton dist.	f_A	resummed
F:	Phys sc. amp.	$\alpha(\mu)\, G_R(m, \mu)$	Hadronic S.F.'s	F_A	$f_A(\mu) \times \widehat{F}(\mu)$

Some common features:

A : divergent; but, independent of “scheme” and scale μ;

B : divergent; scale and scheme dependent;
universal; absorbs all ultra-violet/soft/collinear divergences;

C & D : finite; scheme-dependent;
D controls the μ dependence of E & F;

E : physical parameters to be obtained from experiment;

F : Theoretical “prediction”; μ-indep. to all orders,
but μ-dep. at finite order n; $\mu\frac{d}{d\mu} \sim \mathcal{O}(\alpha^{n+1})$

Note: “Renormalization” is factorization (of UV divergences);
“factorization” is renormalization (of soft/collinear div.)

Hadron Collider Physics

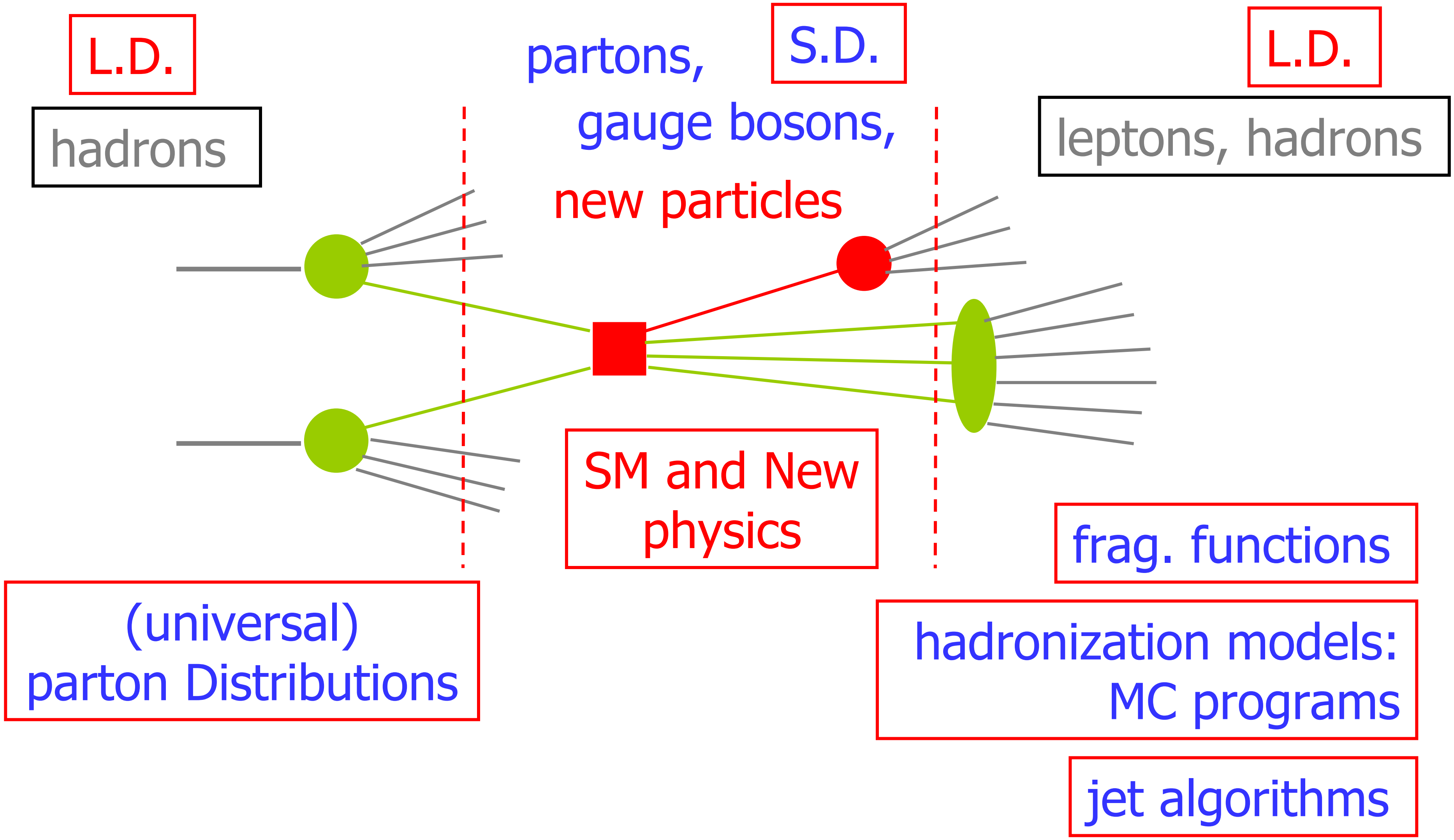

L.D.

hadrons

partons,

gauge bosons,

new particles

S.D.

L.D.

leptons, hadrons

SM and New physics

(universal)
parton Distributions

frag. functions

hadronization models:
MC programs

jet algorithms

Factorization Theorem

$$\sigma_{hh'} = \sum_{i,j} \int_0^1 dx_1 dx_2\, \phi_{i/h}\left(x, Q^2\right) H_{ij}\left(\frac{Q^2}{x_1 x_2 S}\right) \phi_{j/h'}\left(x_2, Q^2\right)$$

Nonperturbative,
but universal,
hence measurable

Infrared safe (IRS),
calculable in pQCD

CTEQ
MSTW
NNPDF

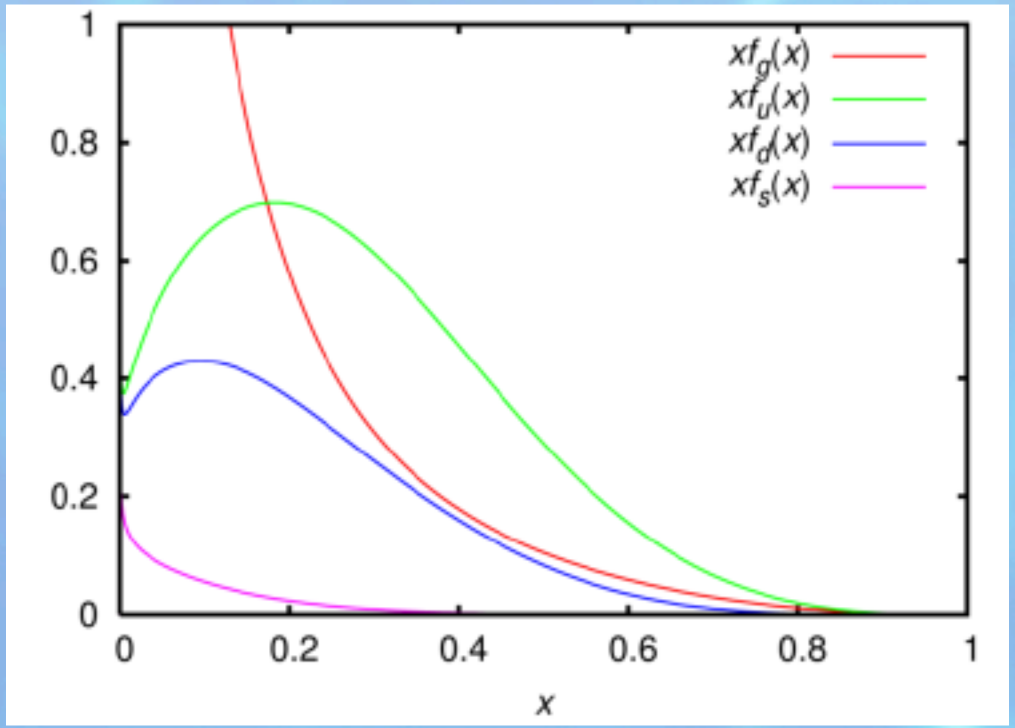

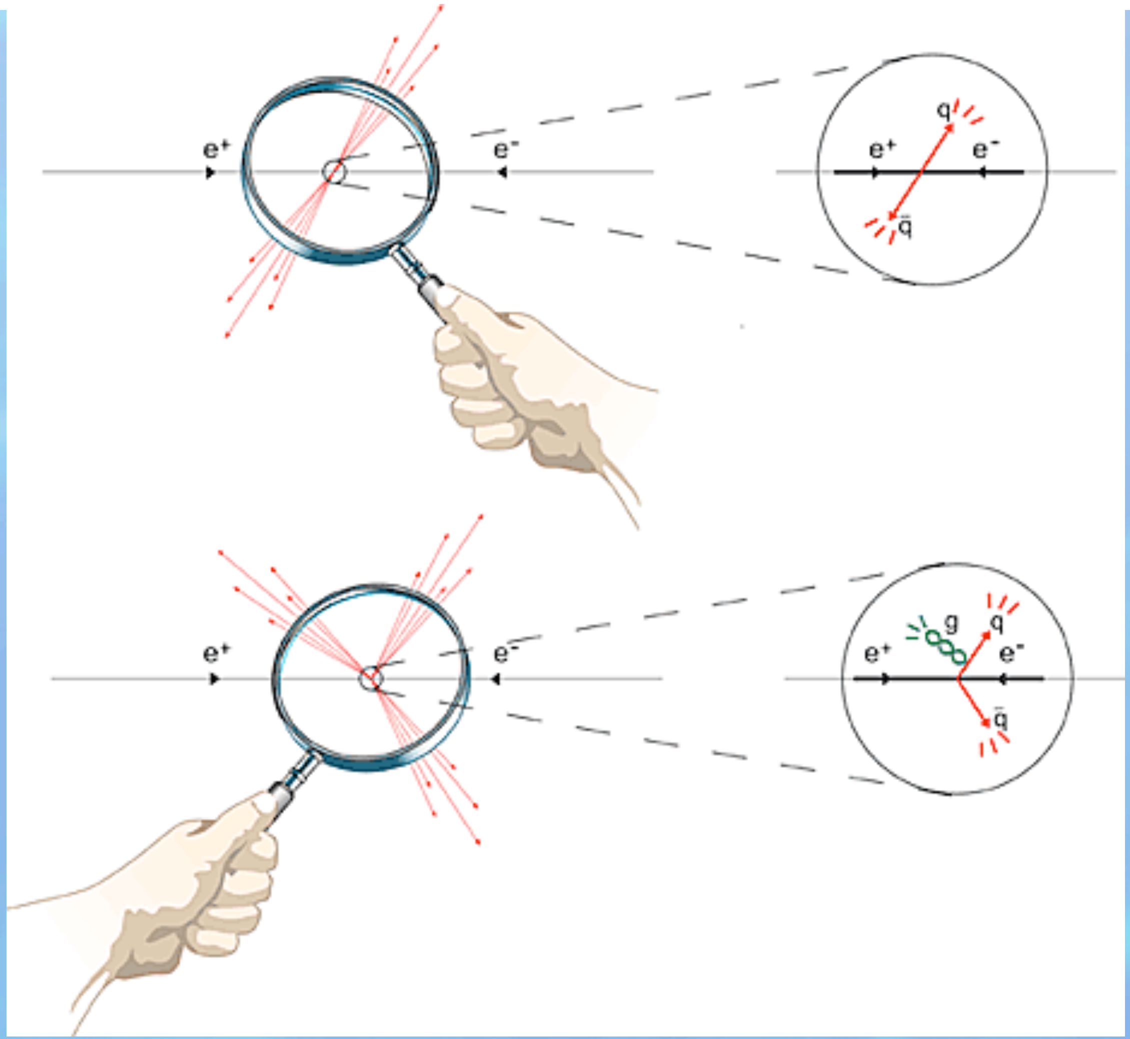

Hard part calculations

- Precision measurements at hadron colliders
- Precision Electroweak Physics at hadron colliders
- Physics of Drell-Yan pairs, W and Z bosons, and Higgs boson

W-boson production at hadron colliders

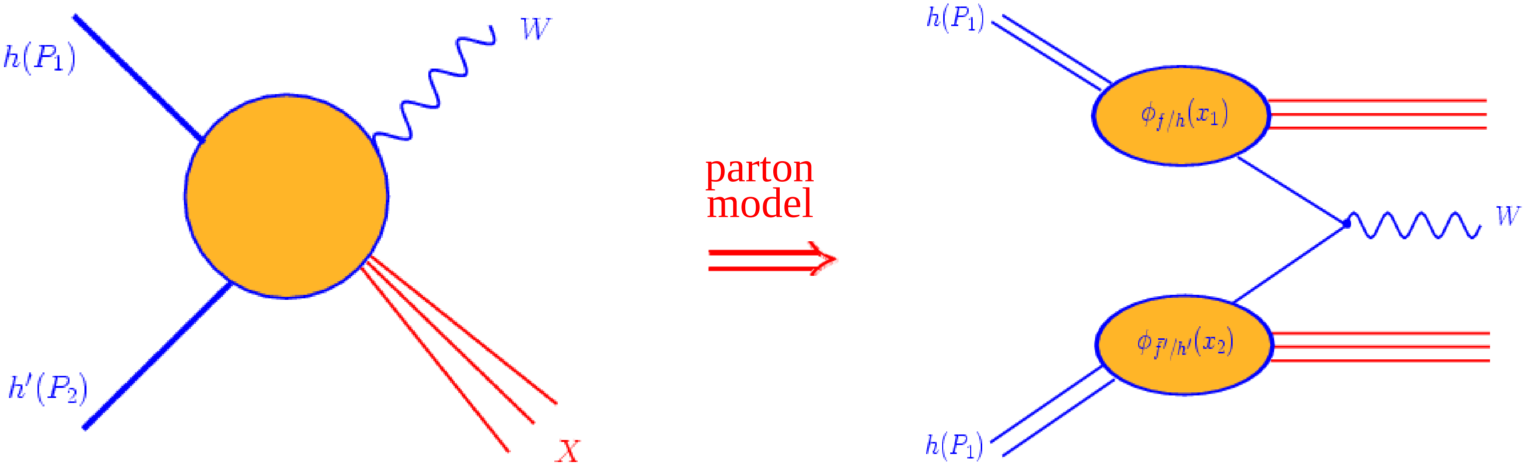

$$\sigma_{hh'\to W+X} = \sum_{f,f'} \int_0^1 dx_1 dx_2 \left\{ \phi_{f/h}(x_1)\, \hat{\sigma}_{ff'} \phi_{\bar{f}'/h'}(x_2) + (x_1 \leftrightarrow x_2) \right\}$$

PDFs are known from deep inelastic scattering

partonic “Born” cross section of $f\bar{f}' \to W^+$

W-boson production at hadron colliders

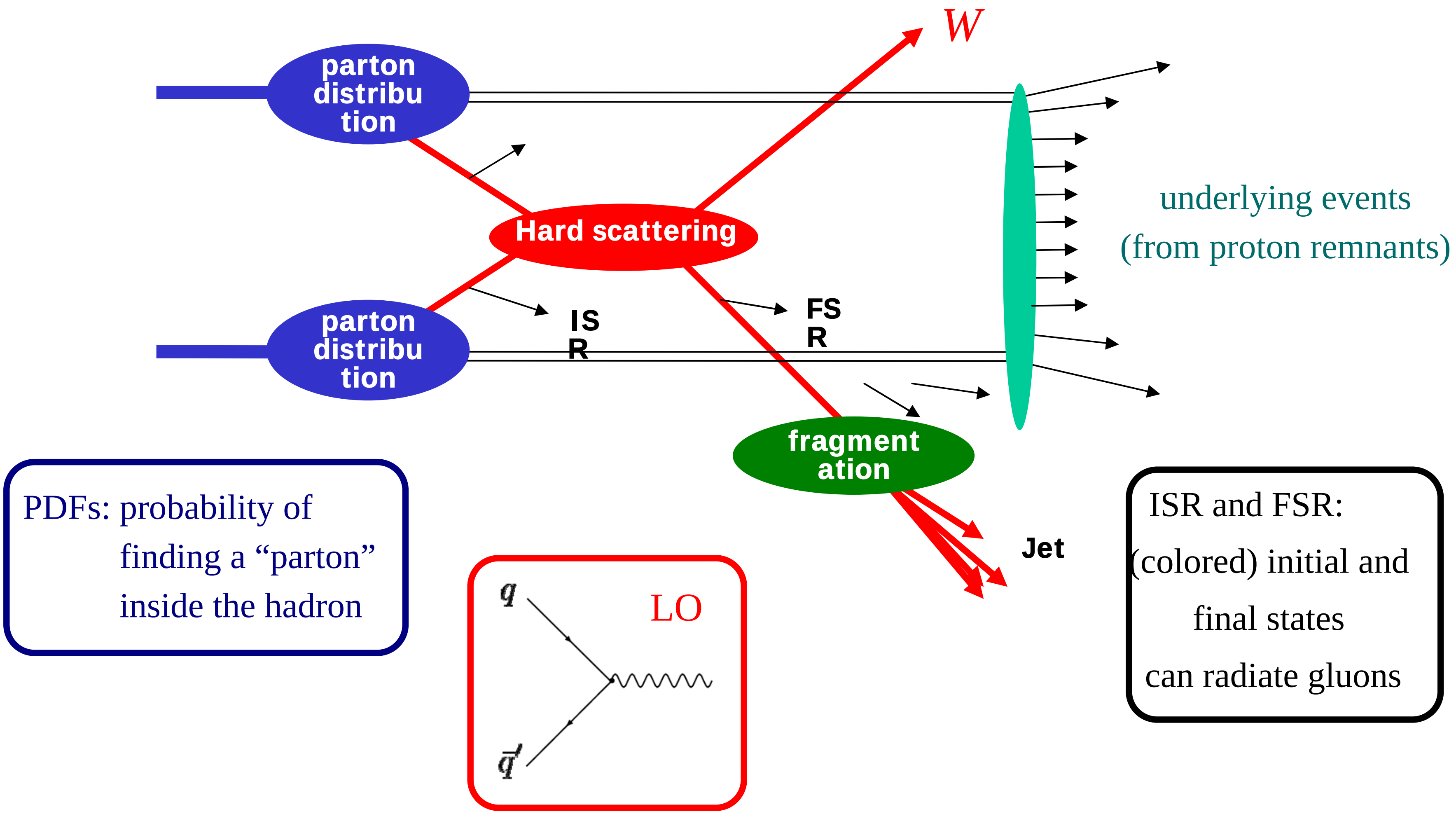

PDFs: probability of
finding a "parton"
inside the hadron

ISR and FSR:
(colored) initial and
final states
can radiate gluons

Fixed order pQCD prediction

$\alpha_S^{(0)}$

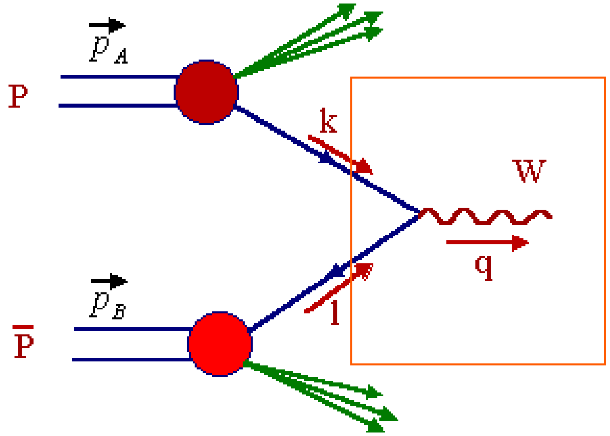

$$\sigma = \frac{1}{2S}\int \frac{d\xi_A}{\xi_A}\frac{d\xi_B}{\xi_B} f_{i/A}(\xi_A,\mu)\, f_{i/B}(\xi_B,\mu)\cdot d\hat{\sigma}$$

$$d\hat{\sigma} = \underbrace{\overline{|M|^2}}(2\pi)^4\,\delta^{(4)}(q-k-l)\frac{d^3q}{(2\pi)^3\,2q_0}$$

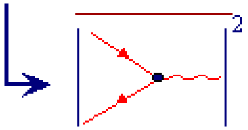

$$\frac{\mathrm{d}\sigma}{\mathrm{d}q_T^2\,\mathrm{d}y\,\mathrm{d}Q^2} = \frac{1}{S}\int \frac{\mathrm{d}\xi_A}{\xi_A}\frac{\mathrm{d}\xi_B}{\xi_B} f_{i/A}(\xi_A,\mu)\, f_{i/B}(\xi_B,\mu)$$

$$\cdot\left(\frac{\pi^2}{Q^2}\right)\cdot\overline{|M|^2}\cdot\delta\left(1-\frac{x_A}{\xi_A}\right)\cdot\delta\left(1-\frac{x_B}{\xi_B}\right)$$

$$\cdot\delta\left(q_T^2\right)\cdot\delta\left(Q^2-M_W^2\right)$$

$$s = \left(p_A + p_B\right)^2$$

$$k = \xi_A p_A$$

$$l = \xi_B p_B$$

$$Q \equiv \sqrt{Q^2} = \sqrt{q^2},\ \mu = Q = M_W,\ x_A = \frac{Q}{\sqrt{S}}e^{y},\ x_B = \frac{Q}{\sqrt{S}}e^{-y}$$

$\alpha_S^{(1)}$

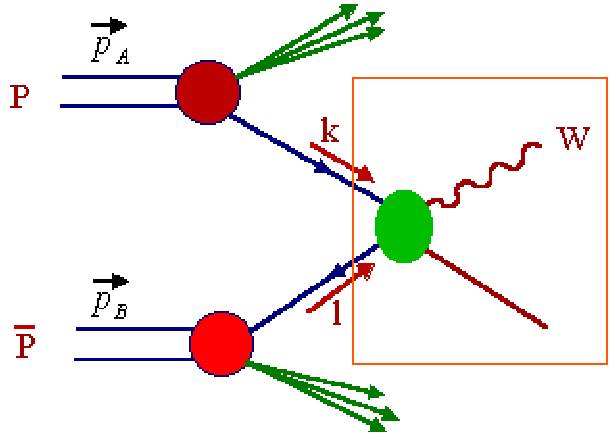

$$\begin{aligned}\frac{\mathrm{d}\sigma}{\mathrm{d}q_T^2\mathrm{d}y\mathrm{d}Q^2} = &\int \frac{\mathrm{d}\xi_A}{\left(\xi_A S + U - Q^2\right)}\left(\frac{\hat{s}\mathrm{d}\hat{\sigma}}{\mathrm{d}\hat{t}}\right)\cdot f_{i/A}\left(\xi_A,\mu\right)\\ &\cdot f_{j/B}\left(\xi_B = \frac{-Q^2-\xi_A\left(T-Q^2\right)}{\xi_A S + U - Q^2},\mu\right)\cdot\delta\left(Q^2-M_W^2\right)\\ &+\int \frac{\mathrm{d}\xi_B}{\left(\xi_B S + T - Q^2\right)}\left(\frac{\hat{s}\mathrm{d}\hat{\sigma}}{\mathrm{d}\hat{t}}\right)\cdot f_{j/B}\left(\xi_B,\mu\right)\\ &\cdot f_{i/A}\left(\xi_A = \frac{-Q^2-\xi_B\left(U-Q^2\right)}{\xi_B S + T - Q^2},\mu\right)\cdot\delta\left(Q^2-M_W^2\right)\end{aligned}$$

$$T = Q^2 - \sqrt{q_T^2+Q^2}\sqrt{S}\ e^{-y},$$

$$U = Q^2 - \sqrt{q_T^2+Q^2}\sqrt{S}\ e^{y},$$

$$\hat{s} = \xi_A\xi_B S$$

$$\hat{t} = \xi_A\left(T-Q^2\right)+Q^2$$

$$\frac{\hat{s}\,\mathrm{d}\hat{\sigma}}{\mathrm{d}\,\hat{t}} = \frac{1}{16\pi^2}\overline{\left|M\right|^2}$$

$M =$

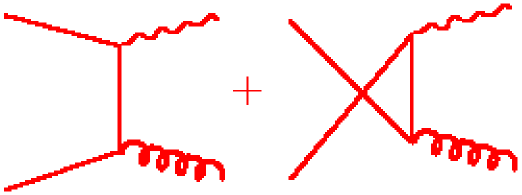

(For simplicity, only consider qq→Wg)

$\alpha_S^{(2)}$

- Virtual Corrections

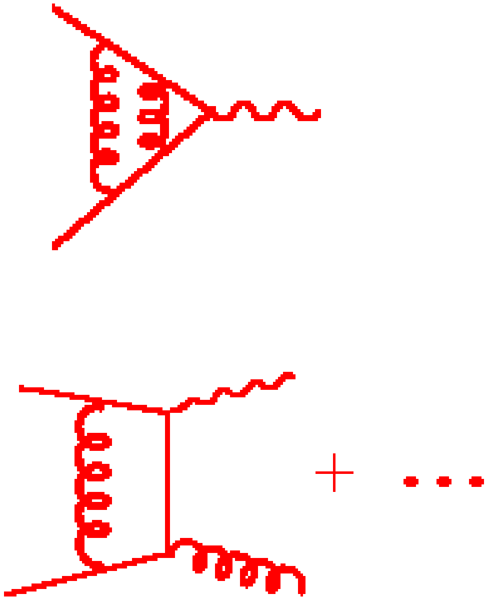

- Real emission contributions

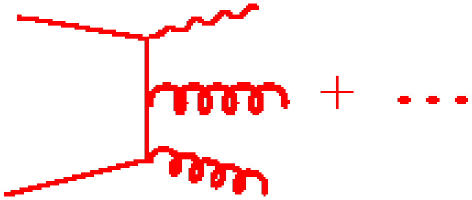

Theory Calculations

There are a variety of programs available for comparison of data to theory and/or predictions.

- Tree level (Alpgen, CompHEP, Grace, Madgraph…)

Les Houches accord

- Parton shower Monte Carlos (Herwig, Pythia,…

MC@NLO

- N^nLO (EKS, Jetrad, Dyrad, Wgrad, Zgrad,…Horace

recover NLO (NNLO?) normalization

- Resummed (ResBos)

Important to know strengths/weaknesses of each.

Shortcoming of fixed order calculation

- Cannot describe data with small q_T of W-boson.
- Cannot precisely determine m_W at hadron colliders without knowing the transverse momentum of W-boson. Most events fall in the small q_T region.

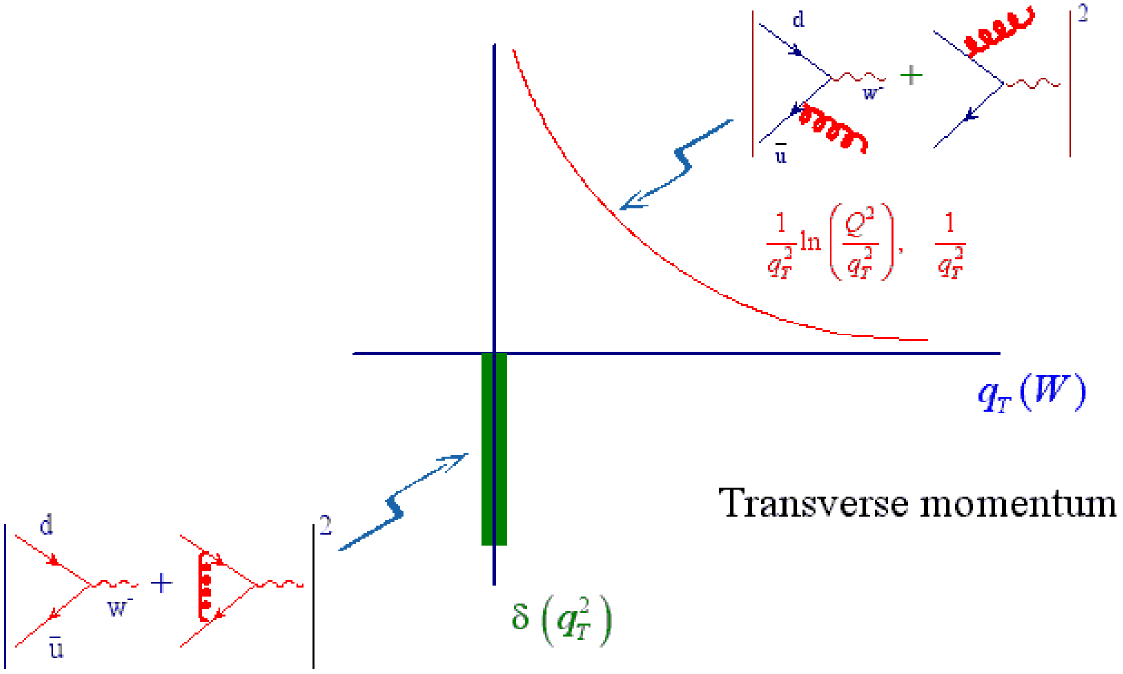

(at NLO)

QCD Resummation is needed

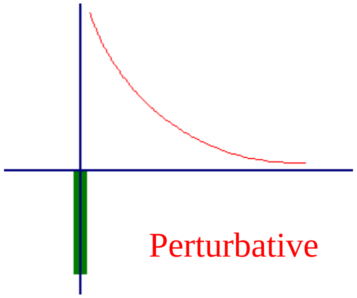

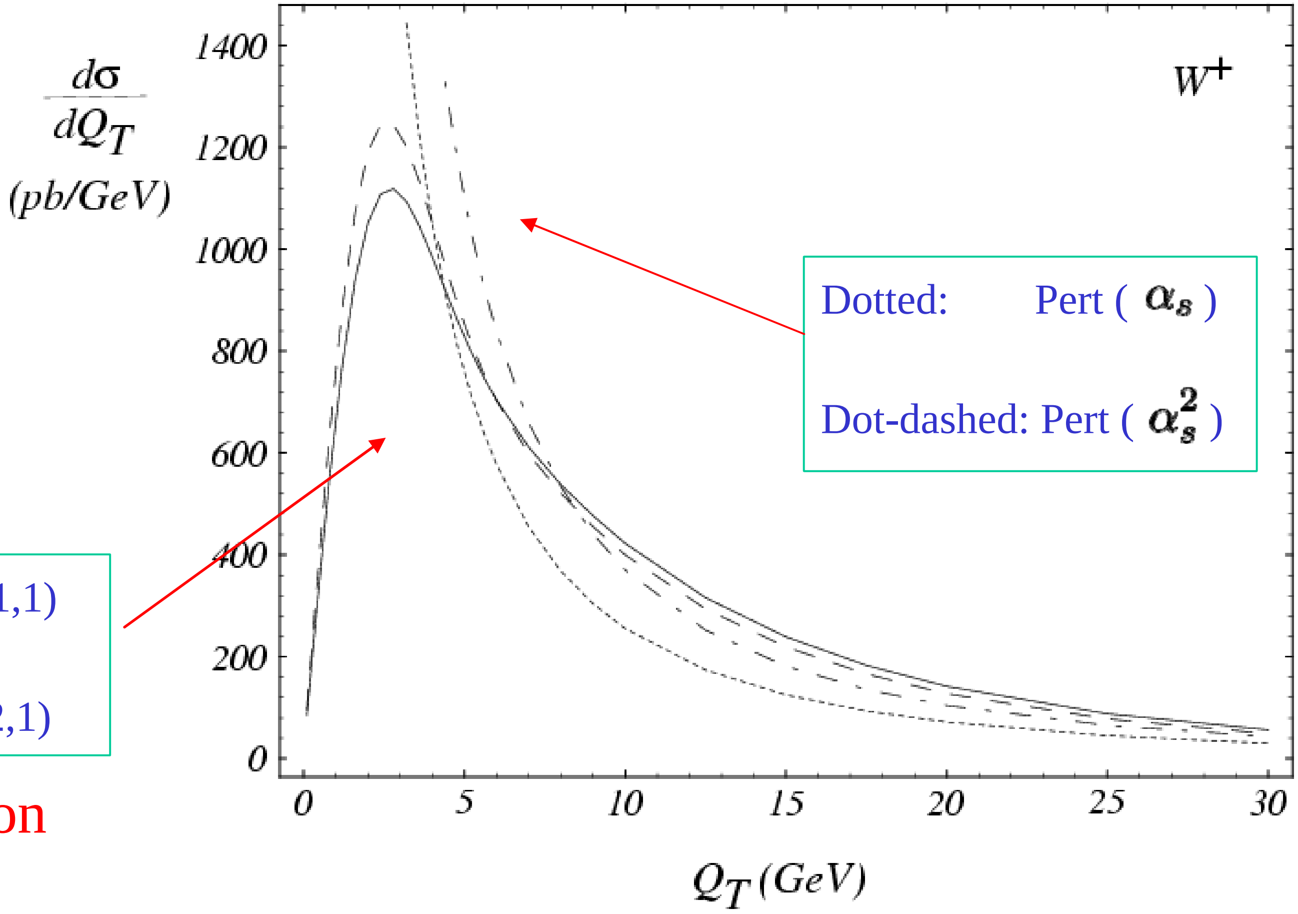

Dotted: Pert (α_s)

Dot-dashed: Pert (α_s^2)

Dashed: CSS (1,1,1)

Solid: CSS (2,2,1)

Resummation

Resummation calculations agree with data very well

Predicted by ResBos:

A program that
includes the effect of
multiple soft gluon emission
on the production of
W and Z bosons
in hadron collisions.

$P\bar{P} \to Z$ @ Tevatron

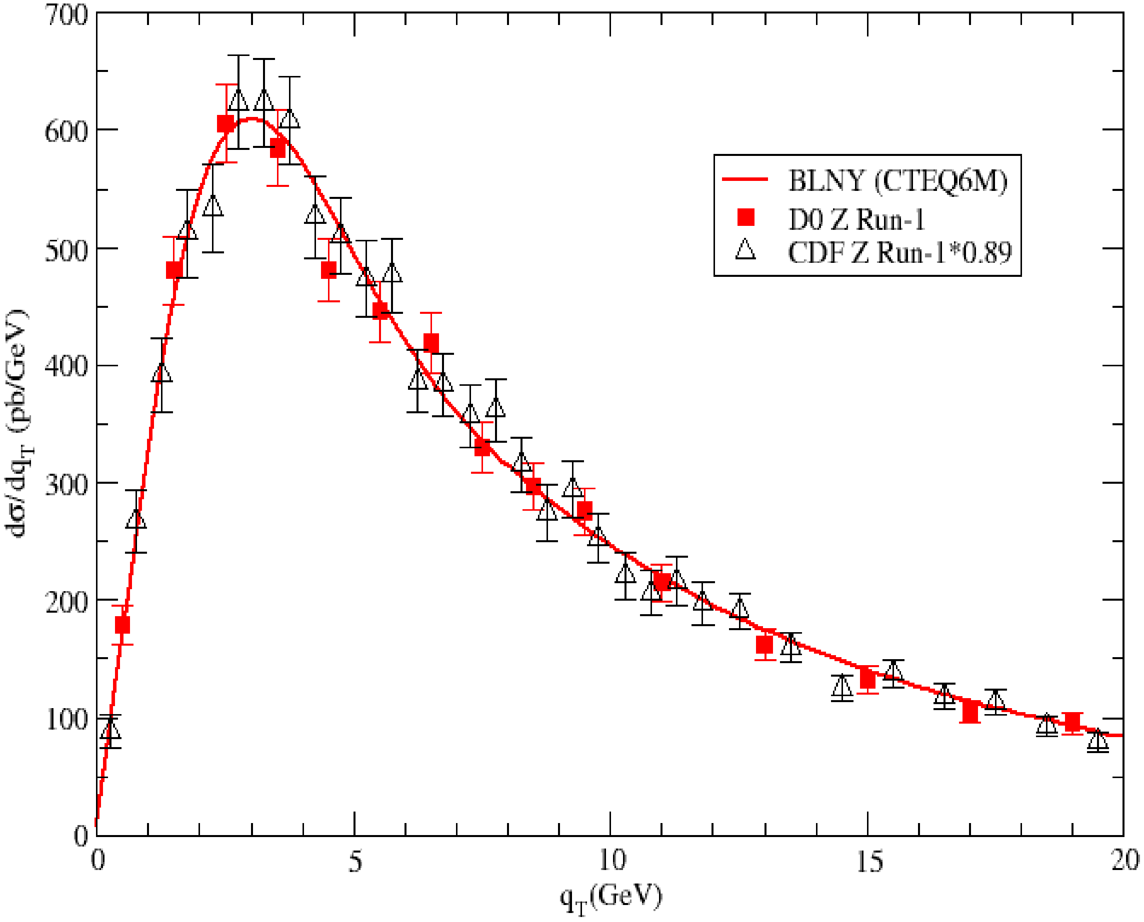

ResBos

(Resummation for Bosons)

Initial state QCD soft gluon resummation
and
Final state QED corrections

In collaboration with

Csaba Balazs, Alexander Belyaev, Ed Berger,
Qing-Hong Cao, Chuan-Ren Chen, Zhao Li,
Steve Mrenna, Pavel Nadolsky, Jian-Wei Qiu,
Carl Schmidt

What’s it for? An Example

- Transverse momentum of

Drell-Yan

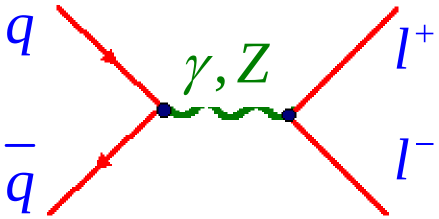

$W^\pm$

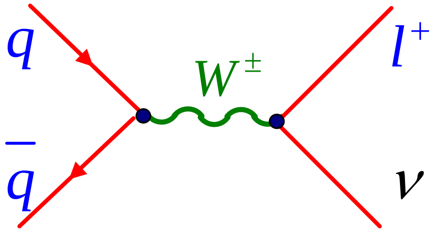

V H

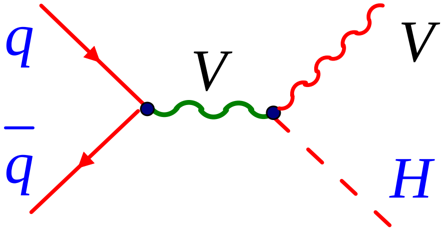

$g\,g \to H$

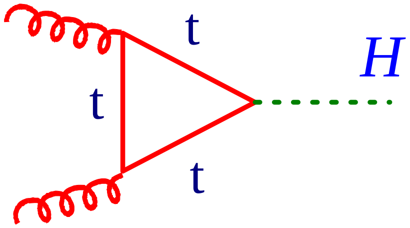

including QCD Resummations.

- Kinematics of Leptons from the decays
  (Spin correlation included)

W Charge Asymmetry: A Monitor of Parton Distribution Functions

- Difference between u(x) and d(x) in proton cause $u\bar{d} \rightarrow W^{+}$and $\bar{u}d \rightarrow W^{-}$ to be boosted in opposite directions

$$A(y_W) = \frac{d\sigma(W^+)/dy_W - d\sigma(W^-)/dy_W}{d\sigma(W^+)/dy_W + d\sigma(W^-)/dy_W}$$

$$A(y_W) \approx \frac{u(x_1)d(x_2) - d(x_1)u(x_2)}{u(x_1)d(x_2) + d(x_1)u(x_2)}$$

Rapidity charge asymmetry is sensitive to d(x)/u(x) ratio at high-**x**
→ primary interest of PDF fitters.

- cannot reconstruct y_W directly
- measure charged lepton only

$$A(\eta_l) = \frac{d\sigma(l^+)/d\eta_l - d\sigma(l^-)/d\eta_l}{d\sigma(l^+)/d\eta_l + d\sigma(l^-)/d\eta_l}$$

$$A(\eta_l) =$$

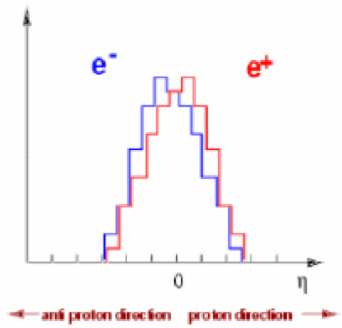

$$\otimes$$

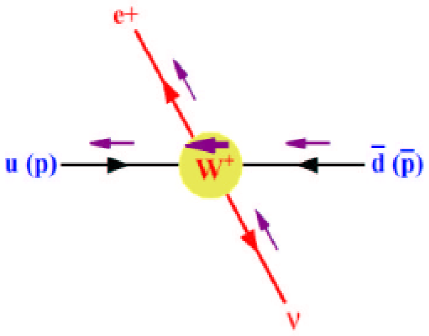

ResBos is also needed for Rapidity distributions

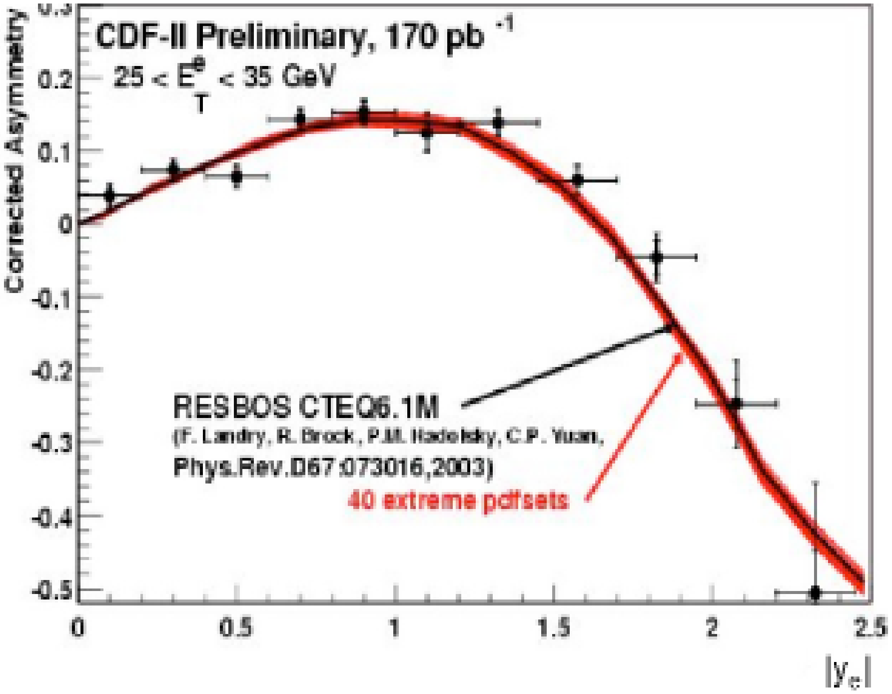

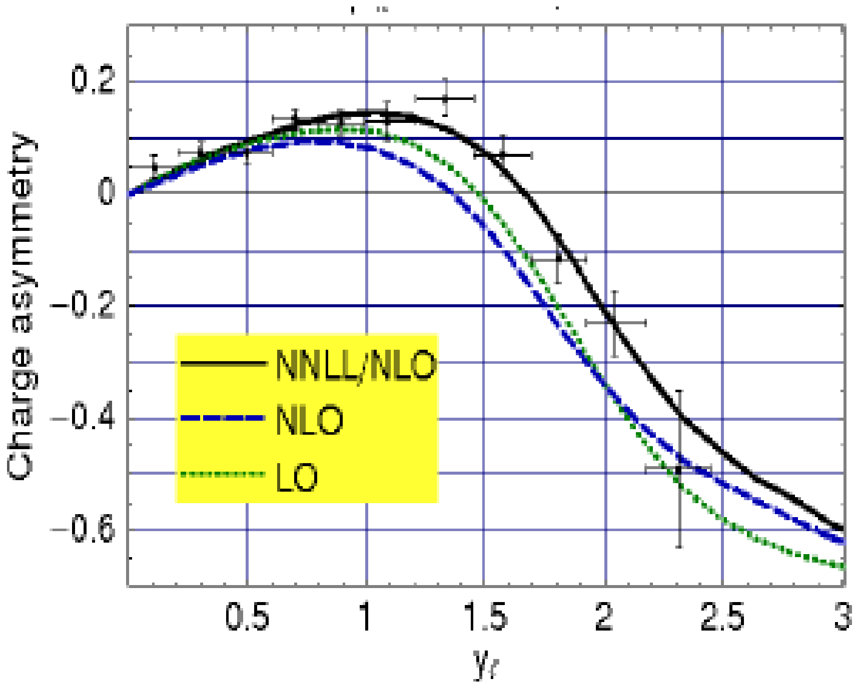

black curve is from ResBos calculation

What's QCD Resummation?

- Perturbative expansion

$$\frac{\mathrm{d}\hat{\sigma}}{\mathrm{d}q_T^2} \sim \alpha_S \left\{ 1 + \alpha_S + \alpha_S^2 + \cdots \right\}$$

- The singular pieces, as $\frac{1}{q_T^2}$ (1 or log's)

$$\frac{\mathrm{d}\hat{\sigma}}{\mathrm{d}q_T^2} \sim \frac{1}{q_T^2} \sum_{n=1}^{\infty} \sum_{m=0}^{2n-1} \alpha_S^{(n)} \ln^{(m)}\left(\frac{Q^2}{q_T^2}\right)$$

$$\sim \frac{1}{q_T^2} \{ \quad \alpha_S \left(\underline{L+1}\right)$$

$$+\alpha_S^2 \left(\underline{L^3 + L^2} + \underline{L+1}\right)$$

$$+\alpha_S^3 \left(\underline{L^5 + L^4} + \underline{L^3 + L^2} + \underline{L+1}\right)$$

$$+ \cdots \quad \}$$

$$L \equiv \ln\left(\frac{Q^2}{q_T^2}\right)$$

Resummation is to reorganize the results in terms of the large Log's.

Resummed results:

Determined by $A^{(1)}$ and $B^{(1)}$

$$\begin{aligned}\frac{d\sigma}{dq_T^2} \sim \frac{1}{q_T^2}\Big\{ & [\alpha_S(L+1) \quad +\alpha_S^2(L^3+L^2)+\alpha_S^3(L^5+L^4) \quad +\cdots\ ] \\ & +[\quad +\alpha_S^2(L+1) \quad +\alpha_S^3(L^3+L^2) \quad +\cdots\ ] \\ & +[\quad +\alpha_S^3(L+1) \quad +\cdots\ ] \\ & +\cdots\ \Big\}\end{aligned}$$

Determined by
$A^{(2)}$ and $B^{(2)}$

Determined by
$A^{(3)}$ and $B^{(3)}$

→ QCD Resummation

In the formalism by Collins-Soper-Sterman, in addition to these perturbative results, the effects from physics beyond the leading twist is also implemented as

[non-perturbative functions].

CSS Resummation Formalism

$$\frac{\mathrm{d}\sigma}{\mathrm{d}q_T^2\,\mathrm{d}y\,\mathrm{d}Q^2}=\frac{\pi}{S}\sigma_0\delta\left(Q^2-M_W^2\right)\cdot$$

$$\left\{\frac{1}{(2\pi)^2}\int \mathrm{d}^2b\quad e^{i\vec{q}_T\cdot\vec{b}}\tilde{W}\left(b,Q,x_A,x_B\right)\cdot\text{[Non-perturbative functions]}\right.$$

$$\left.+Y\left(q_T,y,Q\right)\right\}$$

$$\sum_j\int_{x_A}^1\frac{\mathrm{d}\xi_A}{\xi_A}C_{qj}\left(\frac{x_A}{\xi_A},b,\mu\right)\cdot f_{j/A}\left(\xi_A,\mu\right)$$

$$\tilde{W}=e^{-S(b)}\cdot C\otimes f\left(x_A\right)\cdot C\otimes f\left(x_B\right)$$

$$\sum_k\int_{x_B}^1\frac{\mathrm{d}\xi_B}{\xi_B}C_{qk}\left(\frac{x_A}{\xi_A},b,\mu\right)\cdot f_{k/B}\left(\xi_B,\mu\right)$$

Sudakov form factor $S(b)=\int_{\left(\frac{b_0}{b}\right)^2}^{Q^2}\frac{\mathrm{d}\bar{\mu}^2}{\bar{\mu}^2}\left[\ln\left(\frac{Q^2}{\bar{\mu}^2}\right)A\left(\bar{\mu}\right)+B\left(\bar{\mu}\right)\right]$

[Non-perturbative functions] are functions of (b,Q,x_A,x_B) which include QCD effects beyond Leading Twist.

To recover the "K-factor" in the NLO total rate

➡ To include the C-Functions

$$\frac{\mathrm{d}\sigma}{\mathrm{d}Q^2\,\mathrm{d}y} \sim$$

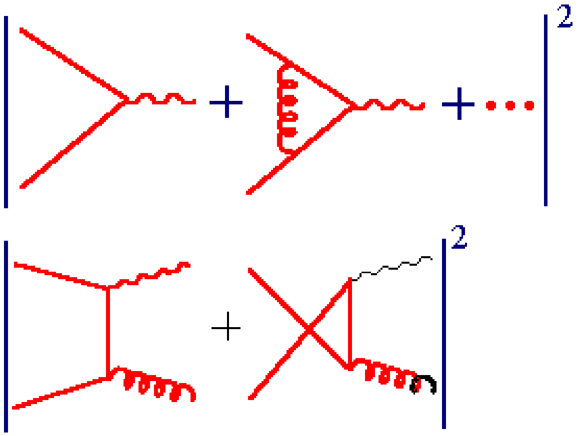

Finite

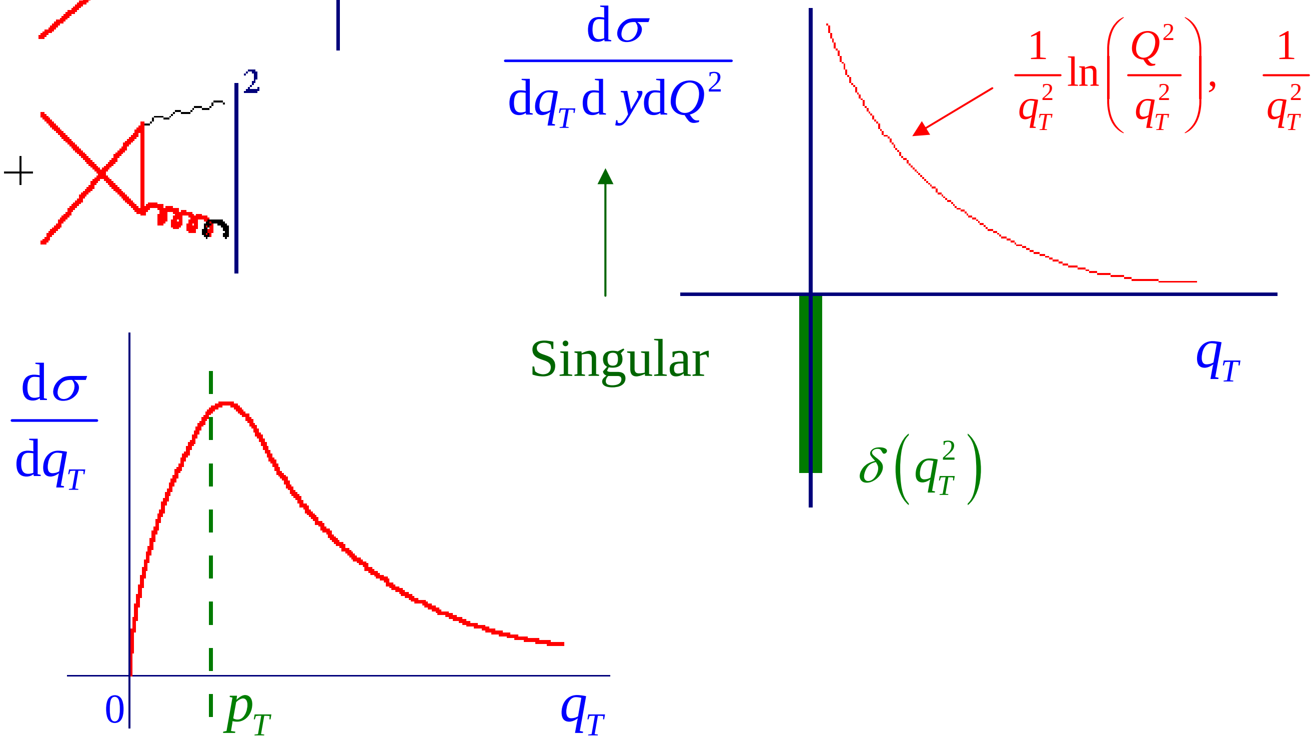

➡ The area under the q_T – curve will reproduce the total rate at the order $\alpha_S^{(1)}$ if Y term is calculated to $\alpha_S^{(1)}$ as well.

Include NNLO in high q_T region

- To improve prediction in high q_T region
- To speed up the calculation, it is implemented through K-factor table which is a function of (Q, q_T, y) of the boson, not just a constant value.

→ ResBos predicts both rate and shape of distributions.

Where is it?

- **ResBos**: http://hep.pa.msu.edu/resum/
- **Plotter**: http://hep.pa.msu.edu/wwwlegacy

ResBos-A (including final state NLO QED corrections)
http://hep.pa.msu.edu/resum/code/resbosa/
has not been updated.
Why? Because it was not used for Tevatron experiments.

The plan is to include final state QED resummation inside ResBos.

Physical processes included in ResBos

$W^{\pm}$

γ, Z

including gauge invariant set amplitude
for Drell-Yan pairs

H

$\gamma\gamma, ZZ, WW$

New physics: W', Z', H^+, A^0, H^0 …

Physics processes inside ResBos

Process	$A^{(i)}$	$B^{(i)}$	$C^{(i)}$	order of Pert. part
$A+B \rightarrow W^{+} \rightarrow l^{+}+\nu+X$	3	2	1	NNLO
$A+B \rightarrow W^{-} \rightarrow l^{-}+\bar{\nu}+X$	3	2	1	NNLO
$A+B \rightarrow Z^{0} \rightarrow l^{-}+l^{+}+X$	3	2	1	NNLO
$A+B \rightarrow Z^{0}/\gamma^{*} \rightarrow l^{+}+l^{-}+X$	3	2	1	NNLO
$A+B \rightarrow \gamma^{*} \rightarrow l^{+}+l^{-}+X$	3	2	1	NNLO
$A+B \rightarrow gg \rightarrow H^{0} \rightarrow \gamma\gamma+X$	3	2	1	NNLO
$A+B \rightarrow gg \rightarrow H^{0} \rightarrow Z^{0}Z^{0}/W^{+}W^{-} \rightarrow 4l+X$	3	2	1	NNLO
$A+B \rightarrow W^{+*} \rightarrow W^{+}+H^{0}+X$	3	2	1	NNLO
$A+B \rightarrow W^{-*} \rightarrow W^{-}+H^{0}+X$	3	2	1	NNLO
$A+B \rightarrow Z^{0*} \rightarrow Z^{0}+H^{0}+X$	3	2	1	NNLO
$A+B \rightarrow q\bar{q} \rightarrow \gamma\gamma+X$	3	2	1	NLO
$A+B \rightarrow gg \rightarrow \gamma\gamma+X$	3	2	1	NLO
$A+B \rightarrow q\bar{q} \rightarrow Z^{0}Z^{0}+X$	3	2	1	NLO
$A+B \rightarrow W^{+}W^{-}+X$ (upcoming)	3	2	1	NLO

New Physics (upcoming)

Process	$A^{(i)}$	$B^{(i)}$	$C^{(i)}$	order of Pert. part
$A+B \rightarrow W' \rightarrow l^{-}+\bar{\nu}+X$	3	2	1	NNLO
$A+B \rightarrow Z' \rightarrow l^{-}+l^{+}+X$	3	2	1	NNLO
$A+B \rightarrow bb \rightarrow A^{0}/H^{0}+X$ (THDM)	3	2	1	NNLO
$A+B \rightarrow c\bar{s} \rightarrow H^{+}+X$ (THDM)	3	2	1	NNLO

PYTHIA predicts a different shape (and rate)

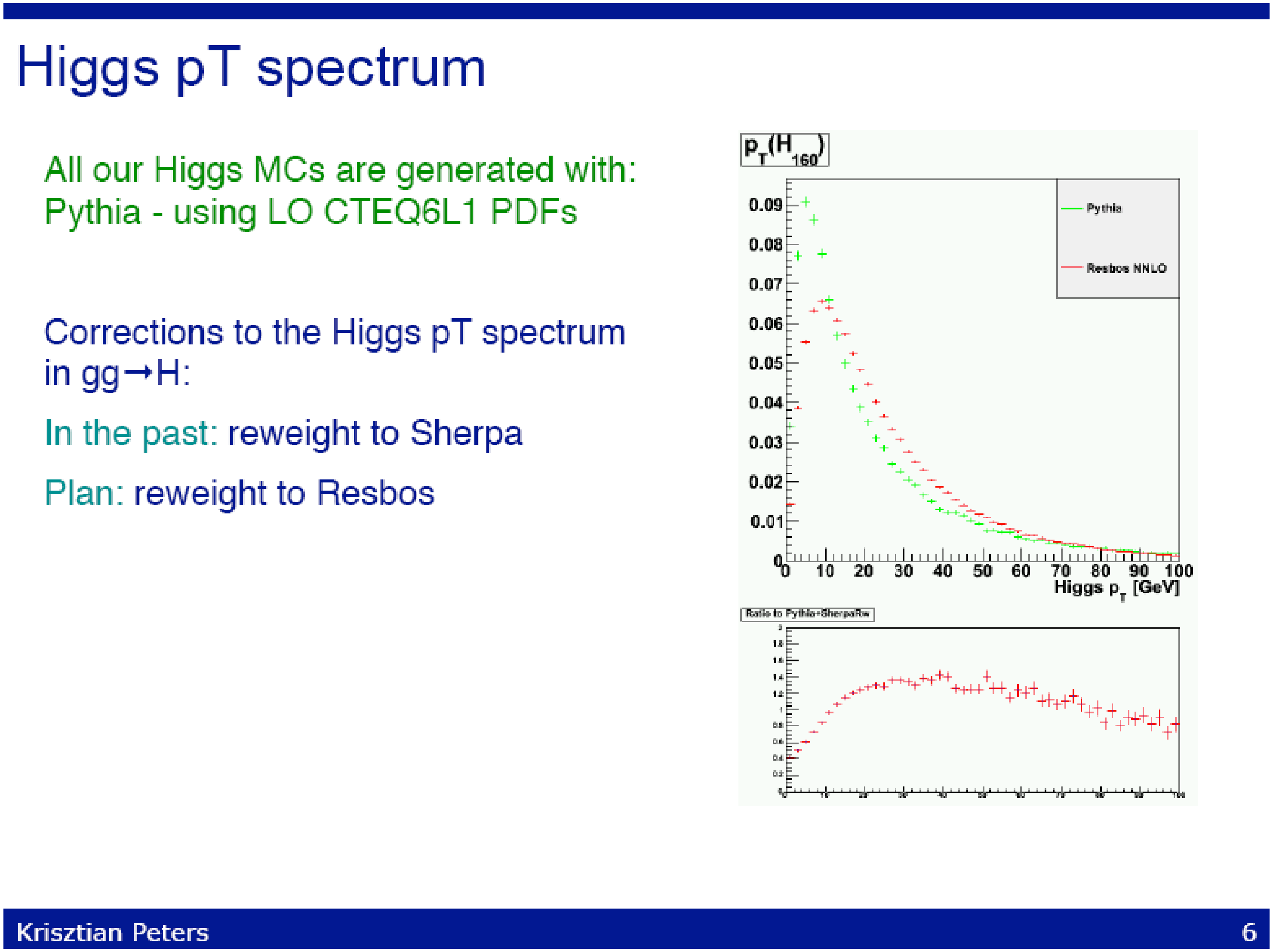

Higgs pT spectrum

All our Higgs MCs are generated with:
Pythia - using LO CTEQ6L1 PDFs

Corrections to the Higgs pT spectrum in gg→H:

In the past: reweight to Sherpa

Plan: reweight to Resbos

Limitations of ResBos

- Any perturbative calculation is performed with some approximation, hence, with limitation.
- To make the best use of a theory calculation, we need to know what it is good for and what the limitations are.

It does not give any information about the hadronic activities of the event.

→ It could be used to reweight the distributions generated by (PYTHIA) event generator, by comparing the boson (and it decay products) distributions to ResBos predictions.

This has been done for W-mass analysis by CDF and D0)

CTEQ-TEA
Parton Distribution Function Global Analysis

- CT10 NNLO PDFs
- Some remarks about the precision of global analysis at LO, NLO and NNLO

CTEQ-Tung et al (TEA) Collaboration:

S. Dulat, J. Gao, M. Guzzi, T.J. Hou, J. Huston,
H.-L. Lai, Z. Li, P. Nadolsky, J. Pumplin,
C. Schmidt, D. Stump, C.-P. Yuan

CT10NNLO and CT1X NNLO PDFs

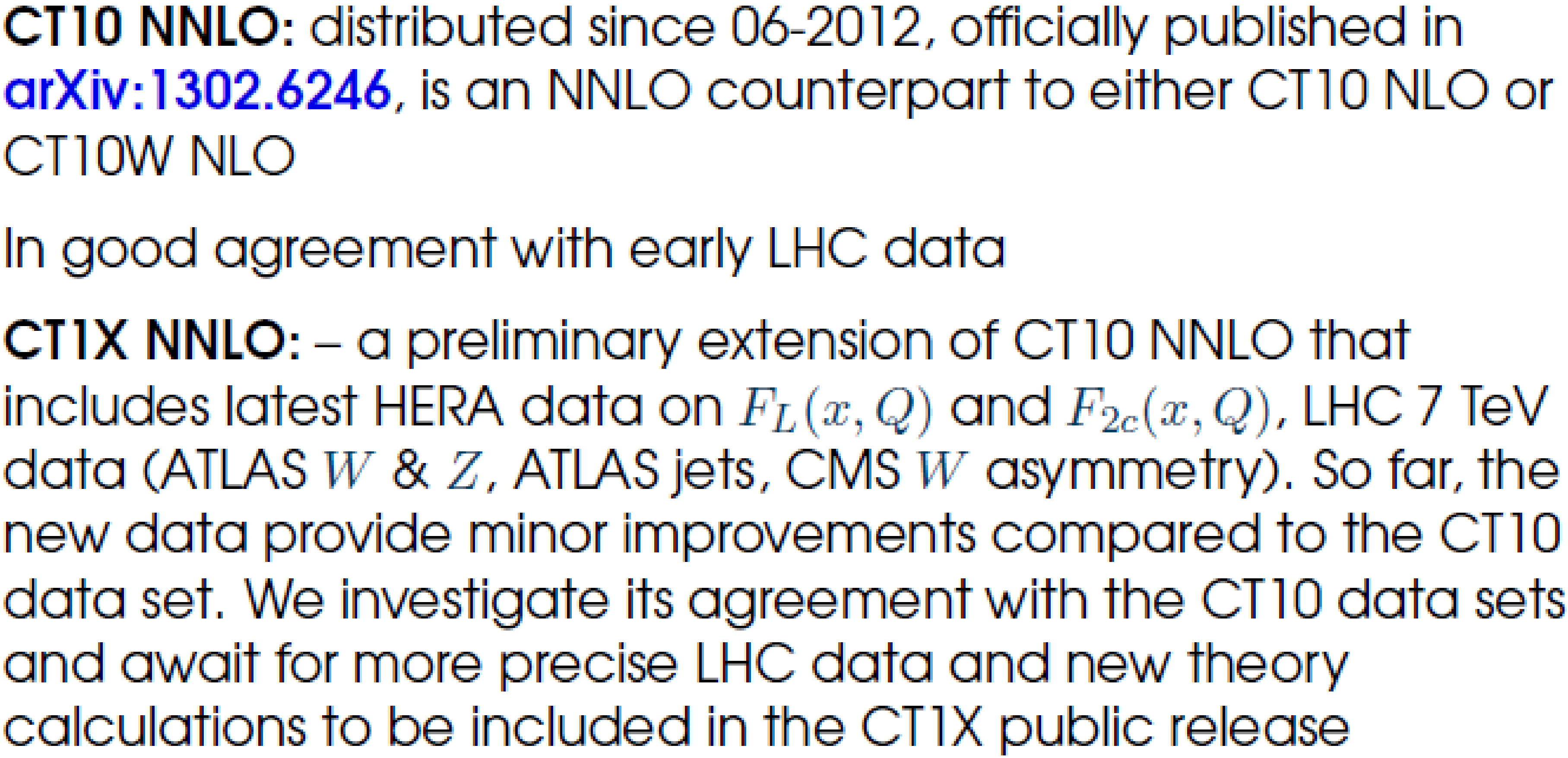

CT10 NNLO: distributed since 06-2012, officially published in arXiv:1302.6246, is an NNLO counterpart to either CT10 NLO or CT10W NLO

In good agreement with early LHC data

CT1X NNLO: – a preliminary extension of CT10 NNLO that includes latest HERA data on $F_L(x,Q)$ and $F_{2c}(x,Q)$, LHC 7 TeV data (ATLAS W & Z, ATLAS jets, CMS W asymmetry). So far, the new data provide minor improvements compared to the CT10 data set. We investigate its agreement with the CT10 data sets and await for more precise LHC data and new theory calculations to be included in the CT1X public release

CT10 Website:
http://hep.pa.msu.edu/cteq/public/ct10.html

Interpretation of experimental data at LO, NLO and NNLO

- Factorization Theorem

⇨ Data depends on
PDFs and Wilson coefficients

- Higher order calculation (including both PDFs and Wilson coefficients) yields better description of experimental data.

Compare the quality of global fits at LO, NLO and NNLO

- Chi-square per data point is

  about 1.1 at NNLO and NLO, and

  about 1.5 at LO.
- The overall data points included in the global analysis is at the order of 3000, including DIS, Drell-Yan (W/Z) and jet data.

(LHC data are not yet included in the released PDF sets.)

ID	**Experimental data set**	N_{pt}	CT10 NNLO	CT10 NLO	CT10 LO
159	Combined HERA1 DIS [?]	579	1.07	1.05	1.54
101	BCDMS F_2^p [?]	339	1.16	1.13	1.24
102	BCDMS F_2^d [?]	251	1.16	1.04	1.13
103	NMC F_2^p [?]	201	1.66	1.71	2.19
104	NMC F_2^d/F_2^p [?]	123	1.23	1.01	0.95
108	CDHSW F_2^p [?]	85	0.83	0.73	0.94
109	CDHSW F_3^p [?]	96	0.81	0.70	0.87
110	CCFR F_2^p [?]	69	0.98	1.04	2.29
111	CCFR xF_3^p [?]	86	0.40	0.37	0.66
124	NuTeV ν di-μ SIDIS [?]	38	0.78	0.91	0.72
125	NuTeV $\overline{\nu}$ di-μ SIDIS [?]	33	0.86	0.83	1.47
126	CCFR ν di-μ SIDIS [?]	40	1.20	1.27	0.73
127	CCFR $overline\nu$ di-μ SIDIS [?]	38	0.70	0.79	0.63
140	H1 F_2^c [?]	8	1.17	1.30	3.60
143	H1 $\tilde{\sigma}^{c\bar{c}}$ [?]	10	1.63	1.55	3.19
145	H1 $\tilde{\sigma}^{bb}$ [?]	10		0.78	
156	ZEUS F_2^c [?]	18	0.74	0.95	3.34
157	ZEUS F_2^c [?]	27	0.62	0.81	2.78
201	E605 DY process $\sigma(pA)$ [?]	119	0.80	0.79	0.78
203	E866 DY process $\sigma(pd)/(2\sigma(pp))$ [?]	15	0.65	0.45	0.55
204	E866 DY process $\sigma(pp)$ [?]	184	1.27	1.292	1.38
225	CDF Run-1 W charge asymmetry [?]	11	1.22	0.78	1.57
227	CDF Run-2 W charge asymmetry [?]	11	1.04	1.33	0.99
231	Run-2 W charge asymmetry [?]	12	2.17		1.91
234	Run-2 W charge asymmetry [?]	9	1.65		1.22
260	Run-2 Z rapidity dist. [?]	28	0.56	0.57	1.83
261	CDF Run-2 Z rapidity dist. [?]	29	1.60	1.76	4.47
504	CDF Run-2 inclusive jet [?]	72	1.42	1.56	1.85
514	Run-2 inclusive jet [?]	110	1.04	1.14	1.63
505	CDF Run-2 inclusive jet [?]	33		1.64	
515	Run-2 inclusive jet [?]	90		0.76	
	Totals N_{pt}**:**		2641	2753	2641
	Totals χ^2 **:**		3026	2954	3870

Experimental access to the proton structure

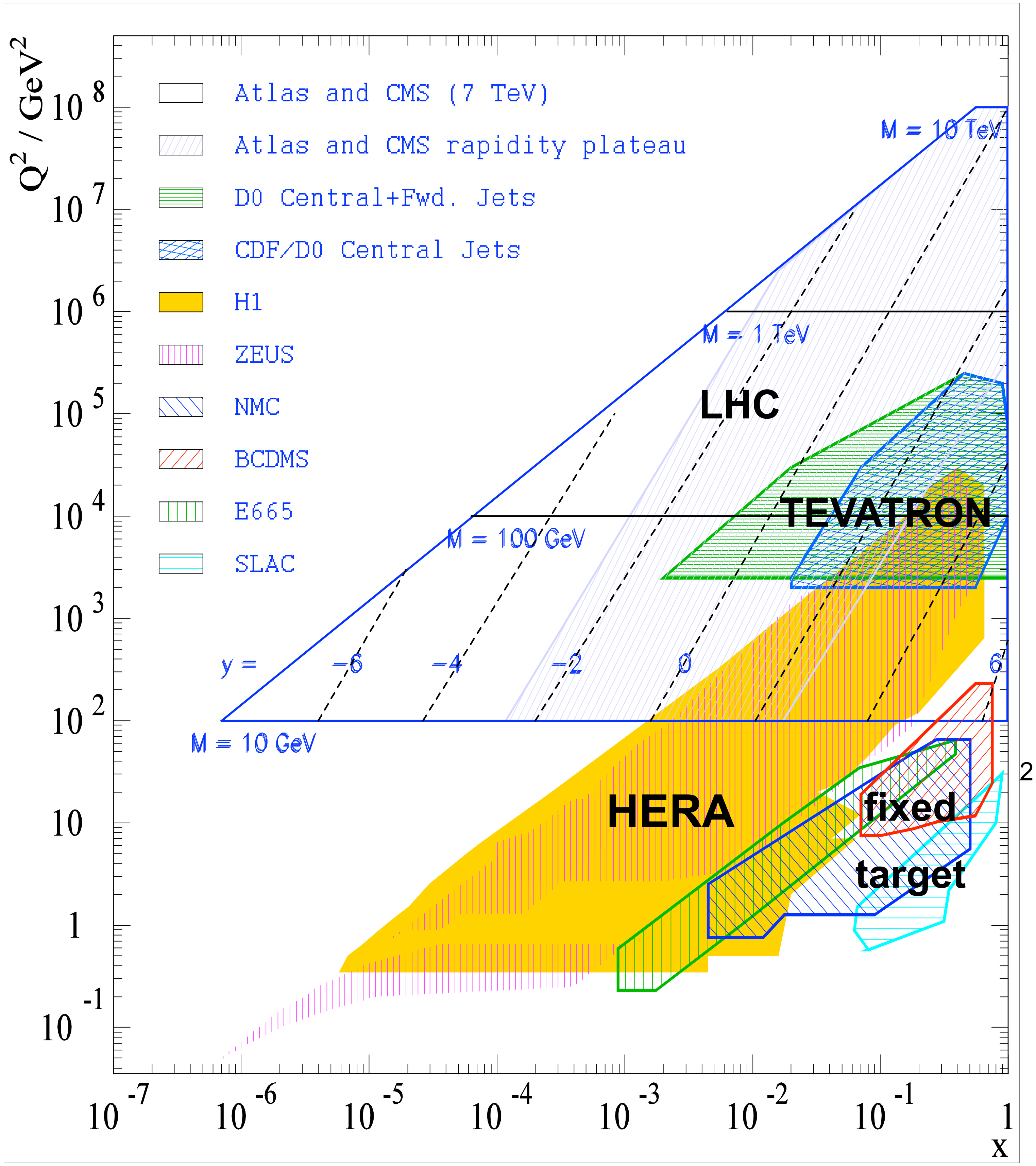

HERA: low and medium x

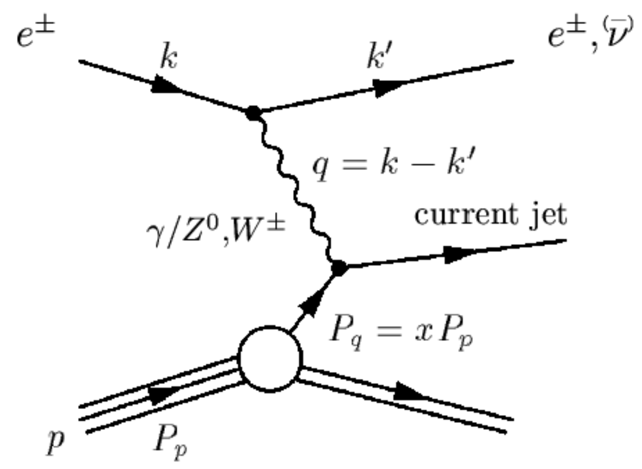

LHC: important constraints on g(x), flavour separation

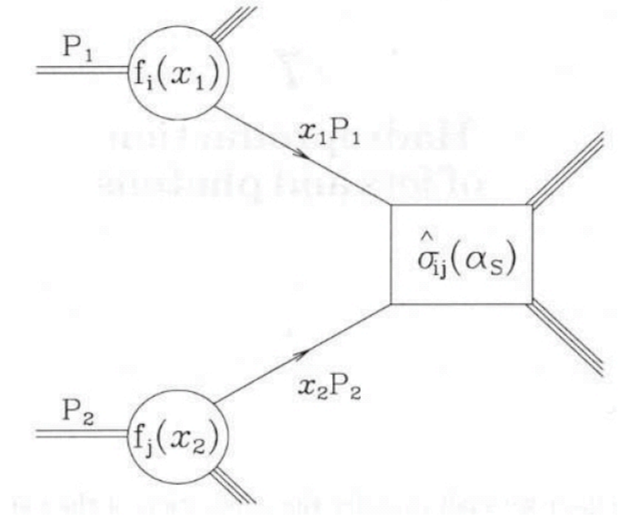

Fixed Target: high x, nuclear PDFs

CT10NNLO Hessian error PDFs

Q=2 GeV

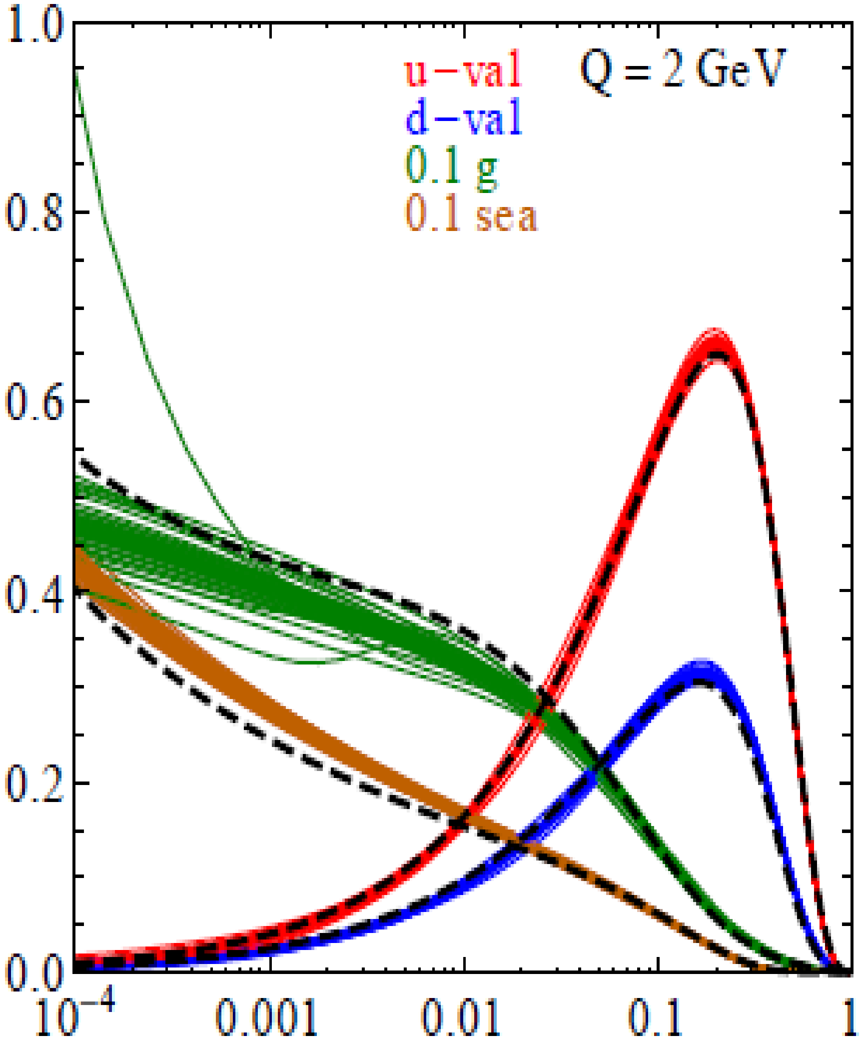

Q=85 GeV

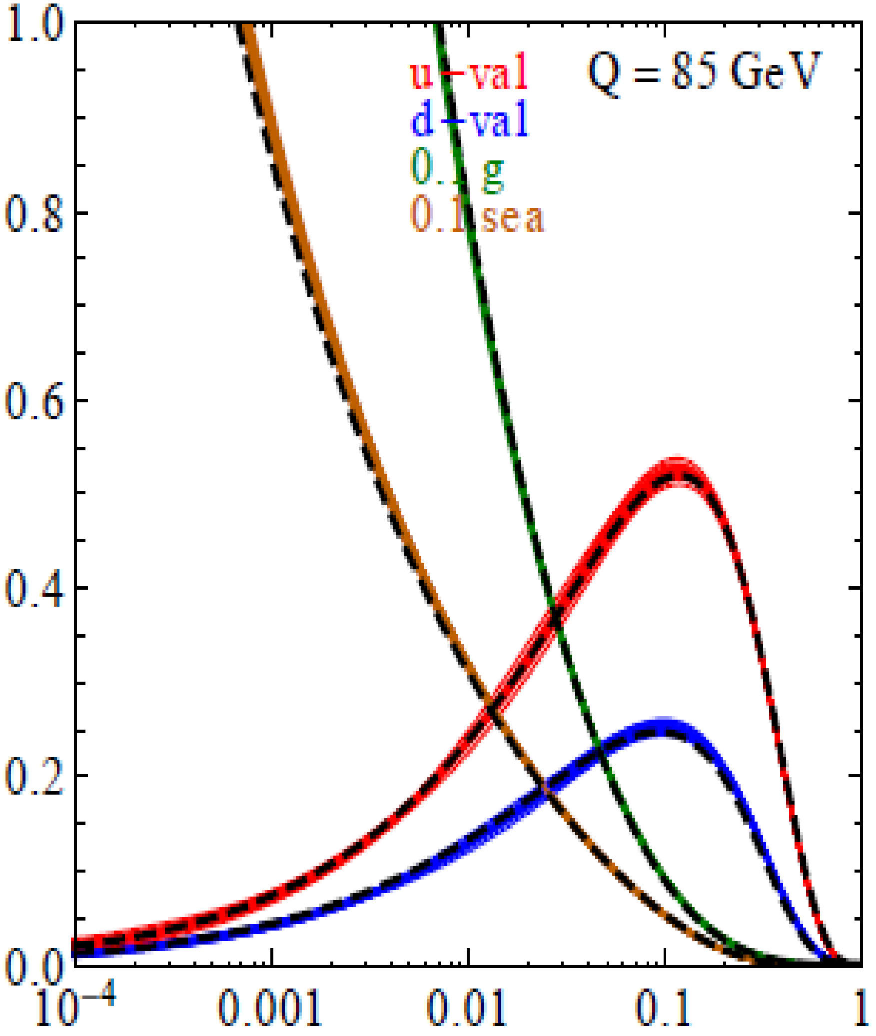

CT10 NNLO error PDFs (compared to CT10W NLO)

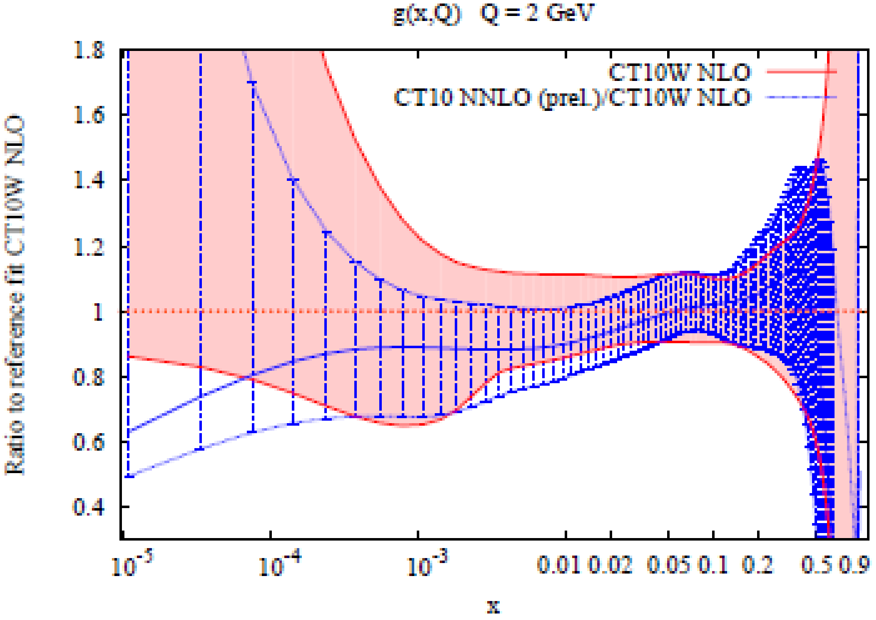

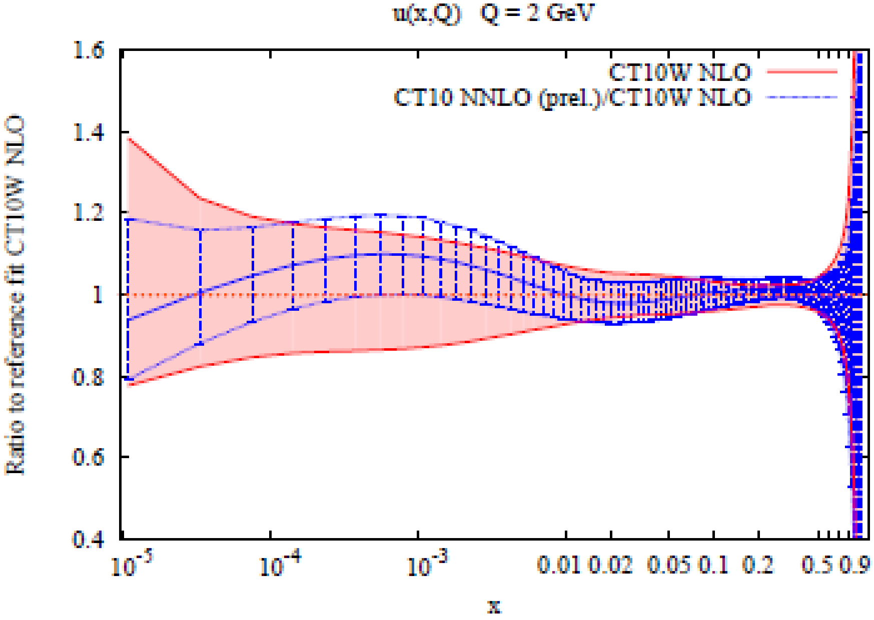

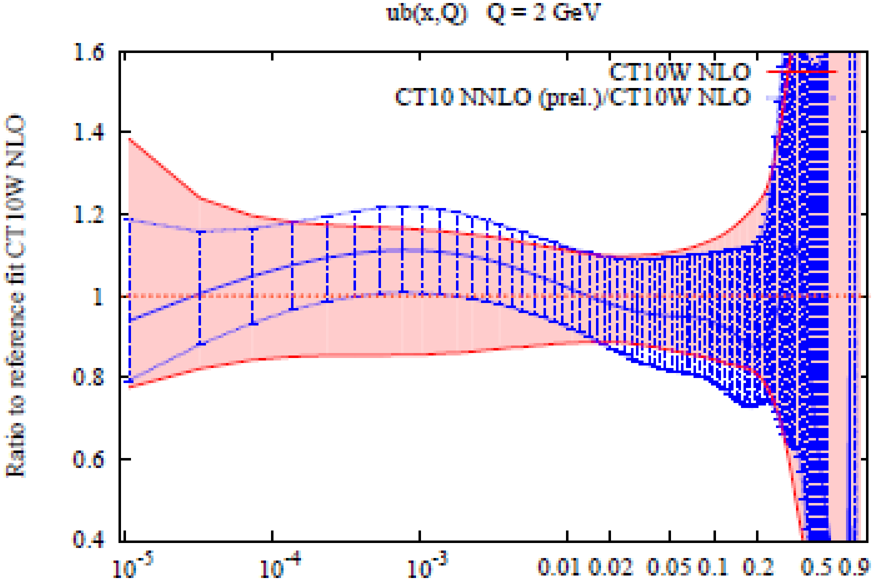

Constraining the gluon PDF in the Higgs production region

(S. Dulat, J. Gao, T.J. Hou, C. Schmidt, et al.)

The goal: find ways to reduce PDF uncertainty on $g(x, Q)$ at $x \sim 0.01$ relevant for Higgs production

- Determine experiments sensitive to $g(x, Q)$ at small x, besides the HERA DIS data
  - LHC jet production, to some extent $t\bar{t}$ production
- Obtain reliable (N)NLO predictions for these processes; benchmarking of MEKS, ApplGrid, FastNLO codes for NLO inclusive jet production
- Understand theoretical and experimental systematic errors on $g(x, Q)$

Correlations of Higgs cross sections to PDFs

GF strongly correlates to
g(x) around x=0.01
@ 125 GeV

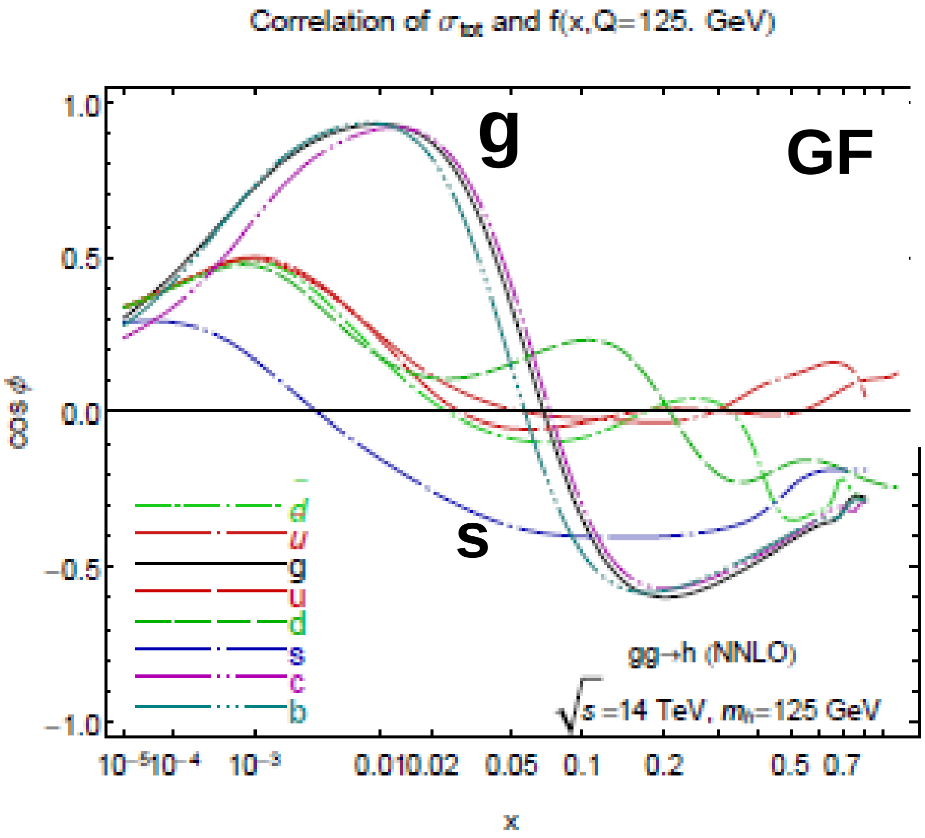

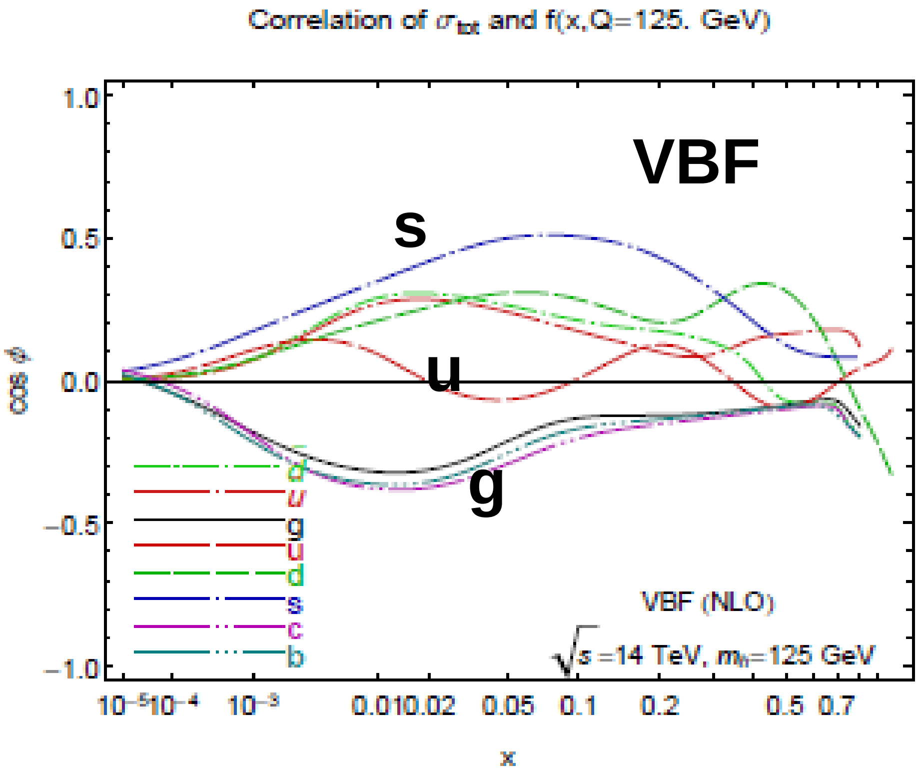

LHC collider energy dependence

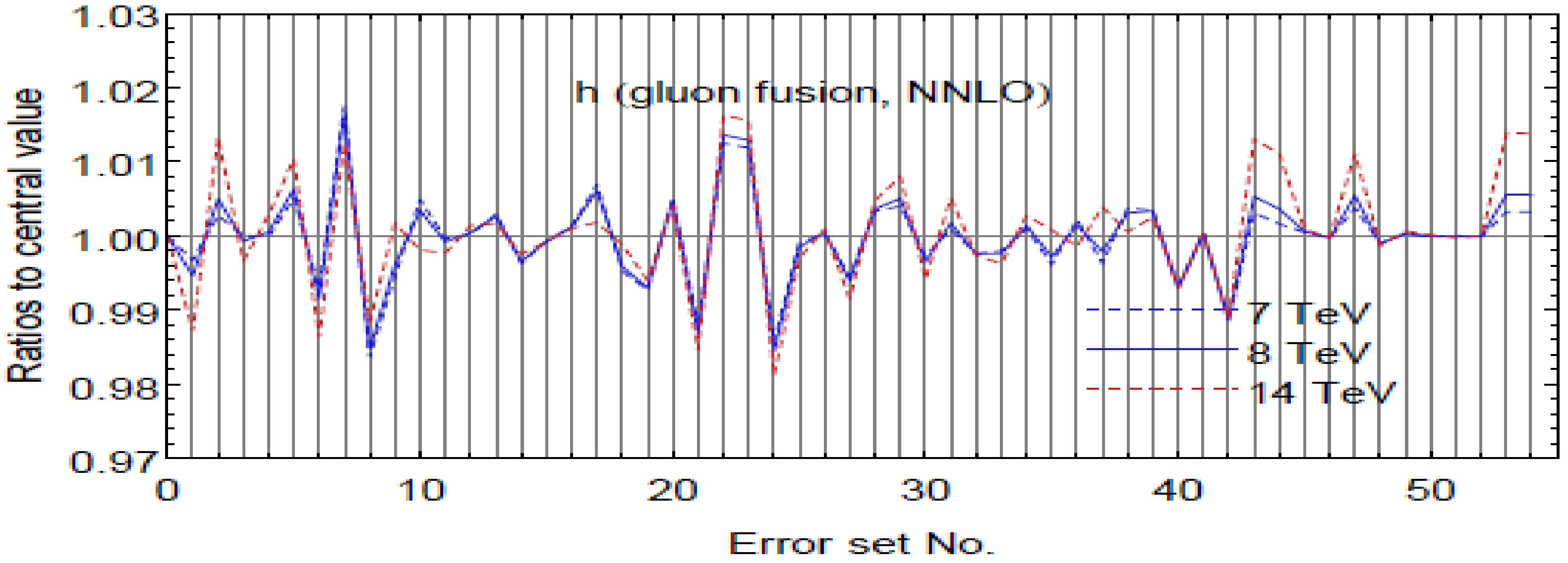

GF

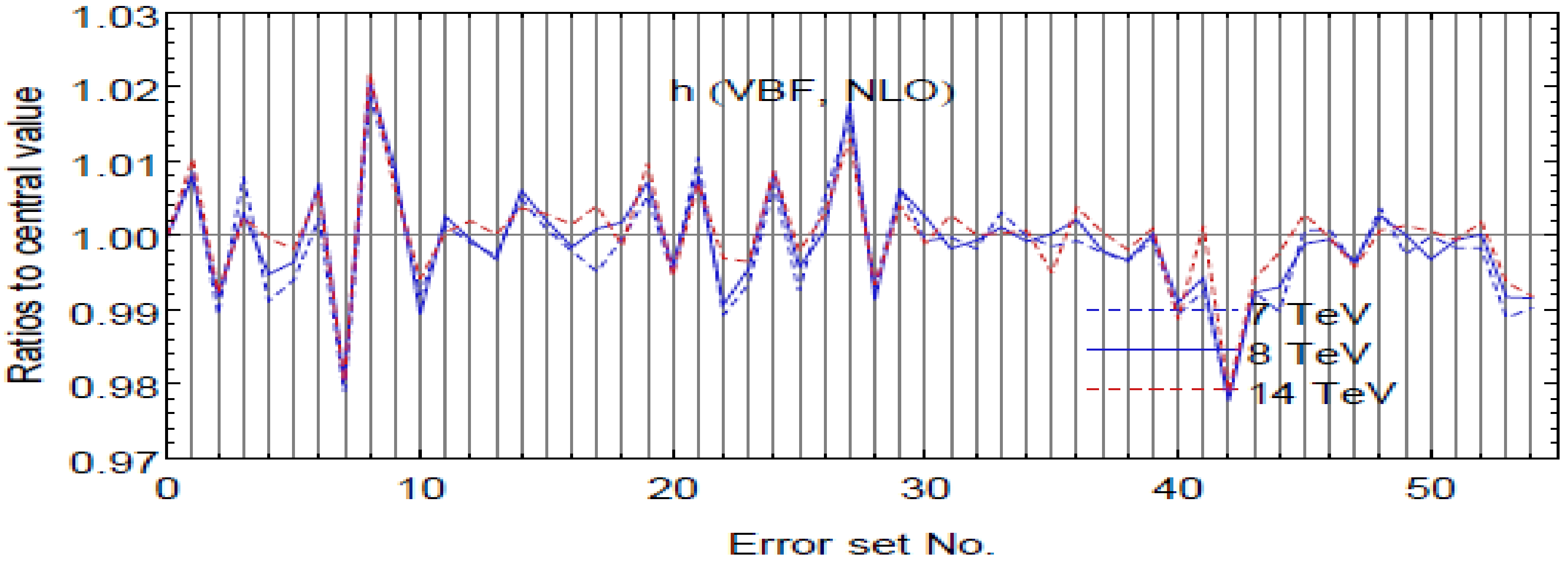

VBF

PDF induced Correlations of $gg \to H$ and $\bar{t}t$ cross sections

$\sigma(t\bar{t})$ and $\sigma(ggH)$ at the LHC are not correlated at the same $\sqrt{s}$, mildly (anti-)correlated at different $\sqrt{s}$

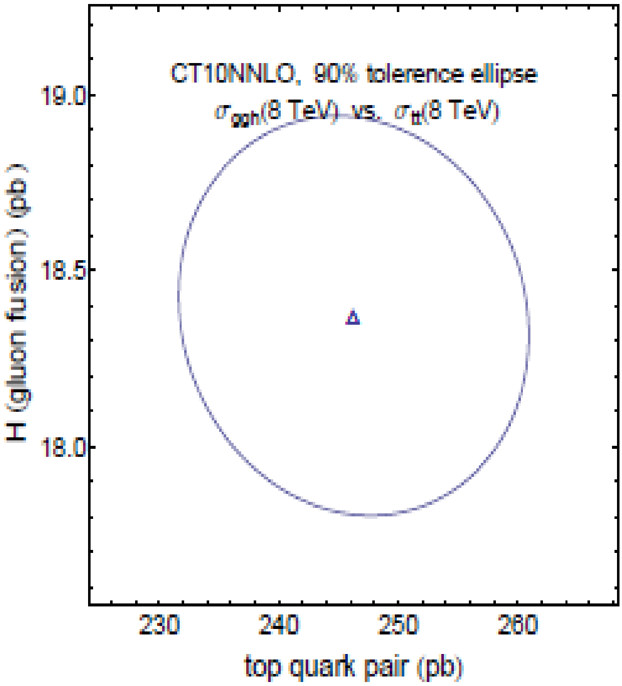

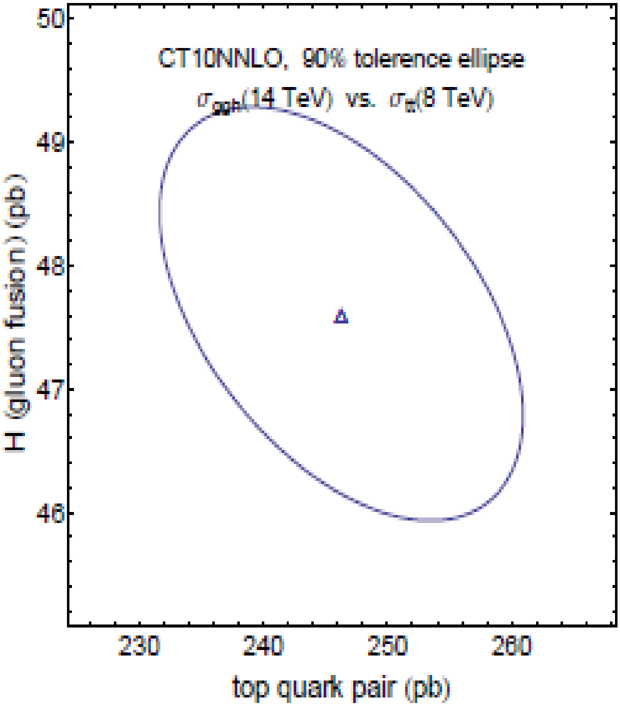

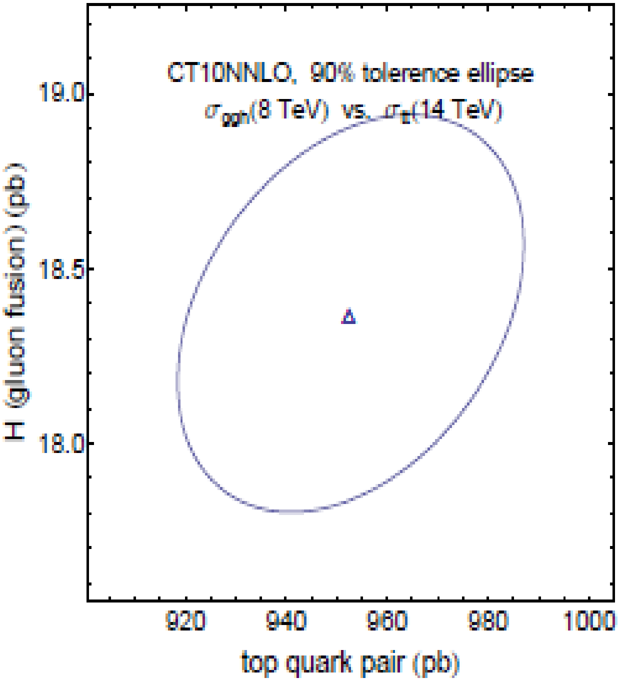

Higgs Boson
Cross Sections
and
Distributions

NNLO cross section and PDF induced uncertainty for gg->H (using ResBos2 program)

$$\Delta\sigma_{\rm PDF} = \frac{1}{2}\sqrt{\sum_{i=1}^{d}\left(\sigma_i^{(+)} - \sigma_i^{(-)}\right)^2}.$$

arXiv:1205.4311 [hep-ph]

M=125 GeV

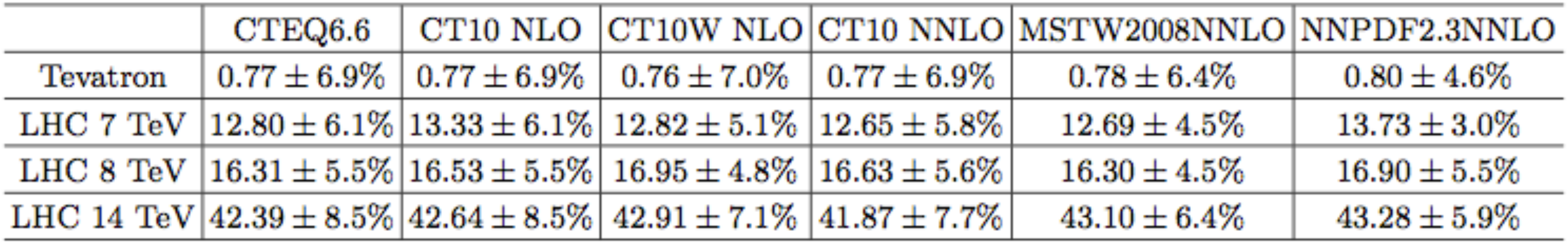

	CTEQ6.6	CT10 NLO	CT10W NLO	CT10 NNLO	MSTW2008NNLO	NNPDF2.3NNLO
Tevatron	$0.77 \pm 6.9\%$	$0.77 \pm 6.9\%$	$0.76 \pm 7.0\%$	$0.77 \pm 6.9\%$	$0.78 \pm 6.4\%$	$0.80 \pm 4.6\%$
LHC 7 TeV	$12.80 \pm 6.1\%$	$13.33 \pm 6.1\%$	$12.82 \pm 5.1\%$	$12.65 \pm 5.8\%$	$12.69 \pm 4.5\%$	$13.73 \pm 3.0\%$
LHC 8 TeV	$16.31 \pm 5.5\%$	$16.53 \pm 5.5\%$	$16.95 \pm 4.8\%$	$16.63 \pm 5.6\%$	$16.30 \pm 4.5\%$	$16.90 \pm 5.5\%$
LHC 14 TeV	$42.39 \pm 8.5\%$	$42.64 \pm 8.5\%$	$42.91 \pm 7.1\%$	$41.87 \pm 7.7\%$	$43.10 \pm 6.4\%$	$43.28 \pm 5.9\%$

TABLE II: The total cross sections (in pb) for Higgs boson production via $g + g \to H + X$ at the Tevatron (1.96 TeV) and LHC (7 TeV, 8 TeV and 14 TeV) by using different PDF sets in ResBos2. The PDF induced uncertainties are estimated at 90% confidence-level, and expressed in the form of percentages.

PDF induced uncertainty at NNLO

- Default $\boldsymbol{\alpha}_s$ values at M_Z are different for

  CT10: 0.118

  MSTW08: 0.120

  NNPDF2.3: 0.119
- They predict different cross sections for GF and VBF processes (not even within each other's error bars, e.g., CT10 vs. NNPDF).

CT10 vs. NNPDF2.3 @NNLO

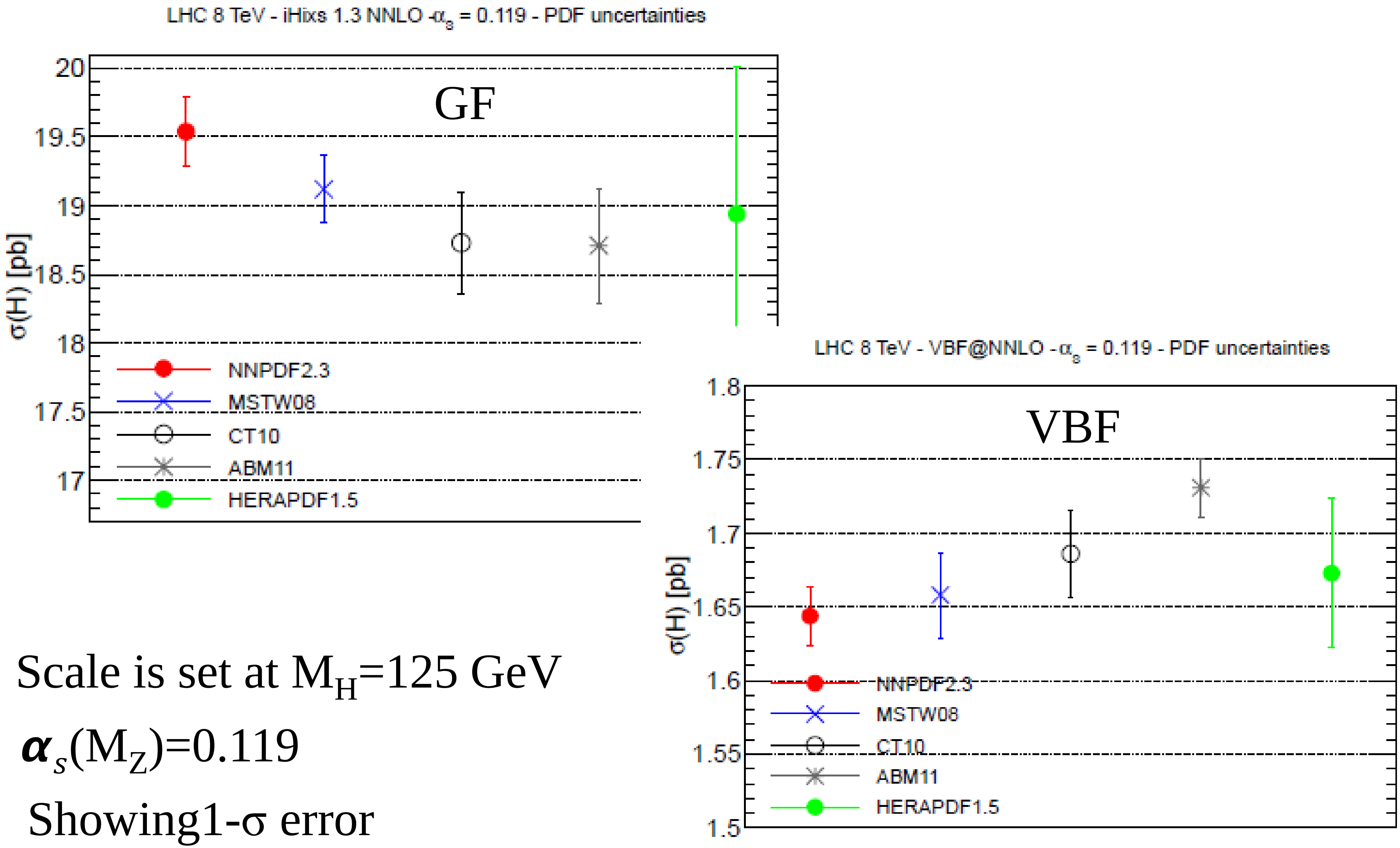

Scale is set at M_H=125 GeV

$\boldsymbol{\alpha}_s(M_Z)$=0.119

Showing1-σ error

Further Checks with LMM

- Apply Lagrangian Multiplier Method (LMM) to study the Higgs boson cross section from gluon fusion processes.
- In contrast to the Hessian Method (HM), the LMM does not require quadratic approximation.
- We find only small increase in the PDF and $\boldsymbol{\alpha}_s$ induced uncertainties, as compared to the HM predictions.

Uncertainties of cross sections for gg->H (using ResBos2 program)

$$\Delta\sigma_{\alpha_s} = \frac{1}{2}\sqrt{[\sigma_0(A_{-2}) - \sigma_0(A_2)]^2}.$$

(at 90% CL, with the range of 0.116 to 0.120)

$$(\Delta\sigma)^2 = (\Delta\sigma_{\mathrm{PDF}})^2 + (\Delta\sigma_{\alpha_s})^2\,.$$

M=125 GeV

CT10-NNLO	σ_0	$\Delta\sigma_{\mathrm{PDF}}$	$\Delta\sigma_{\alpha_s}$	$\Delta\sigma = \sqrt{(\Delta\sigma_{\mathrm{PDF}})^2 + (\Delta\sigma_{\alpha_s})^2}$
Tevatron	0.77	±6.9%	±1.8%	±7.1%
LHC 7 TeV	12.65	±5.8%	±2.5%	±6.3%
LHC 8 TeV	16.63	±5.6%	±3.5%	±6.6%
LHC 14 TeV	41.87	±7.7%	±5.3%	±9.3%

Transverse momentum distribution of Higgs boson via gg->H

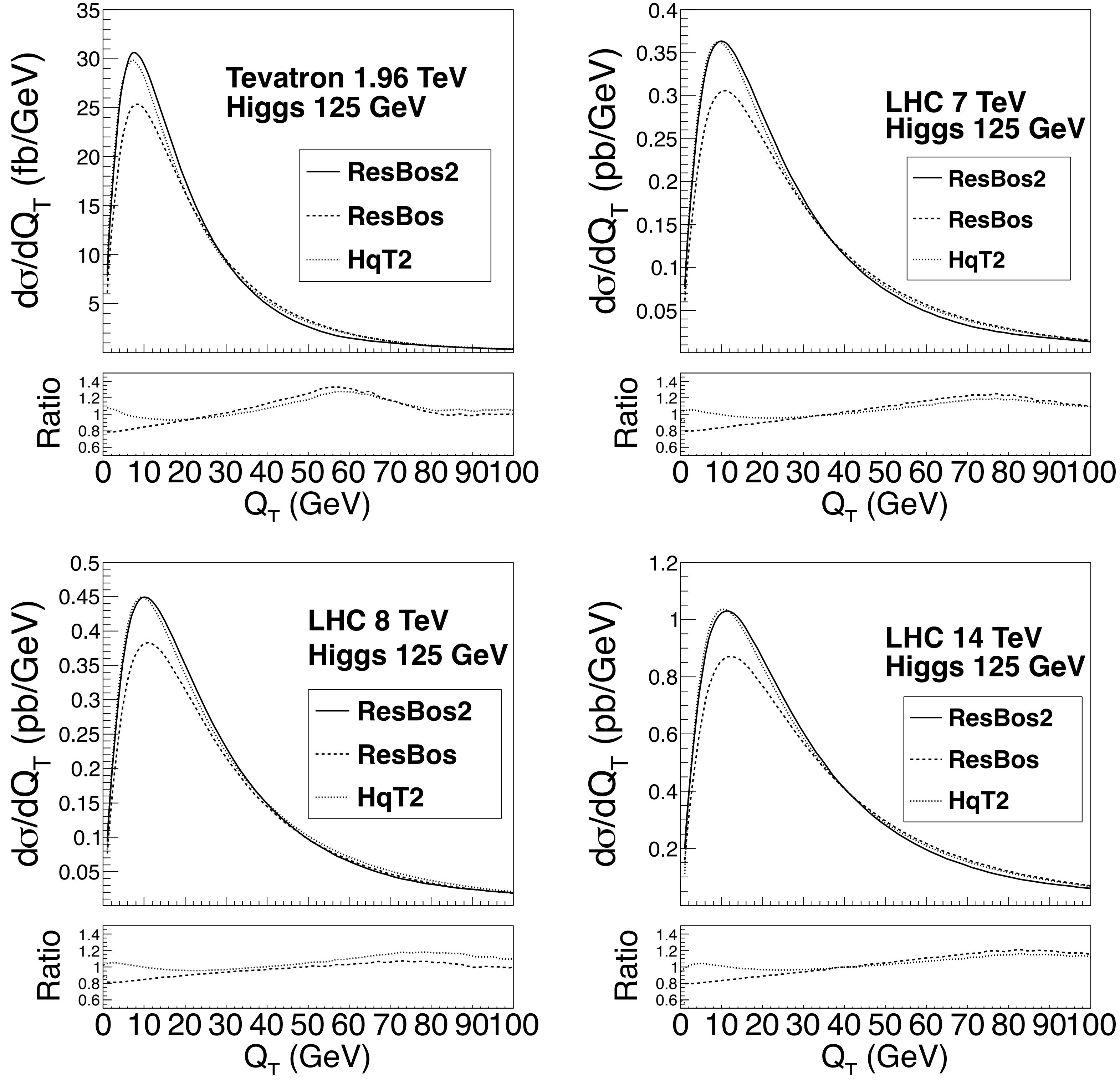

FIG. 1: The different theoretical predictions on the transverse momentum distributions for the Higgs boson production at the Tevatron (1.96 TeV) and the LHC (7 TeV, 8 TeV and 14 TeV). In the bottom of each plot, the ratios to ResBos2 predictions are also shown.

Total NNLO cross section for gg->H (comparing various codes)

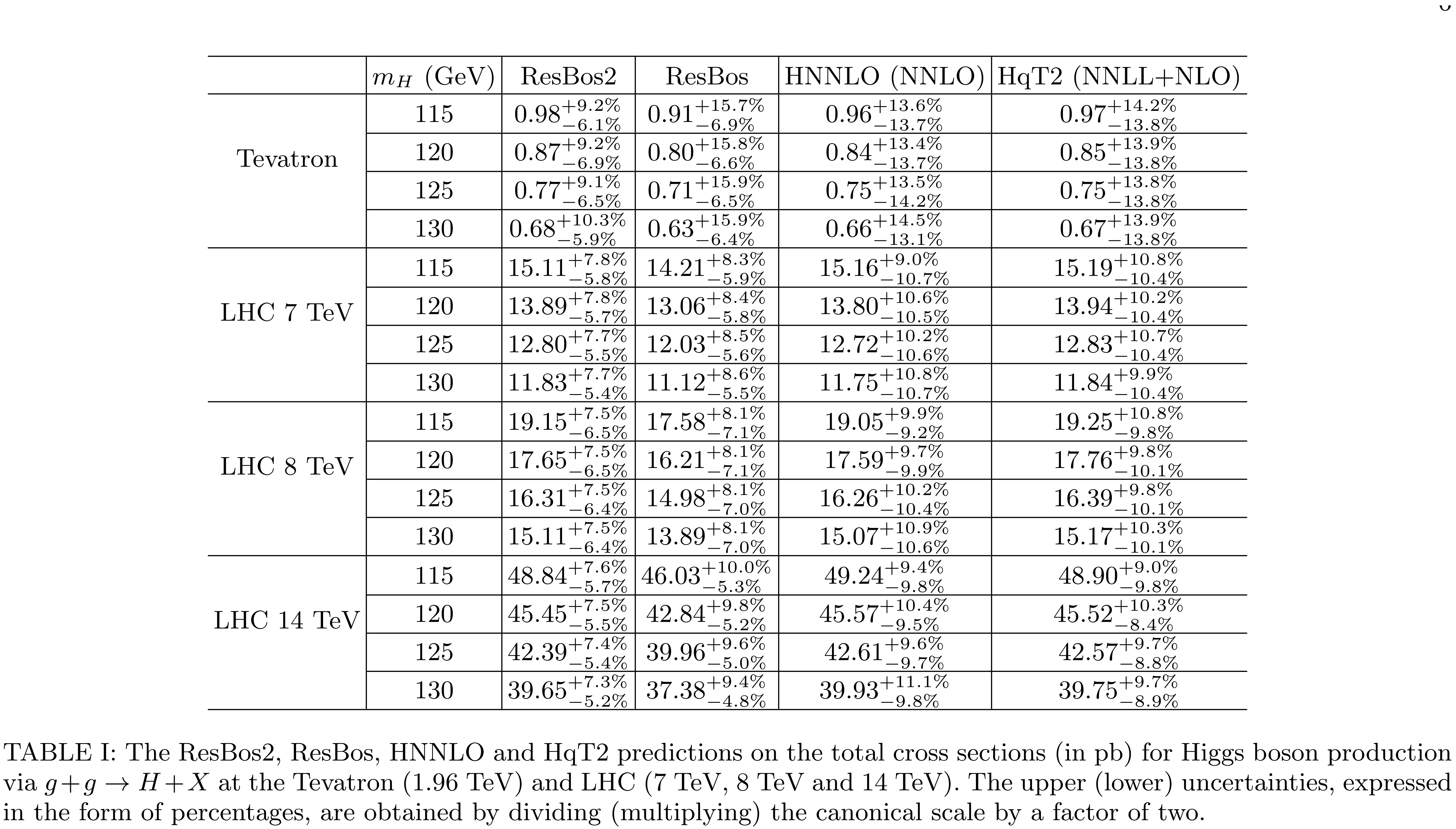

	m_H (GeV)	ResBos2	ResBos	HNNLO (NNLO)	HqT2 (NNLL+NLO)
Tevatron	115	$0.98^{+9.2\%}_{-6.1\%}$	$0.91^{+15.7\%}_{-6.9\%}$	$0.96^{+13.6\%}_{-13.7\%}$	$0.97^{+14.2\%}_{-13.8\%}$
	120	$0.87^{+9.2\%}_{-6.9\%}$	$0.80^{+15.8\%}_{-6.6\%}$	$0.84^{+13.4\%}_{-13.7\%}$	$0.85^{+13.9\%}_{-13.8\%}$
	125	$0.77^{+9.1\%}_{-6.5\%}$	$0.71^{+15.9\%}_{-6.5\%}$	$0.75^{+13.5\%}_{-14.2\%}$	$0.75^{+13.8\%}_{-13.8\%}$
	130	$0.68^{+10.3\%}_{-5.9\%}$	$0.63^{+15.9\%}_{-6.4\%}$	$0.66^{+14.5\%}_{-13.1\%}$	$0.67^{+13.9\%}_{-13.8\%}$
LHC 7 TeV	115	$15.11^{+7.8\%}_{-5.8\%}$	$14.21^{+8.3\%}_{-5.9\%}$	$15.16^{+9.0\%}_{-10.7\%}$	$15.19^{+10.8\%}_{-10.4\%}$
	120	$13.89^{+7.8\%}_{-5.7\%}$	$13.06^{+8.4\%}_{-5.8\%}$	$13.80^{+10.6\%}_{-10.5\%}$	$13.94^{+10.2\%}_{-10.4\%}$
	125	$12.80^{+7.7\%}_{-5.5\%}$	$12.03^{+8.5\%}_{-5.6\%}$	$12.72^{+10.2\%}_{-10.6\%}$	$12.83^{+10.7\%}_{-10.4\%}$
	130	$11.83^{+7.7\%}_{-5.4\%}$	$11.12^{+8.6\%}_{-5.5\%}$	$11.75^{+10.8\%}_{-10.7\%}$	$11.84^{+9.9\%}_{-10.4\%}$
LHC 8 TeV	115	$19.15^{+7.5\%}_{-6.5\%}$	$17.58^{+8.1\%}_{-7.1\%}$	$19.05^{+9.9\%}_{-9.2\%}$	$19.25^{+10.8\%}_{-9.8\%}$
	120	$17.65^{+7.5\%}_{-6.5\%}$	$16.21^{+8.1\%}_{-7.1\%}$	$17.59^{+9.7\%}_{-9.9\%}$	$17.76^{+9.8\%}_{-10.1\%}$
	125	$16.31^{+7.5\%}_{-6.4\%}$	$14.98^{+8.1\%}_{-7.0\%}$	$16.26^{+10.2\%}_{-10.4\%}$	$16.39^{+9.8\%}_{-10.1\%}$
	130	$15.11^{+7.5\%}_{-6.4\%}$	$13.89^{+8.1\%}_{-7.0\%}$	$15.07^{+10.9\%}_{-10.6\%}$	$15.17^{+10.3\%}_{-10.1\%}$
LHC 14 TeV	115	$48.84^{+7.6\%}_{-5.7\%}$	$46.03^{+10.0\%}_{-5.3\%}$	$49.24^{+9.4\%}_{-9.8\%}$	$48.90^{+9.0\%}_{-9.8\%}$
	120	$45.45^{+7.5\%}_{-5.5\%}$	$42.84^{+9.8\%}_{-5.2\%}$	$45.57^{+10.4\%}_{-9.5\%}$	$45.52^{+10.3\%}_{-8.4\%}$
	125	$42.39^{+7.4\%}_{-5.4\%}$	$39.96^{+9.6\%}_{-5.0\%}$	$42.61^{+9.6\%}_{-9.7\%}$	$42.57^{+9.7\%}_{-8.8\%}$
	130	$39.65^{+7.3\%}_{-5.2\%}$	$37.38^{+9.4\%}_{-4.8\%}$	$39.93^{+11.1\%}_{-9.8\%}$	$39.75^{+9.7\%}_{-8.9\%}$

TABLE I: The ResBos2, ResBos, HNNLO and HqT2 predictions on the total cross sections (in pb) for Higgs boson production via $g+g \to H+X$ at the Tevatron (1.96 TeV) and LHC (7 TeV, 8 TeV and 14 TeV). The upper (lower) uncertainties, expressed in the form of percentages, are obtained by dividing (multiplying) the canonical scale by a factor of two.

Jets in QCD

Two-jet Events:
Quark – anti-quark Pair Production

Typical $e^+ e^-$ event with hadron final states:

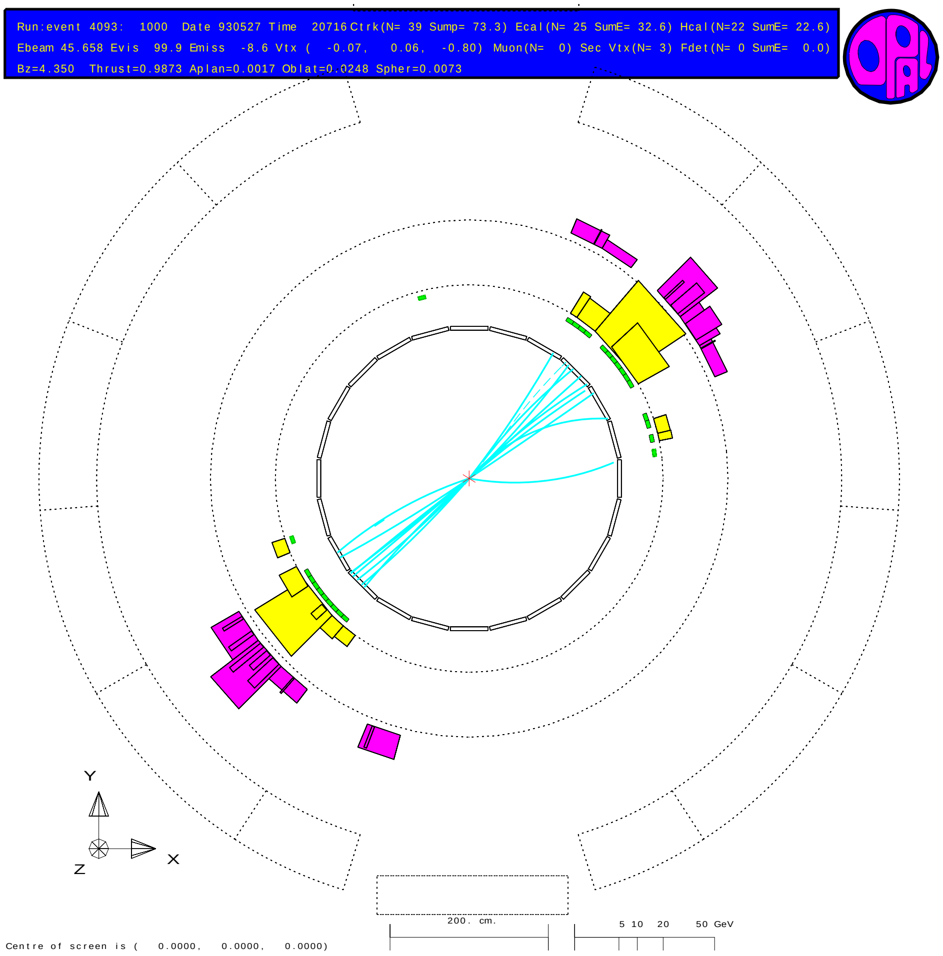

```
Run:event 4093:  1000  Date 930527 Time  20716 Ctrk(N= 39 Sump= 73.3) Ecal(N= 25 SumE= 32.6) Hcal(N=22 SumE= 22.6)
Ebeam 45.658 Evis  99.9 Emiss  -8.6 Vtx (  -0.07,   0.06,  -0.80) Muon(N=  0) Sec Vtx(N= 3) Fdet(N= 0 SumE=  0.0)
Bz=4.350  Thrust=0.9873 Aplan=0.0017 Oblat=0.0248 Spher=0.0073
```

Parton process underlying 2-jet events

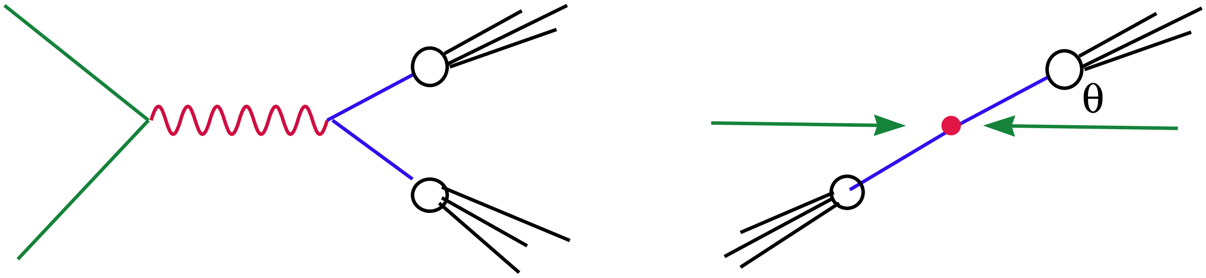

3 Jet Events and the Gluon Parton

A typical 3-jet event (∼ 10% prob.):

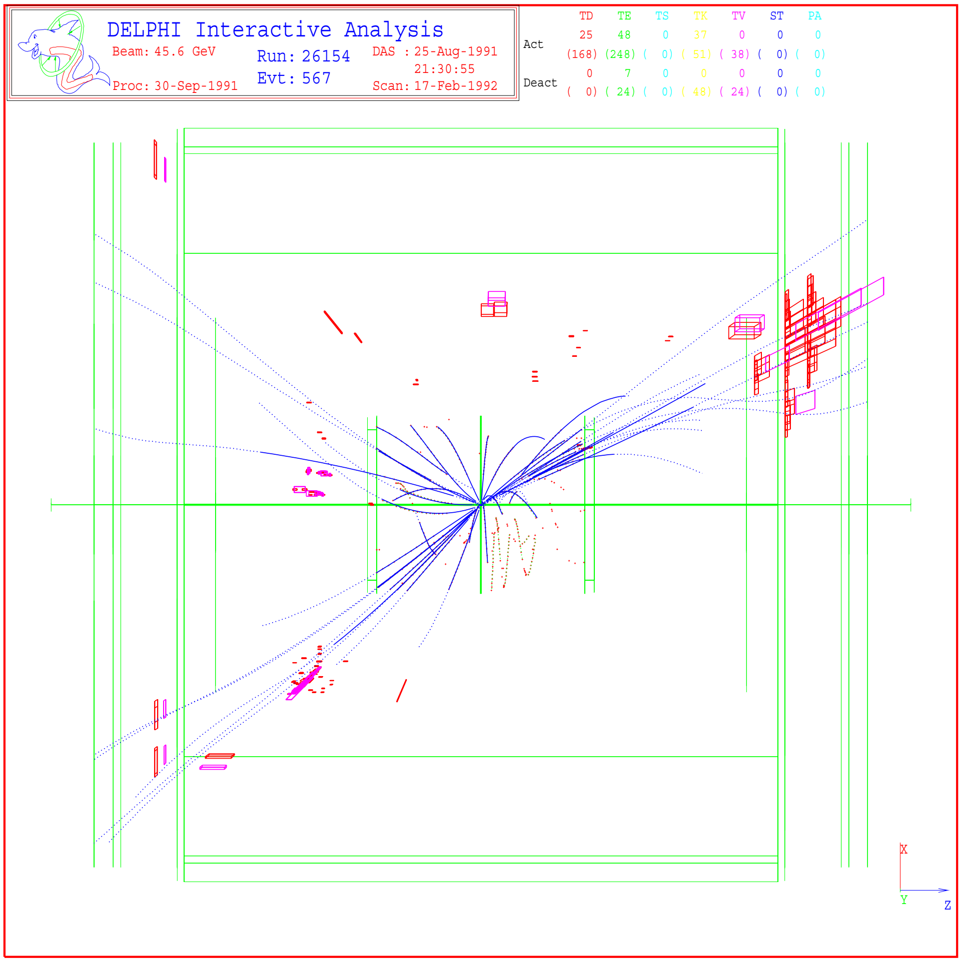

DELPHI Interactive Analysis

Beam: 45.6 GeV

Run: 26154

DAS : 25-Aug-1991 21:30:55

Proc: 30-Sep-1991

Evt: 567

Scan: 17-Feb-1992

	TD	TE	TS	TK	TV	ST	PA
Act	25	48	0	37	0	0	0
	(168)	(248)	(0)	(51)	(38)	(0)	(0)
Deact	0	7	0	0	0	0	0
	(0)	(24)	(0)	(48)	(24)	(0)	(0)

Parton process underlying 3-jet events

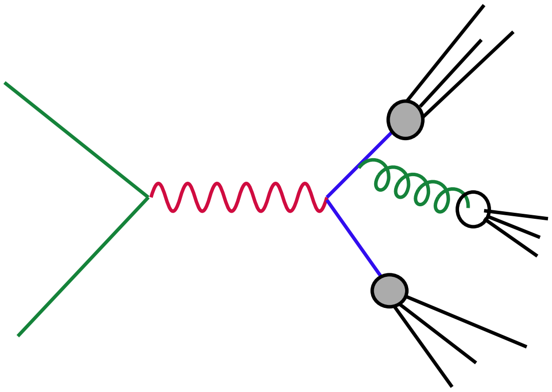

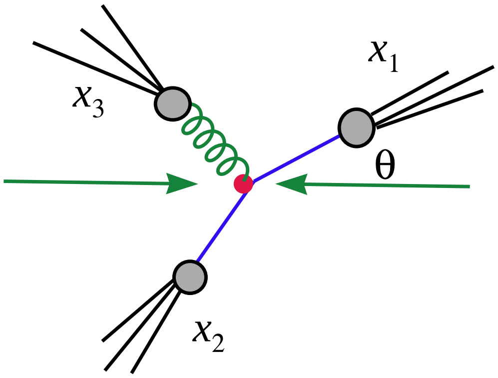

Outlines

- Motivation
- Jet function
- Resummation
- Jet energy profile
- Jet mass distribution
- Summary

arXiv: 1107.4535 [hep-ph]
1206.1344

Jet Production

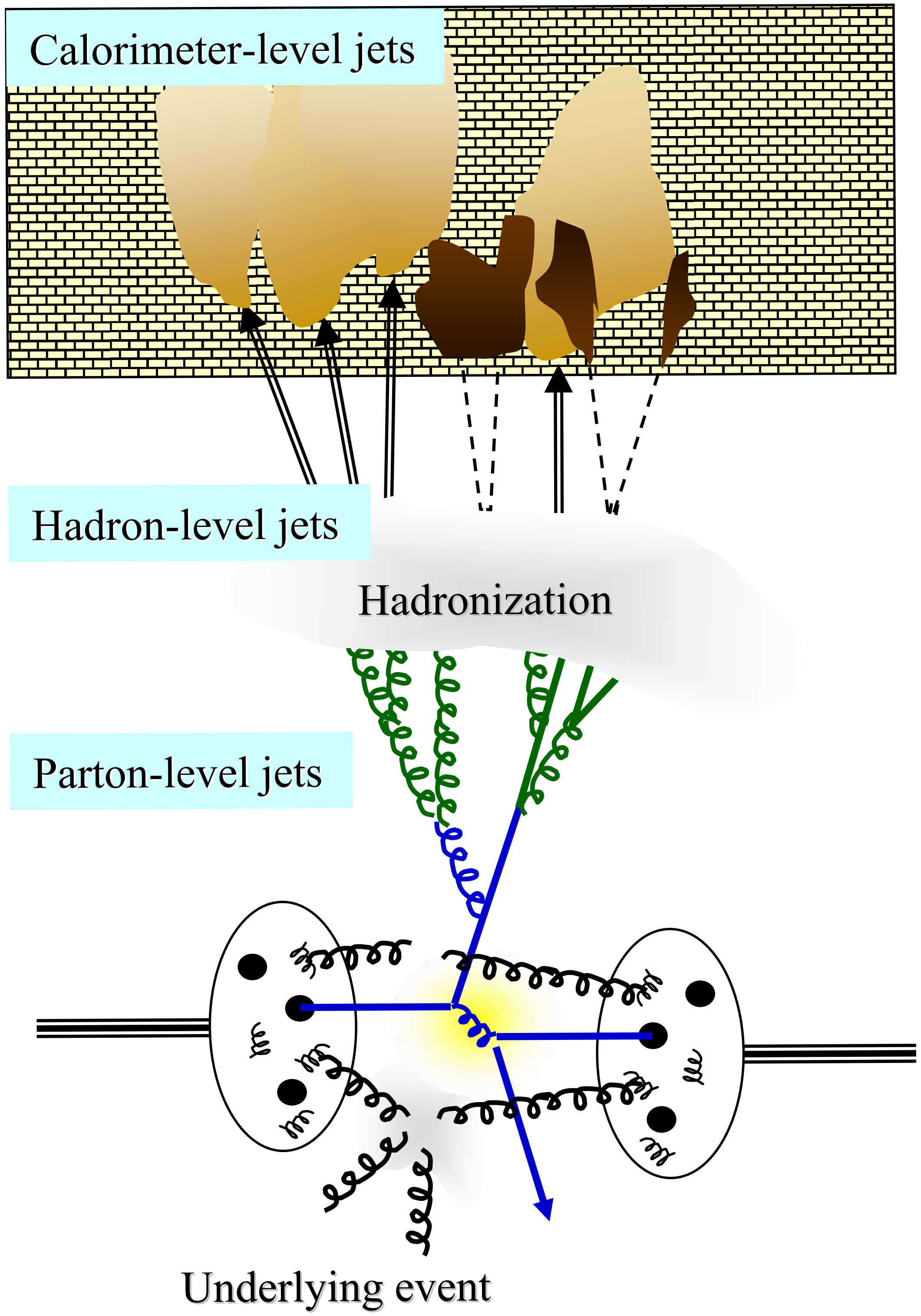

- ☐ Jets are collimated spray of hadrons originating from quarks/gluons coming from the hard scattering

  (Jets are experimental signatures of quarks and gluons)

- ☐ Unlike photons, leptons etc, jets have to be defined by an algorithm for quantitative studies

- ☐ Need a well-defined algorithm that gives close relationship between calorimeter-level jets, hadron-level jets, and parton-level jets

Jet Clustering Algorithms

- ☐ Algorithms should be well-defined so that they map the experimental measurements with theoretical calculations as close as possible.
- ☐ Different algorithms with different parameters provide different sets of resulting jets.

“Simple” event

(all algorithms give essentially the same results)

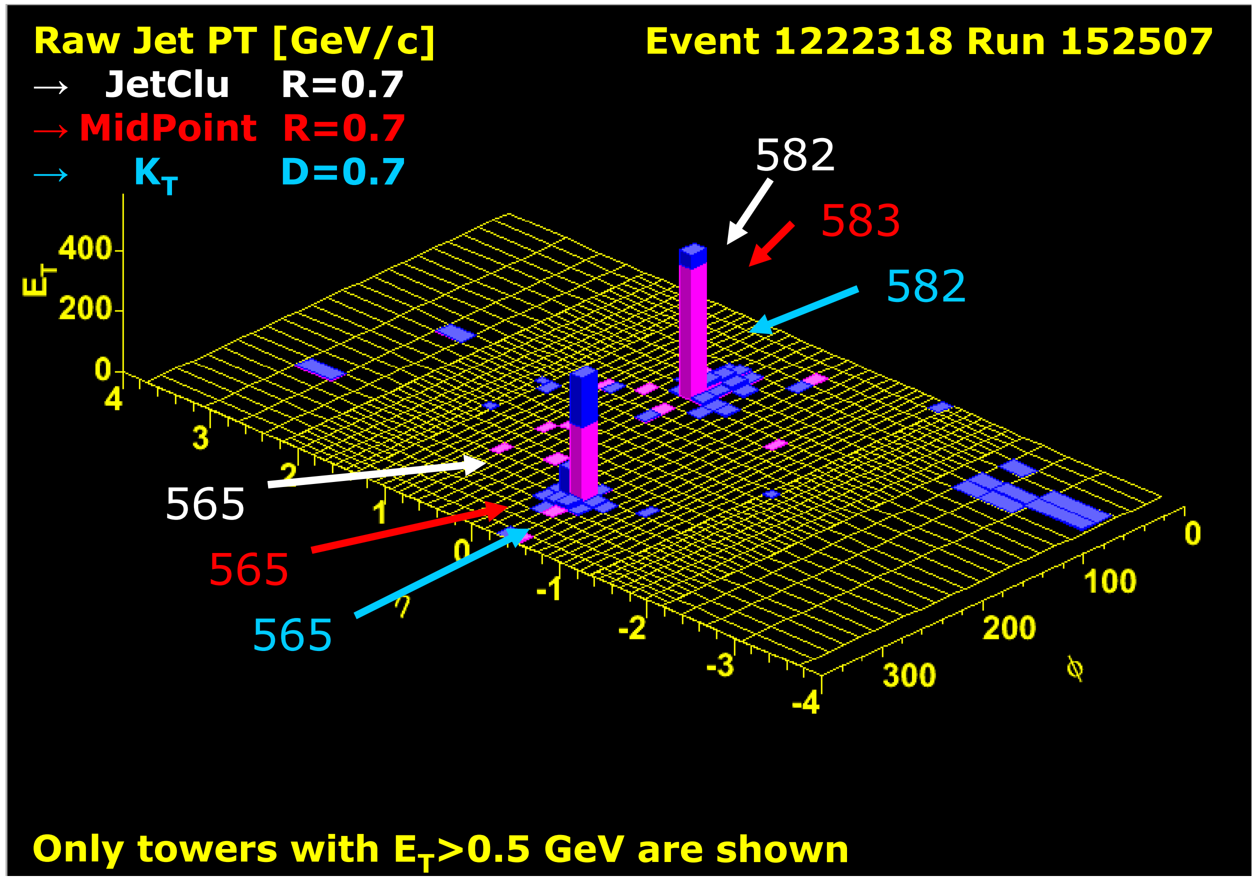

“Complicated” event

(Resulting jets depend on jet algorithms)

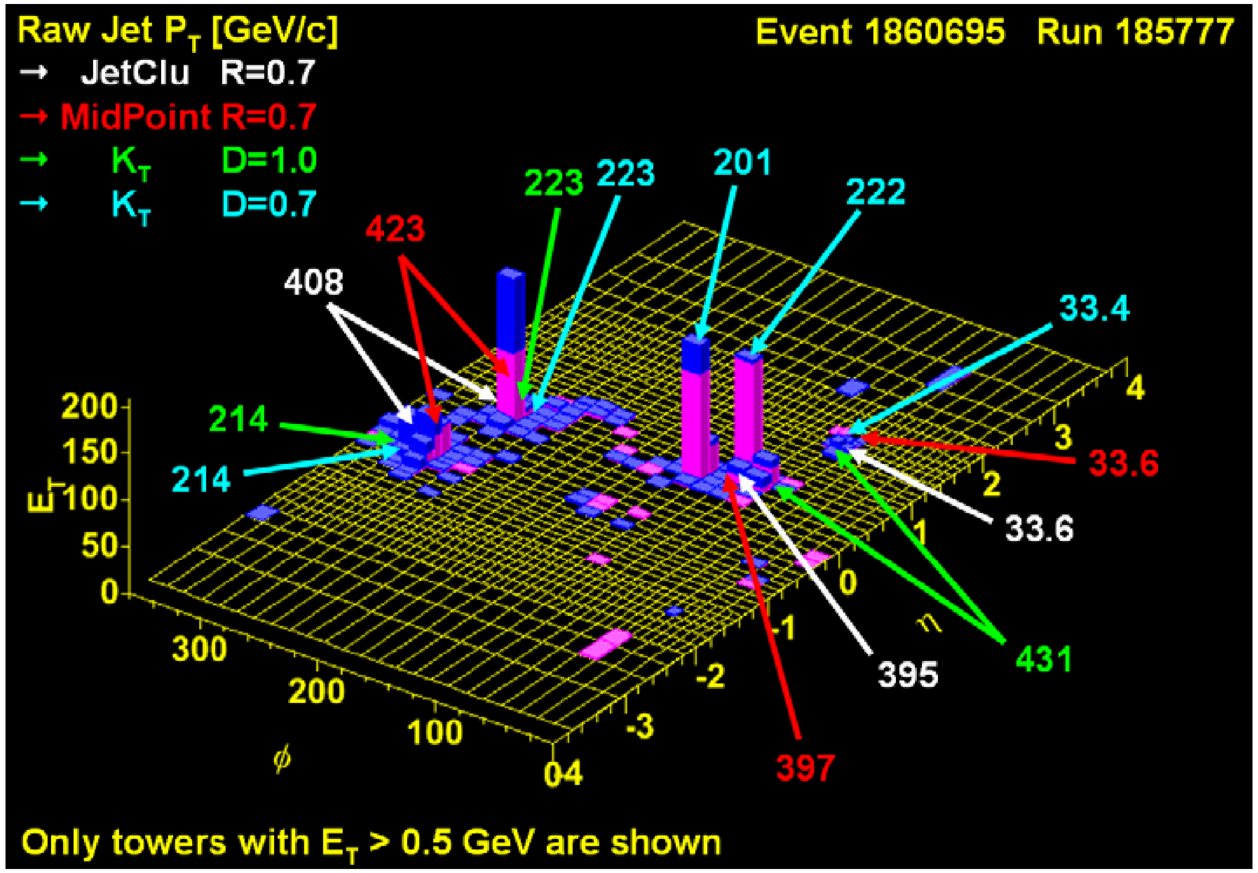

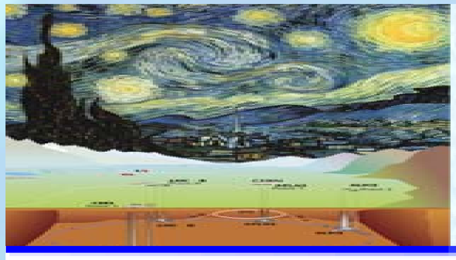

Objects at the LHC

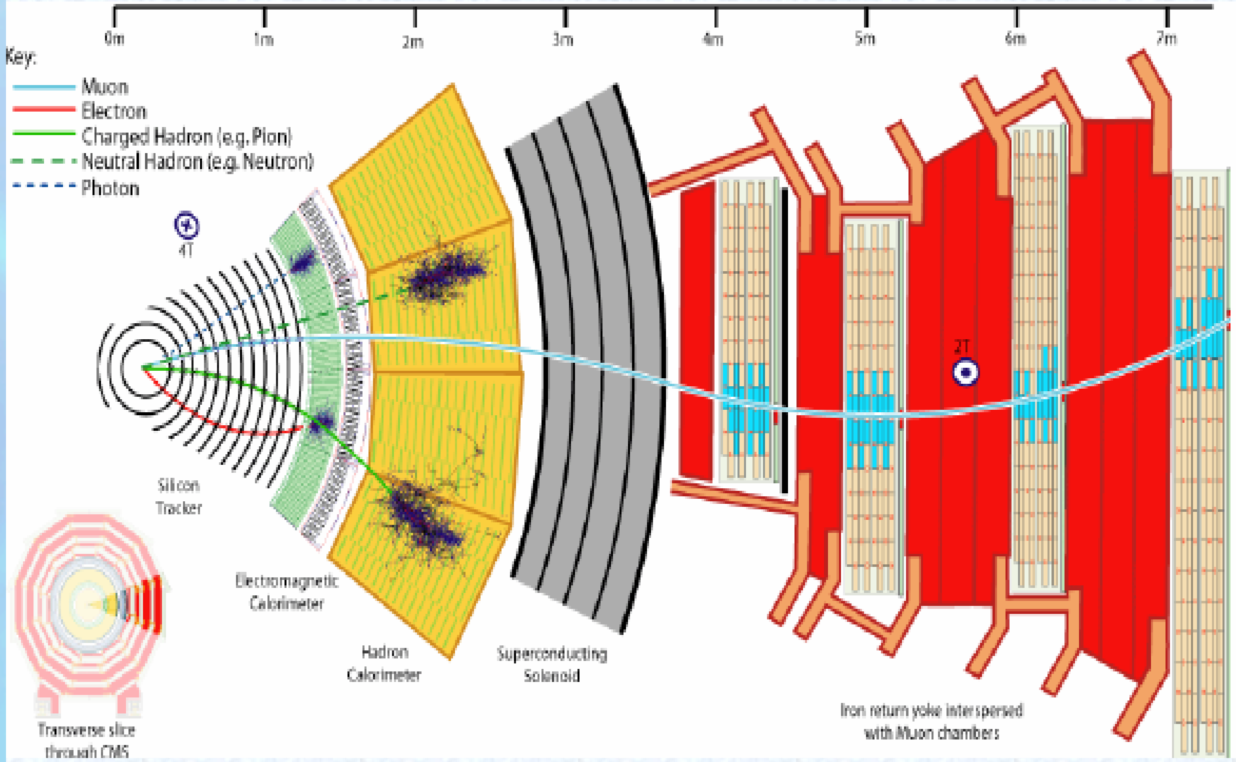

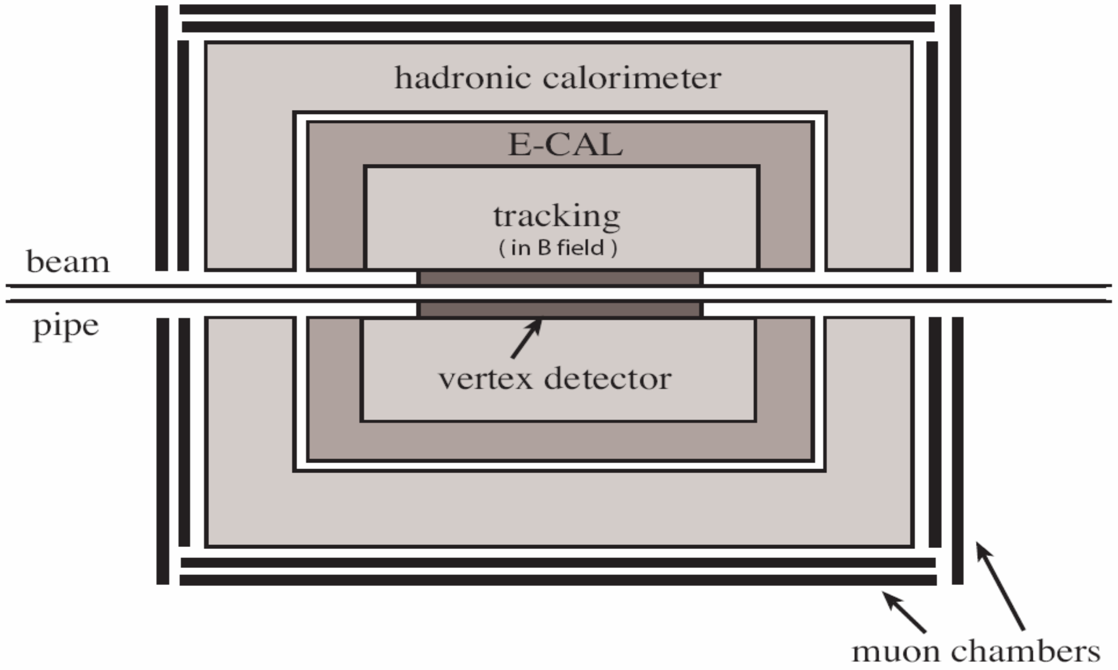

- objects
  - Photons: no tack, energy in ECAL, no energy in HCAL
  - Electrons: tack, energy in ECAL, no energy in HCAL
  - Muons: tack, tack in the muon chamber
  - Jets: tracks and energy in the calorimeter
  - Missing transverse enegy (MET) : inferred from the conservation of momentum in a plane perpendicular to the beam direction

- Typical variables
  - Transverse momentum: p_T
  - Azimuth angle: ϕ
  - Pseudorapidity: $\eta = -\ln(tg(\theta/2))$
  - Relative isolation: $\Delta R=(\Delta \phi^2+ \Delta \eta^2)^{1/2}$

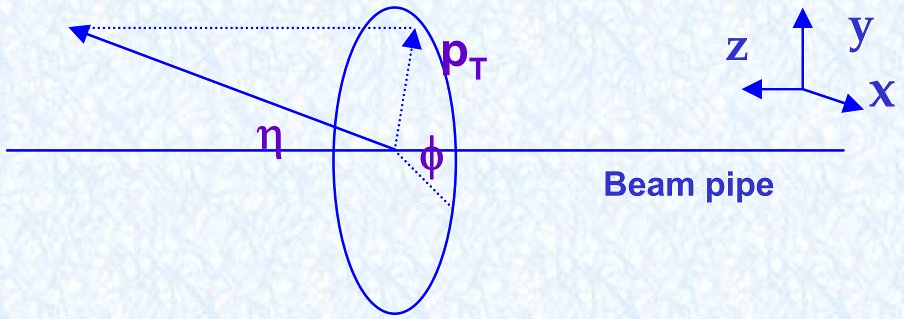

Jet “Definitions” - Algorithms at CDF

- ☐ Cone algorithms (JetClu, Midpoint)
  - Cluster objects based on their proximity in y(η)-ϕ space
  - Starting from seeds (calorimeter towers/particles above threshold), find stable cones (p_T-weighted centroid = geometric center).
  - Seeds have been necessary for speed, but source of infrared unsafety.
  - In Run II QCD studies, often use “Midpoint” algorithm, i.e. look for stable cones from middle points between stable cones → Infrared safety restored up to NNLO.
  - Stable cones sometime overlaps → merge cones when overlap > 75%

Infrared unsafety:

soft parton emission changes jet clustering

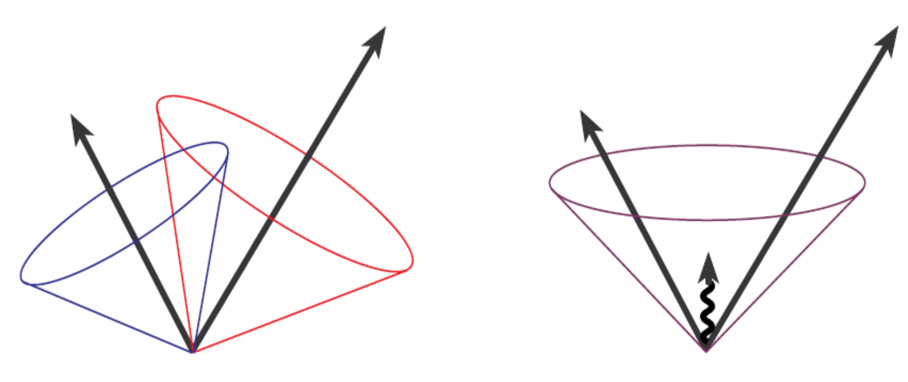

N.B., Recently a new version of seedless algorithm (SIScone) became available which is fast enough for practical use.

Jet "Definitions" - Algorithms at CDF

k_T algorithm

- Cluster objects in order of increasing their relative transverse momentum (k_T)
  - ☐ $d_{ii} = p^2_{T,i}, \quad d_{ij} = \min(p^2_{T,i}, p^2_{T,j}) \dfrac{\Delta R^2}{D^2}$

  until all objects become part of jets
- D parameter controls merging termination and characterizes size of resulting jets

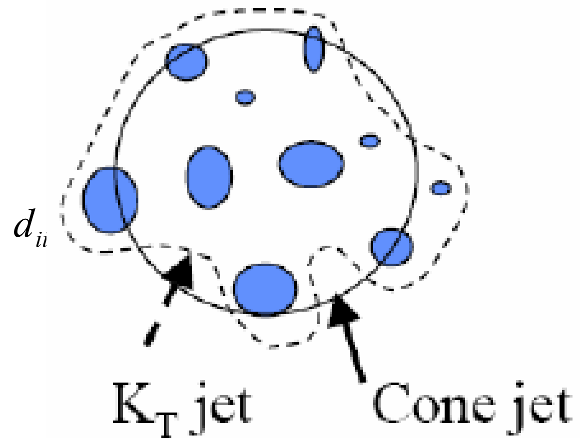

- No issue of splitting/merging. Infrared and collinear safe to all orders of QCD.
- Every object assigned to a jet: concerns about vacuuming up too many particles.
- Successful at LEP & HERA, but relatively new at the hadron colliders
  - ☐ More difficult environment (underlying event, multiple $p\bar{p}$ interactions…)

Other clustering algorithm

- p=1
  - the regular k_T jet algorithm
- p=0
  - Cambridge-Aachen algorithm
- p=-1
  - anti-k_T jet algorithm →
  - Cacciari, Salam, Soyez ’08
  - also P-A Delsart ’07
  - soft particles will first cluster with hard particles before clustering among themselves
  - no split/merge
  - leads mostly to constant area hard jets

$$d_{ij} = \min\left(p_{T,i}^{2p}, p_{T,j}^{2p}\right)\frac{\Delta R_{ij}^2}{D^2}$$

$$d_{ii} = p_{T,i}^{2p}$$

- #1 algorithm for ATLAS, CMS

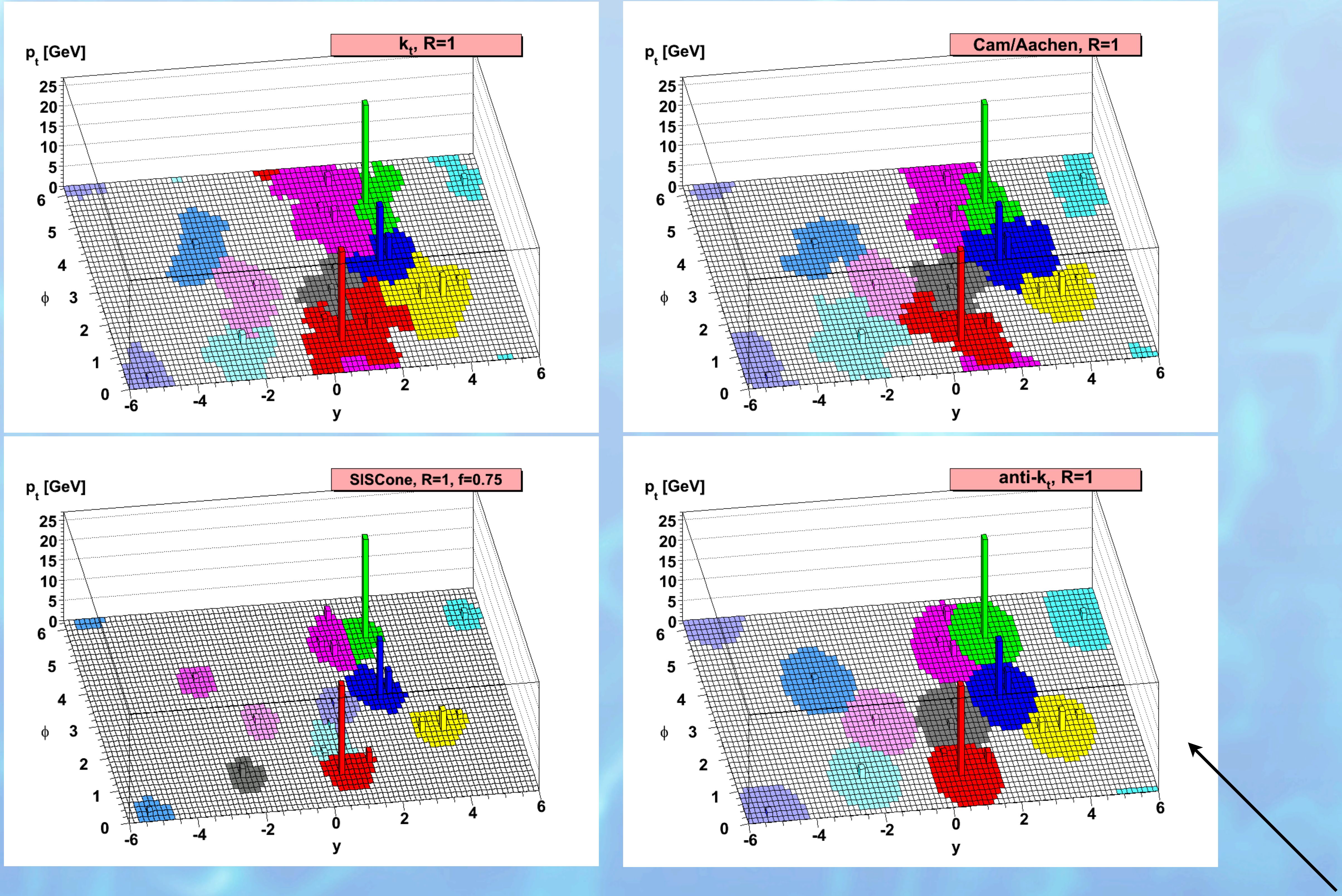

Anti-Kt jet clustering algorithm

arXiv: 0802.1189
Cacciari, Salam, Soyez

Jet Finding

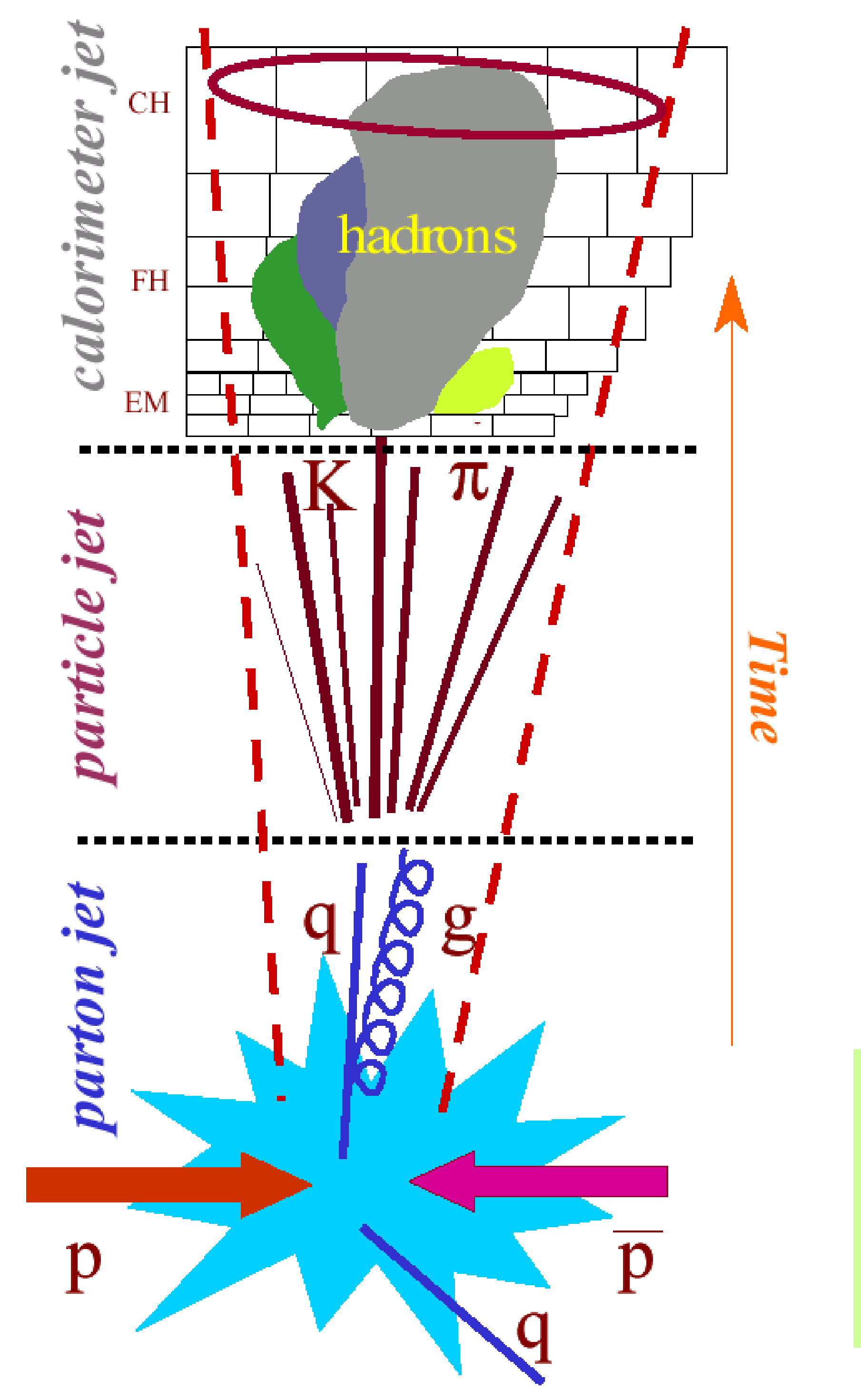

- **Calorimeter jet (cone)**
  - ◆ jet is a collection of energy deposits with a given cone *R*: $R = \sqrt{\Delta\varphi^2 + \Delta\eta^2}$
  - ◆ cone direction maximizes the total E_T of the jet
  - ◆ various clustering algorithms

➜ correct for finite energy resolution

➜ subtract underlying event

➜ add out of cone energy

- **Particle jet**
  - ◆ a spread of particles running roughly in the same direction as the parton after hadronization

Jet Fragmentation Studies

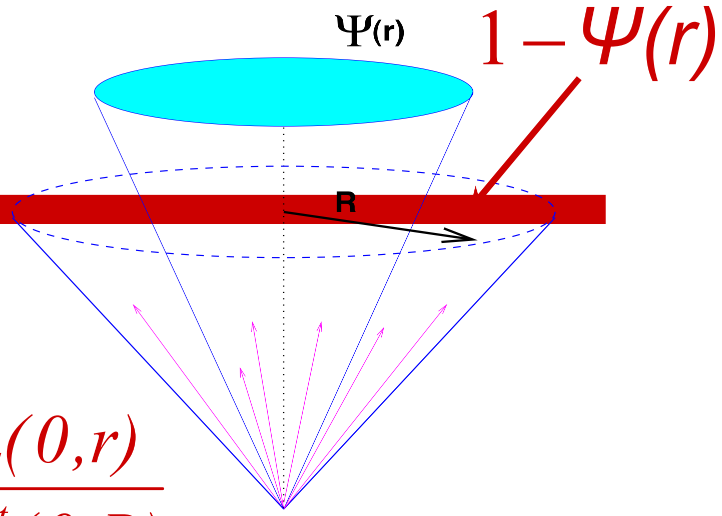

Need to simulate jets properly: particle composition, multiplicity, momentum distribution etc

$$\Psi(r) = \frac{1}{N_{jets}} \Sigma_{jets} \frac{p_T(0,r)}{p_T^{jet}(0,R)}$$

e.g. **$\mathbf{2}$ hadrons with $p_T = 50$ GeV/c**
$\neq 20$ hadrons with $p_T = 5$ GeV/c

due to calorimeter non-linearity

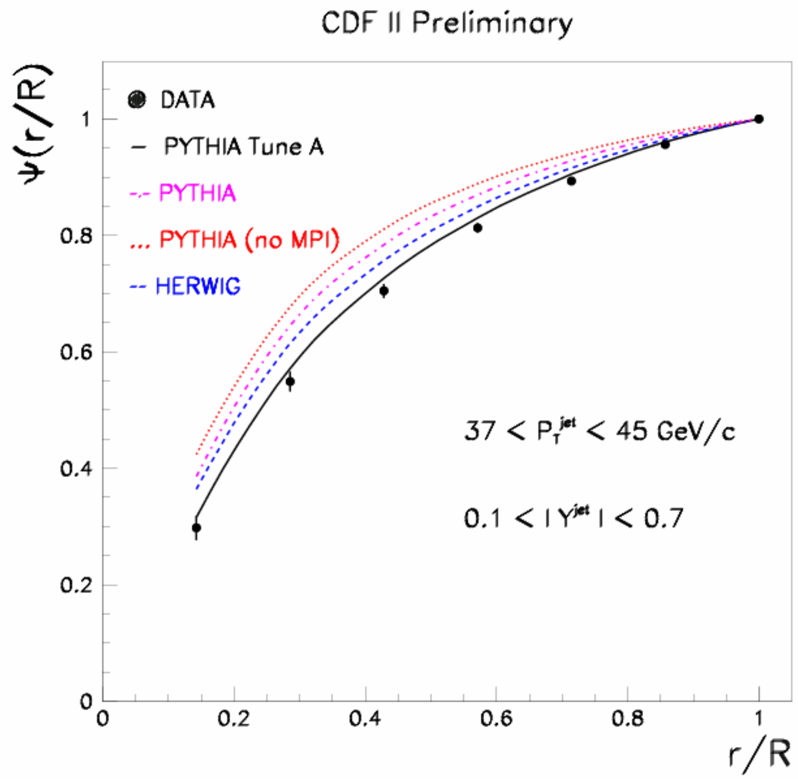

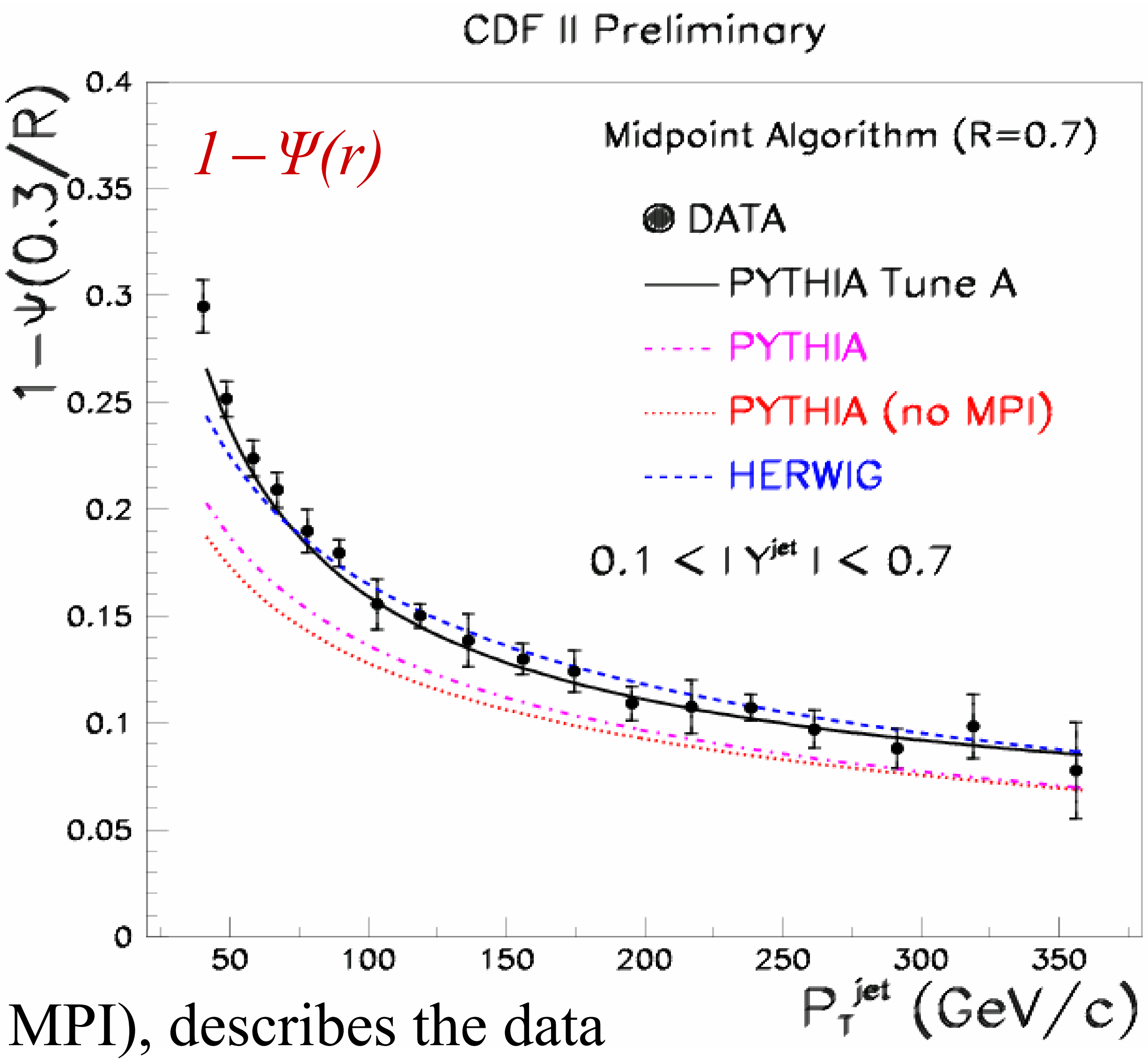

Tuned MC, PYTHIA Tune A (enhanced ISR + MPI), describes the data

We know how to model the jet fragmentation reasonably well !!

Various Theoretical Predictions

Various Theoretical Predictions

- **Event Generators**: leading log radiations, hadronization, underlying events, etc.
- **Fixed order QCD calculation**: finite number of soft/collinear radiations
- **Resummation**: all order soft/collinear radiations

NLO

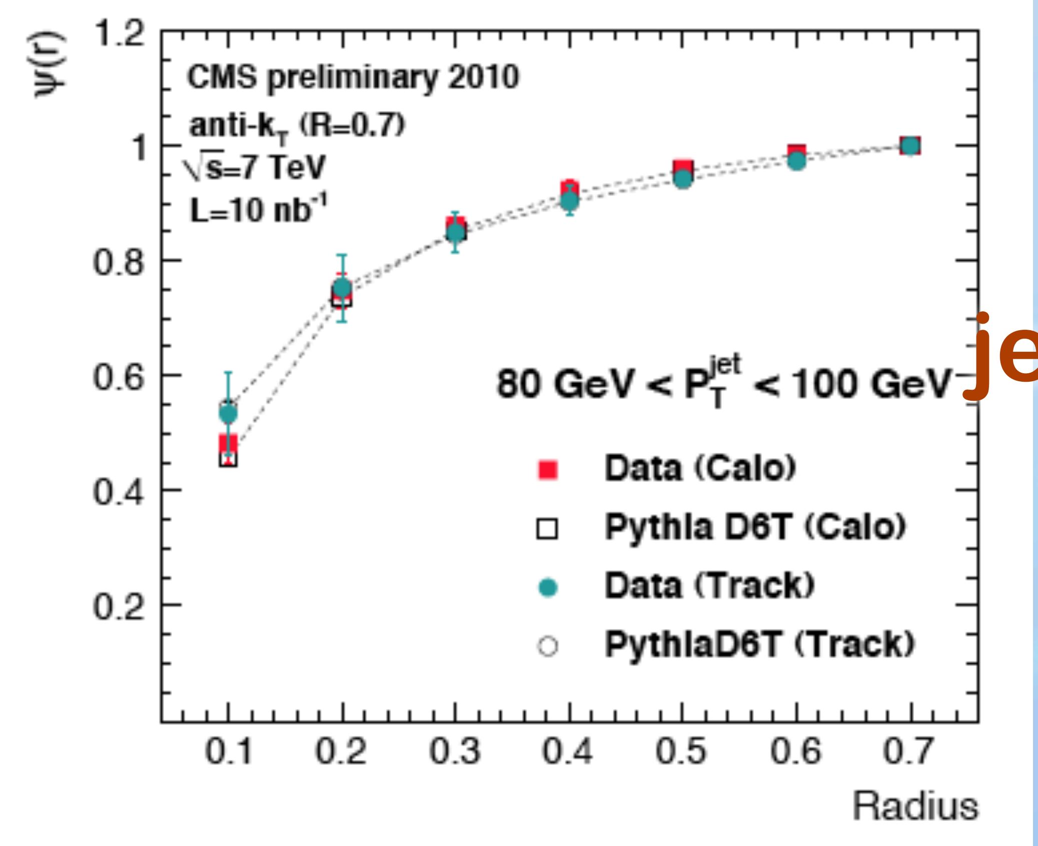

jet energy profile

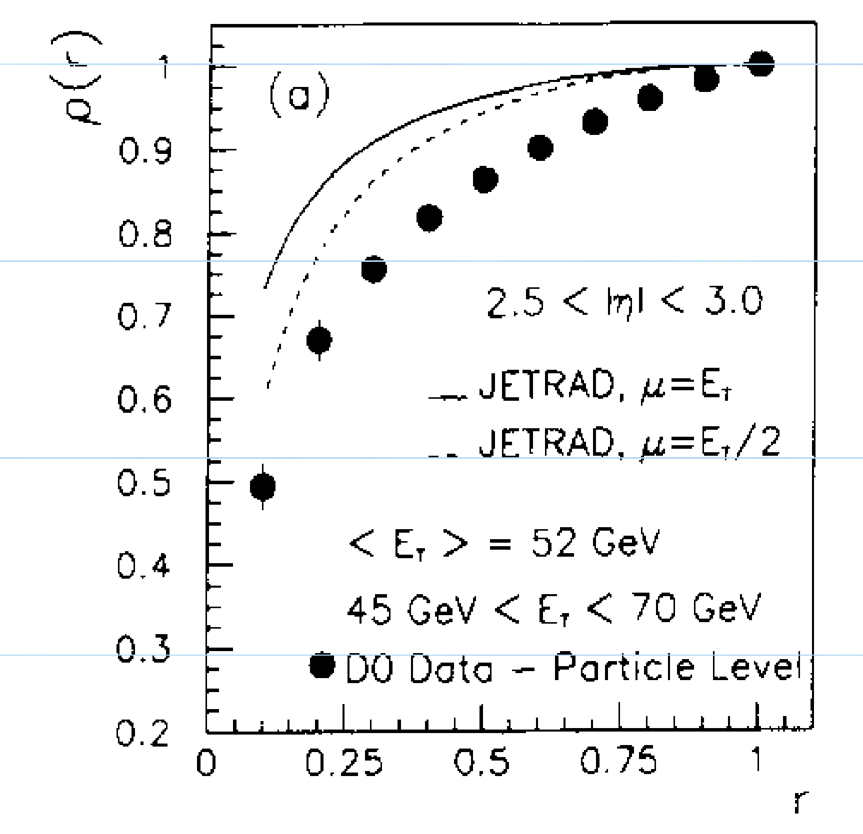

D0 Collaboration/Physics Letters B 357(1995) 500-508

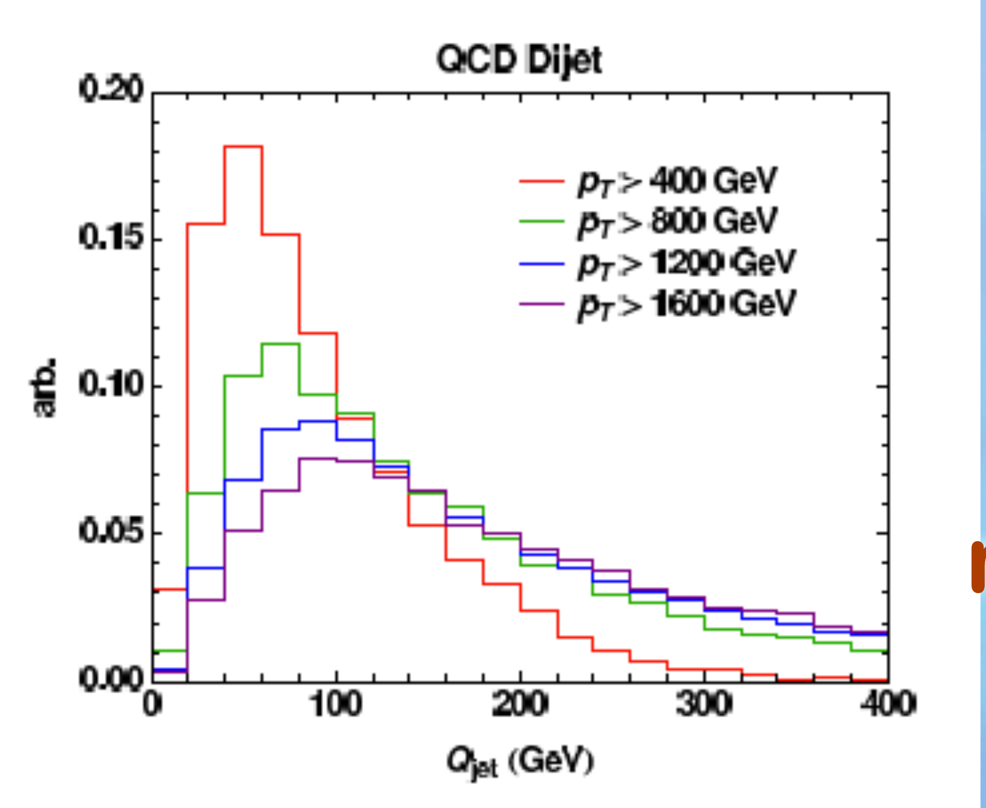

jet mass

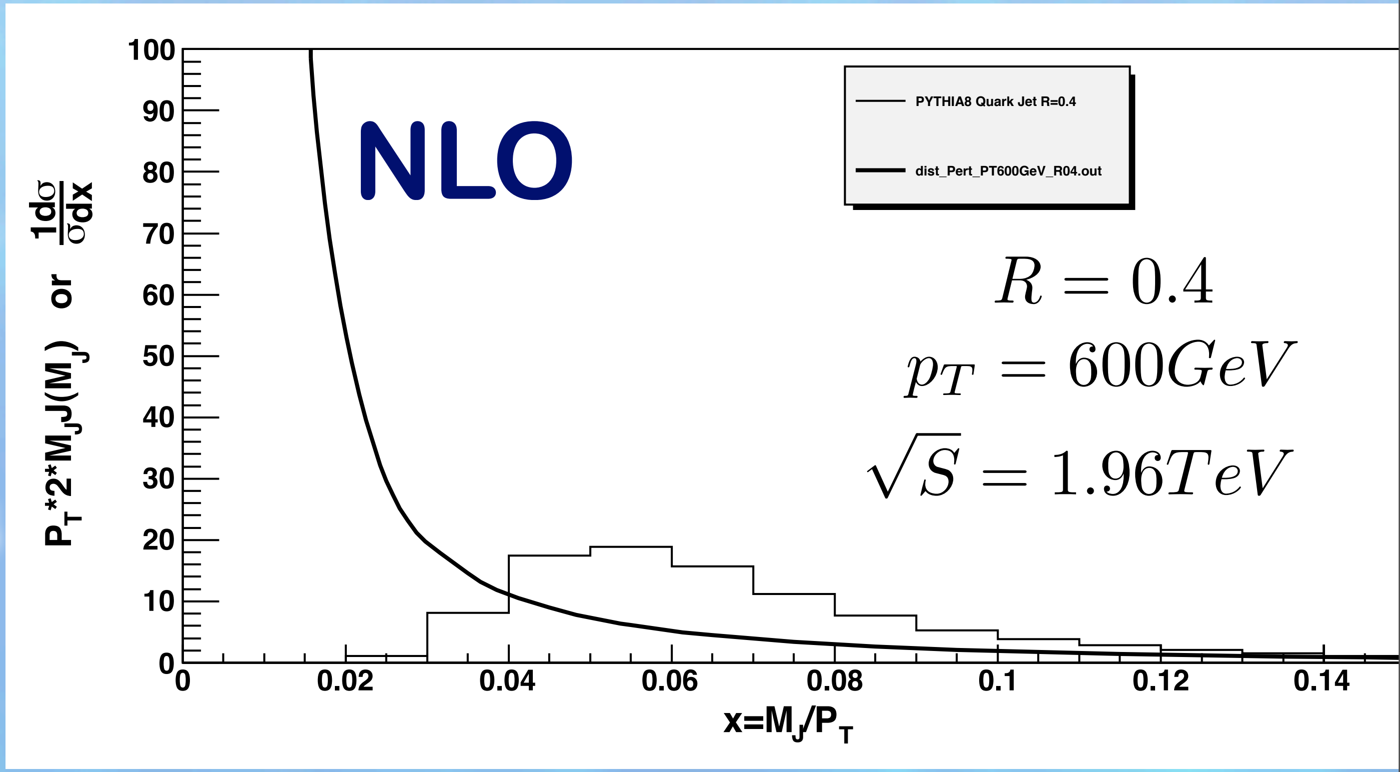

Thaler & Wang, arxiv:0806.0023

Our resummation results

- At the first time that **pQCD resummation approach** is established to investigate jets.

- Improve predictions on Jet **energy profile** and jet **mass distribution** to describe CDF and CMS data.

Jet energy profile @ CDF

$$\Psi_q(r) \equiv \frac{\bar{J}_q^E(1, P_T, \nu_{\rm fi}^2, R, r)}{\bar{J}_q^E(1, P_T, \nu_{\rm in}^2, R, R)},$$

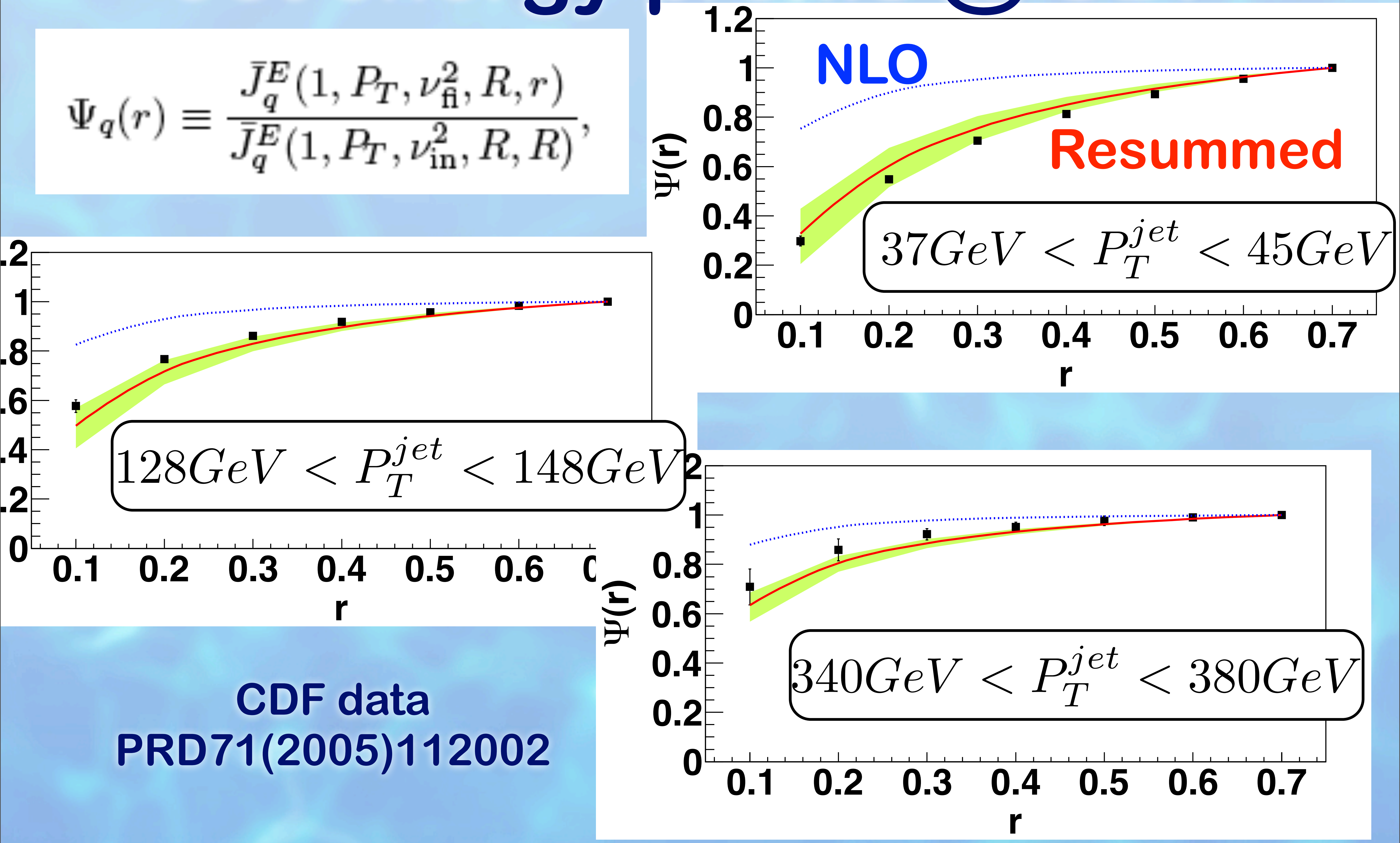

CDF data
PRD71(2005)112002

Gluon jet dominates in low pT region.

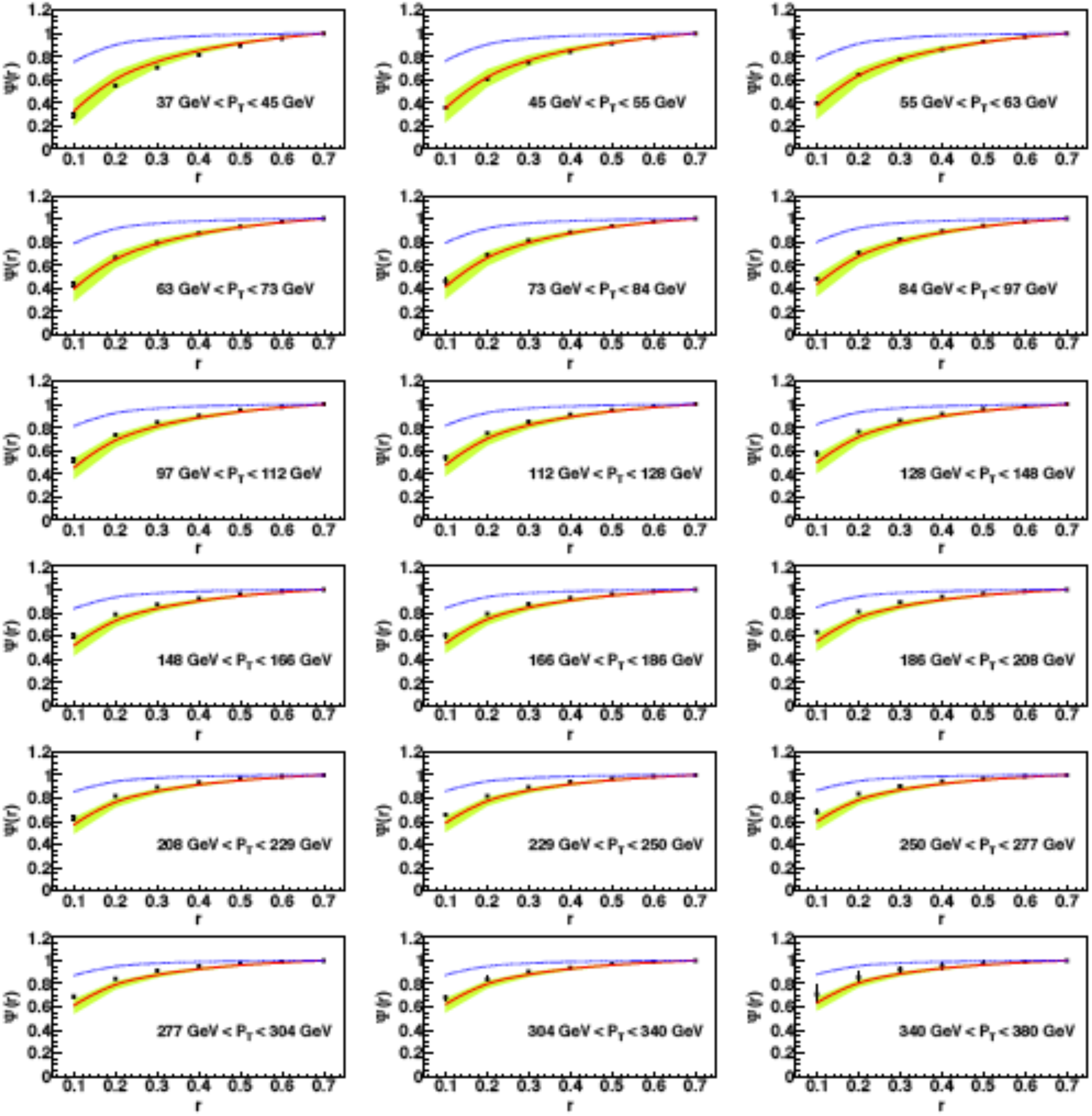
Ψ(r)
r
0
0.2
0.4
0.6
0.8
1
1.2
0.1
0.2
0.3
0.4
0.5
0.6
0.7
37 GeV < P_T < 45 GeV
45 GeV < P_T < 55 GeV
55 GeV < P_T < 63 GeV
63 GeV < P_T < 73 GeV
73 GeV < P_T < 84 GeV
84 GeV < P_T < 97 GeV
97 GeV < P_T < 112 GeV
112 GeV < P_T < 128 GeV
128 GeV < P_T < 148 GeV
148 GeV < P_T < 166 GeV
166 GeV < P_T < 186 GeV
186 GeV < P_T < 208 GeV
208 GeV < P_T < 229 GeV
229 GeV < P_T < 250 GeV
250 GeV < P_T < 277 GeV
277 GeV < P_T < 304 GeV
304 GeV < P_T < 340 GeV
340 GeV < P_T < 380 GeV

Jet energy profile @ CMS

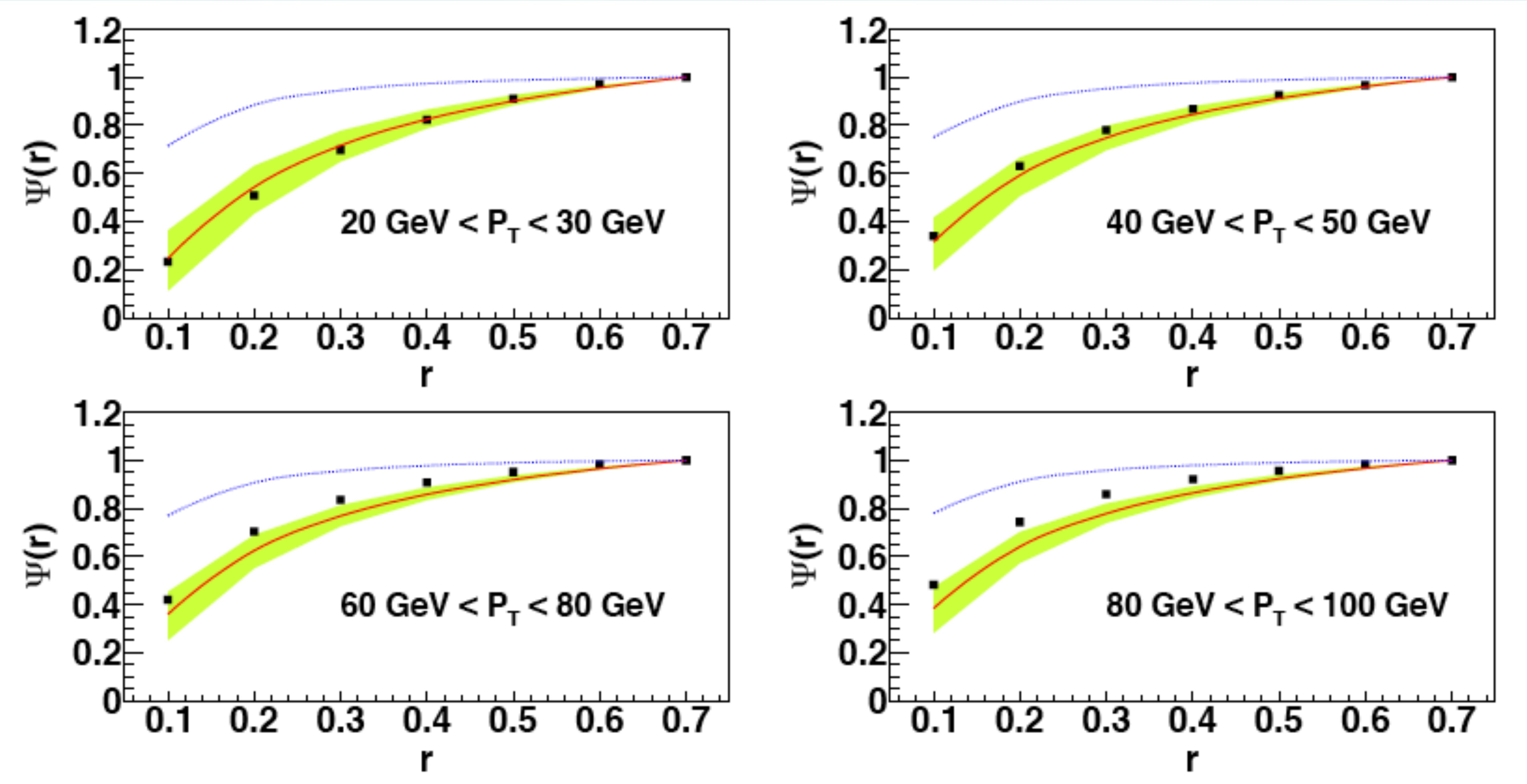

Predicted by perturbative resummation calculation, and non-perturbative physics input is not needed.

Dependence on pT@ LHC

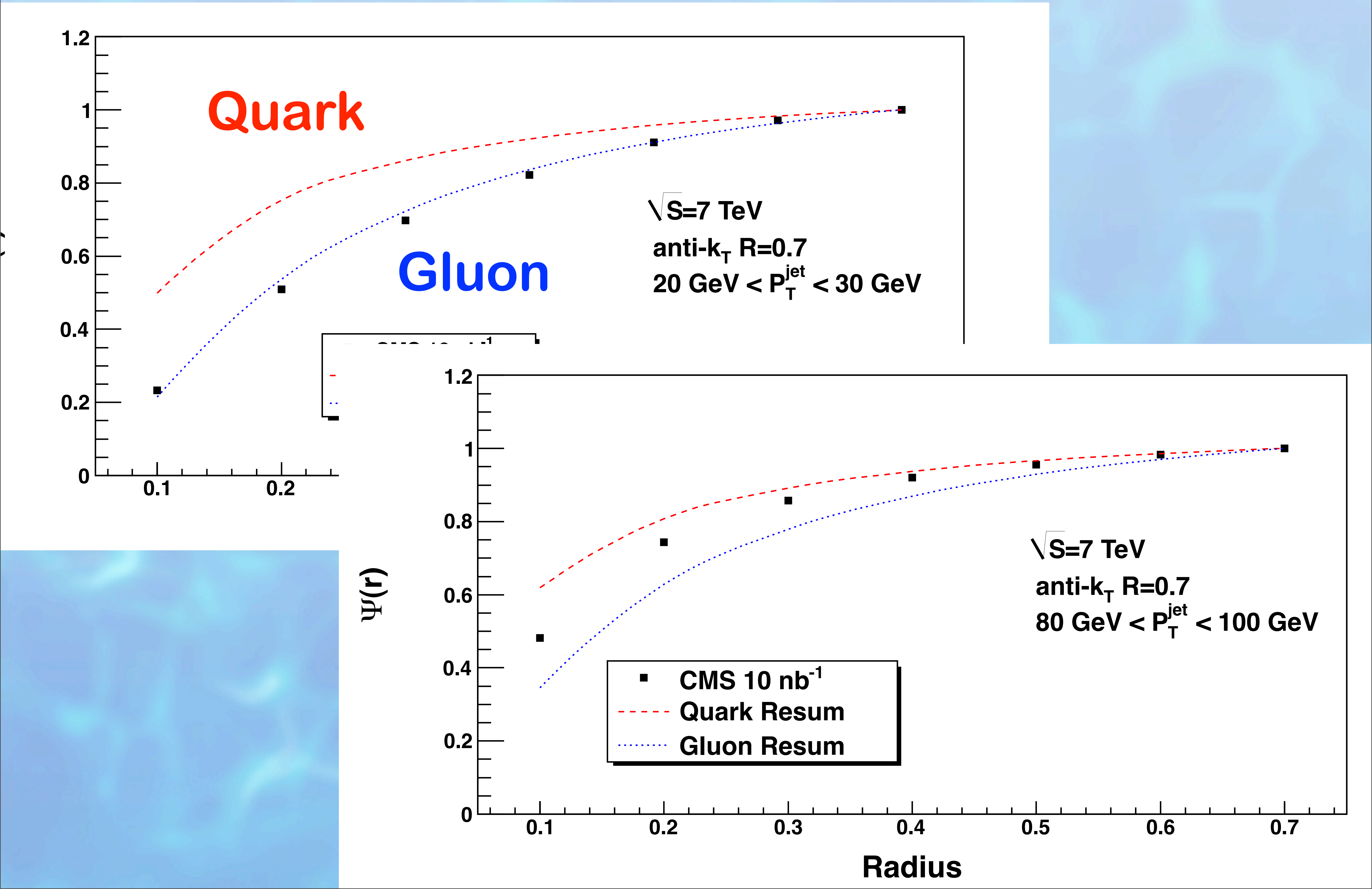

Use Jet Energy Profile to distinguish Higgs Boson Production Mechanisms

(Separating weak boson fusion from gluon fusion processes)

Discriminate Higgs Production Mechanisms Using Jet Energy Profiles

- Important to measure the couplings of Higgs boson to other SM particles.
- Need to separate vector boson fusion (VBF) from gluon fusion (GF) production mechanisms for the Higgs boson.
- Various kinematical distributions look alike after imposing relevant kinematic cuts.
- Propose to study the final state jet energy profiles to discriminate VBF from GF processes.

Hep-ph/1306.0899
V. Rentala, N. Vignaroli, H.-N. Li, Z. Li, CPY

Higgs production mechanisms

SM Higgs Production

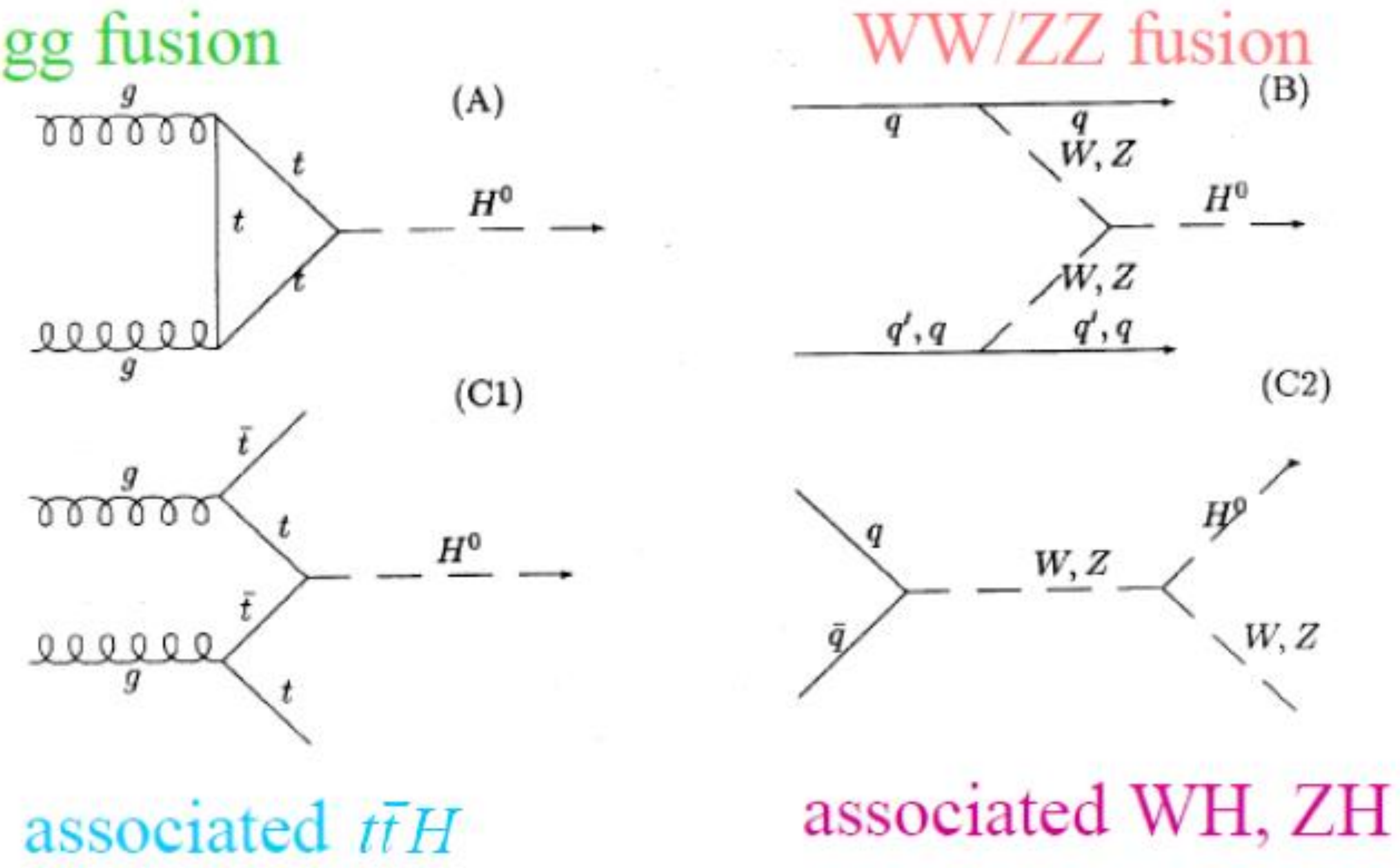

SM Higgs @ 14 TeV LHC

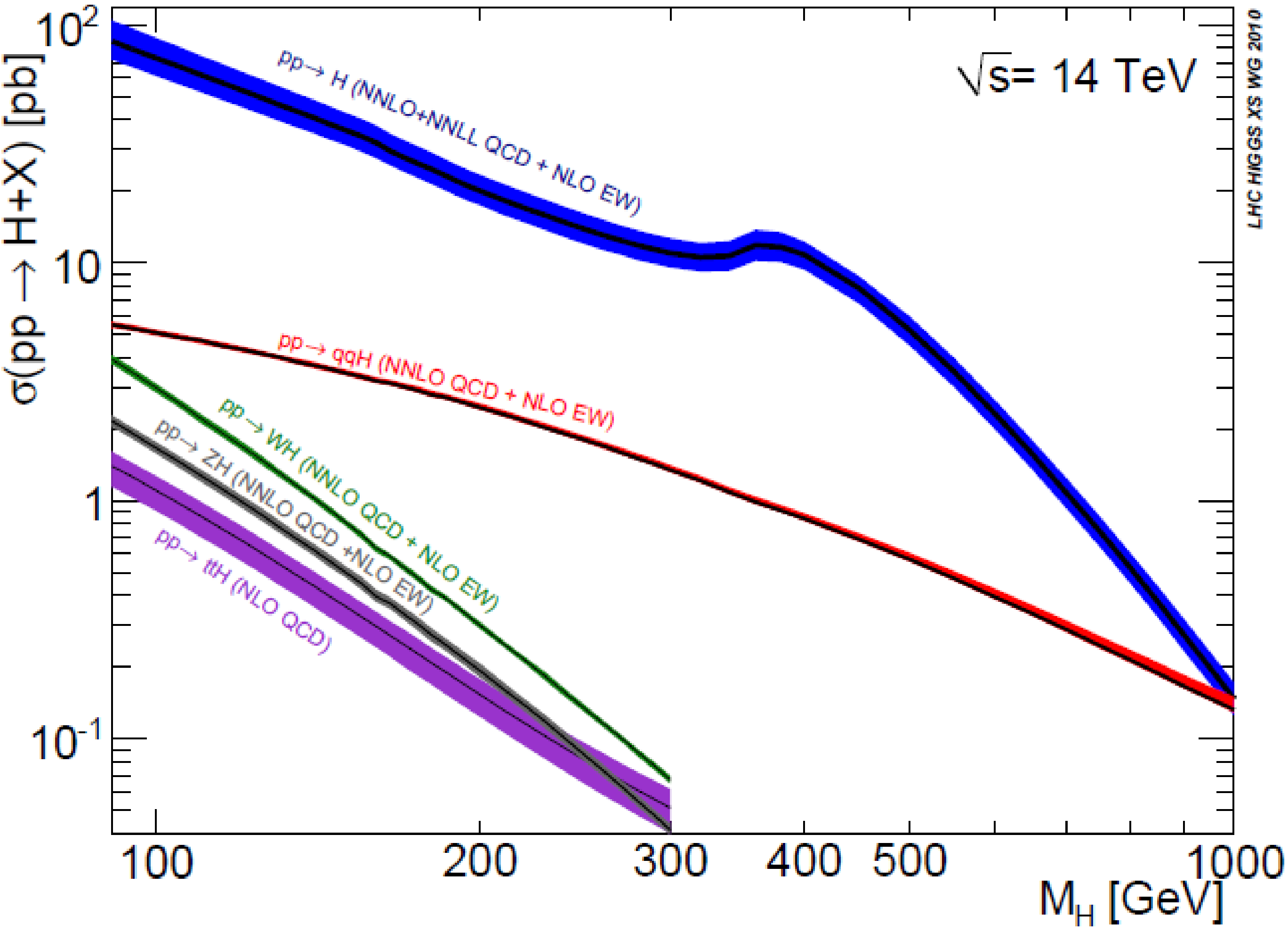

Higgs decay branching ratios

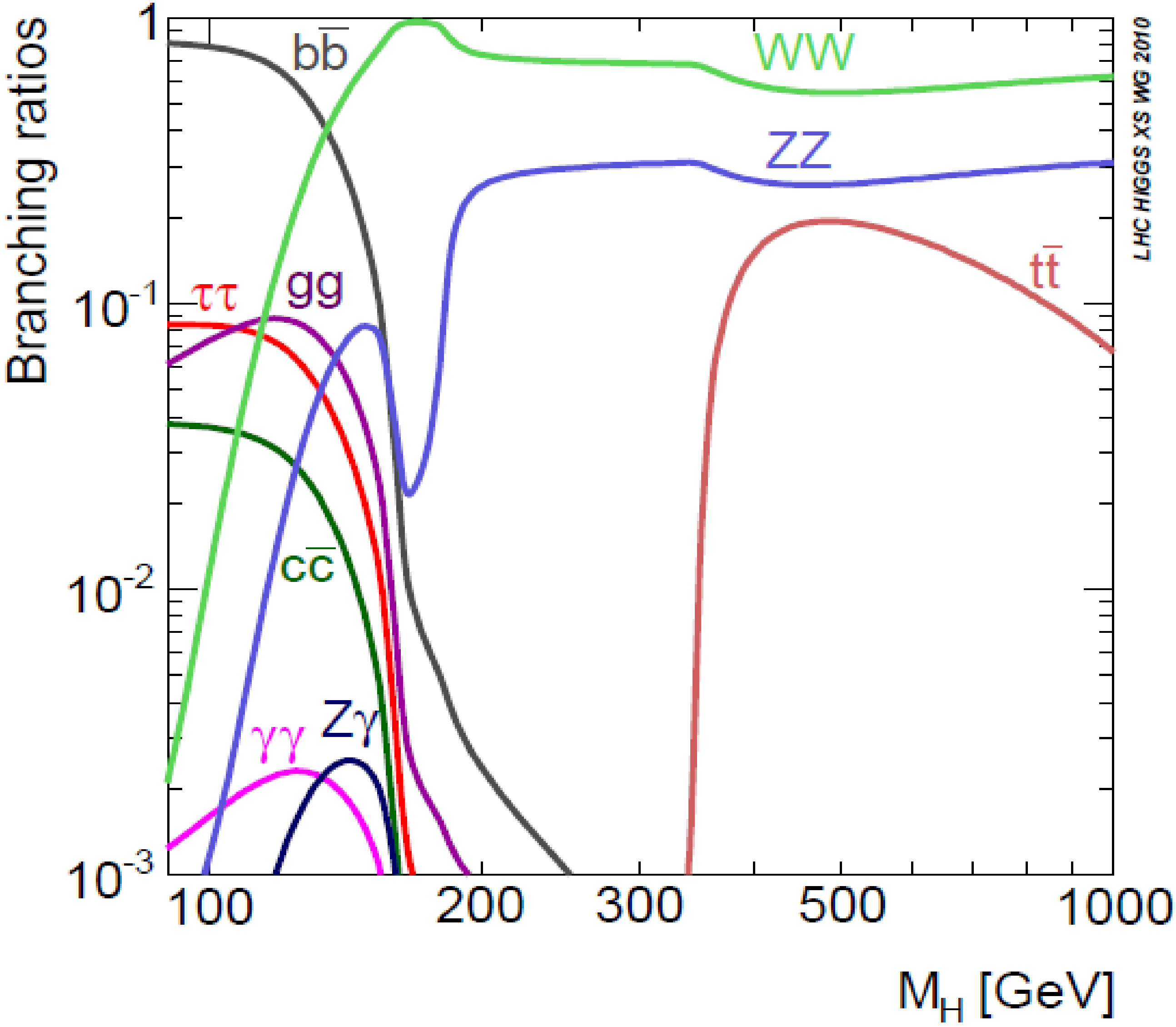

For 125 GeV Higgs, Total decay width is 4.03 MeV.

$$Br(\bar{b}b) = 0.58$$
$$Br(WW) = 0.22$$
$$Br(gg) = 0.086$$
$$Br(\tau\tau) = 0.06$$
$$Br(cc) = 0.028$$
$$Br(ZZ) = 0.027$$
$$Br(\gamma\gamma) = 0.0023$$
$$Br(Z\gamma) = 0.0016$$

Higgs + 2 jets, in di-photon channel

- Following CMS analysis:

$$p_T^{\gamma 1} > m_{\gamma\gamma}/2, \quad p_T^{\gamma 2} > m_{\gamma\gamma}/4, \quad |\eta_\gamma| < 2.5,$$

$$p_T^{j1} > 30 \text{ GeV}, \quad p_T^{j2} > 30 \text{ GeV}, \quad |\eta_j| < 4.7,$$

$$\Delta\eta_{jj} > 3.5,$$

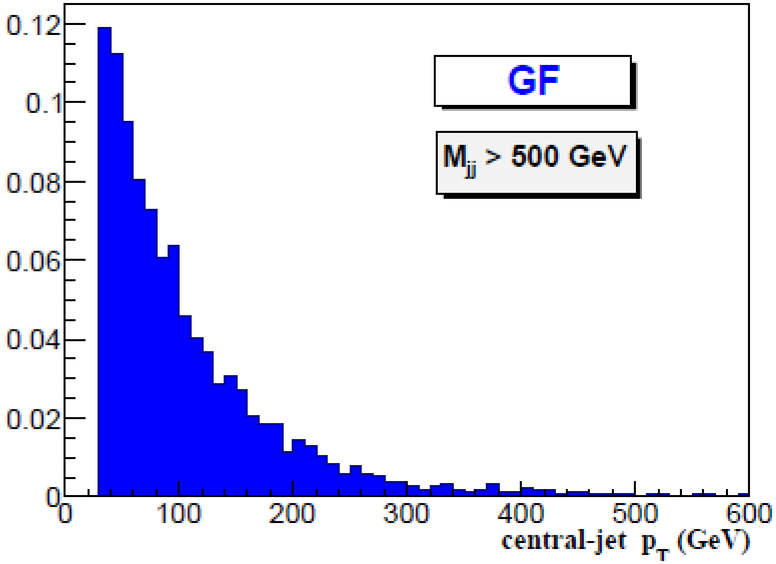

Longer tail in GF, due to large M_{jj} cut.

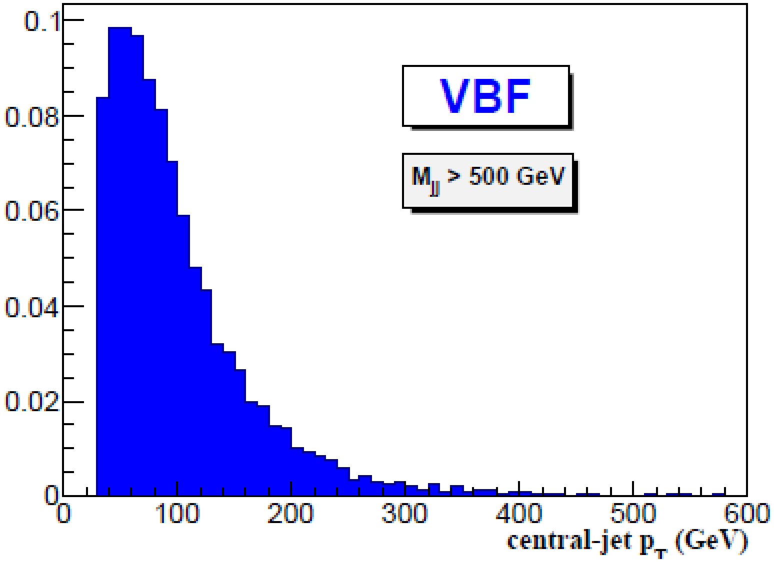

P_T Peaks around $\frac{M_W}{2}$ In VBF, due to weak boson propagators.

Jet Energy Profiles

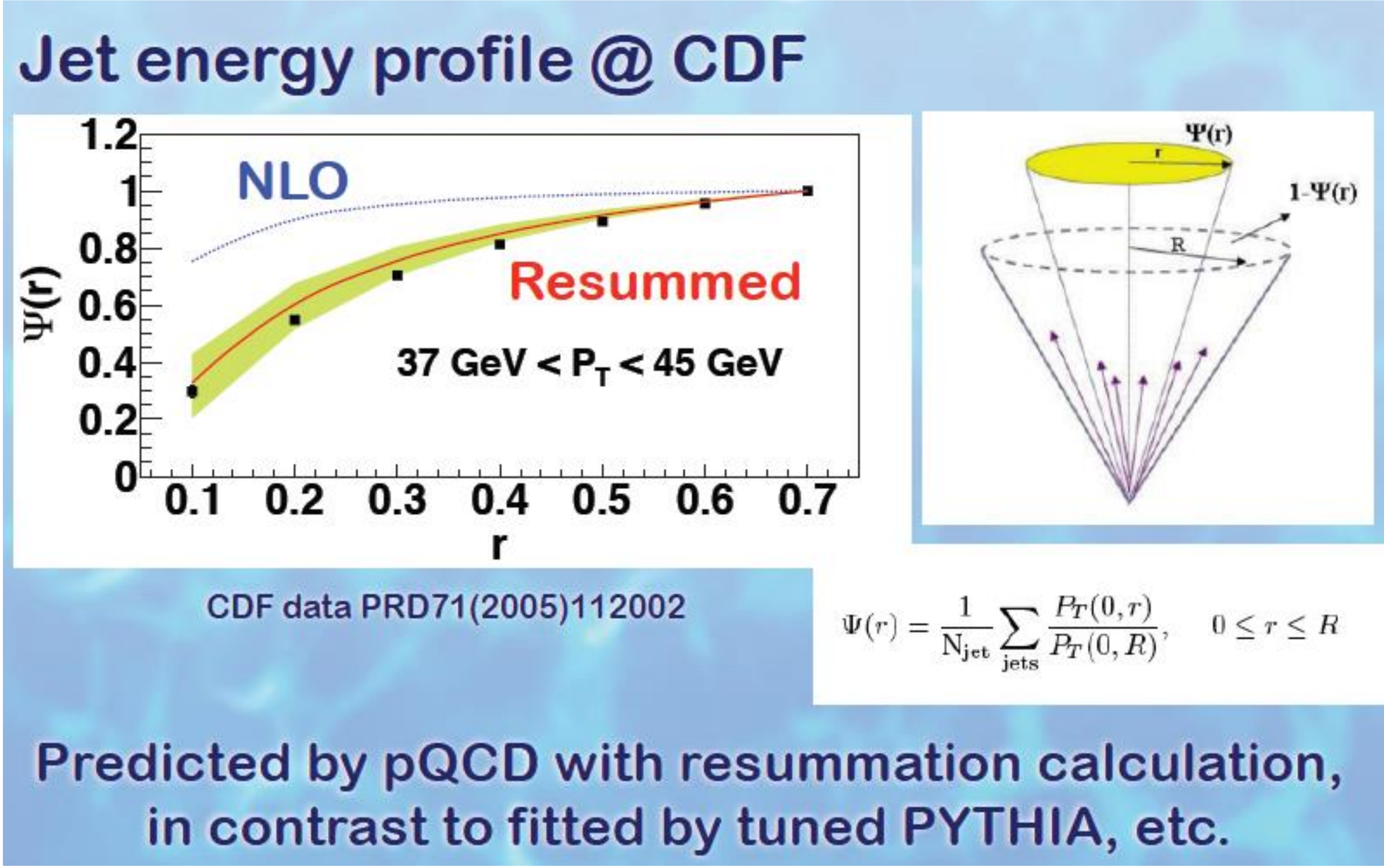

Jet energy profile @ CDF

CDF data PRD71(2005)112002

$$\Psi(r) = \frac{1}{\mathrm{N_{jet}}} \sum_{\mathrm{jets}} \frac{P_T(0,r)}{P_T(0,R)}, \quad 0 \le r \le R$$

Predicted by pQCD with resummation calculation, in contrast to fitted by tuned PYTHIA, etc.

pQCD Resummation calculations

- The perturbative QCD resummation technique is applied to improve prediction on jet energy profile to describe CDF and CMS data.
- Final state quark jets can be statistically separated from gluon jets by studying their corresponding jet energy profiles.

Hep-ph/1107.4535; 1206.1344
H.-N. Li, Z. Li, CPY

Separating Quark from Gluon Jets

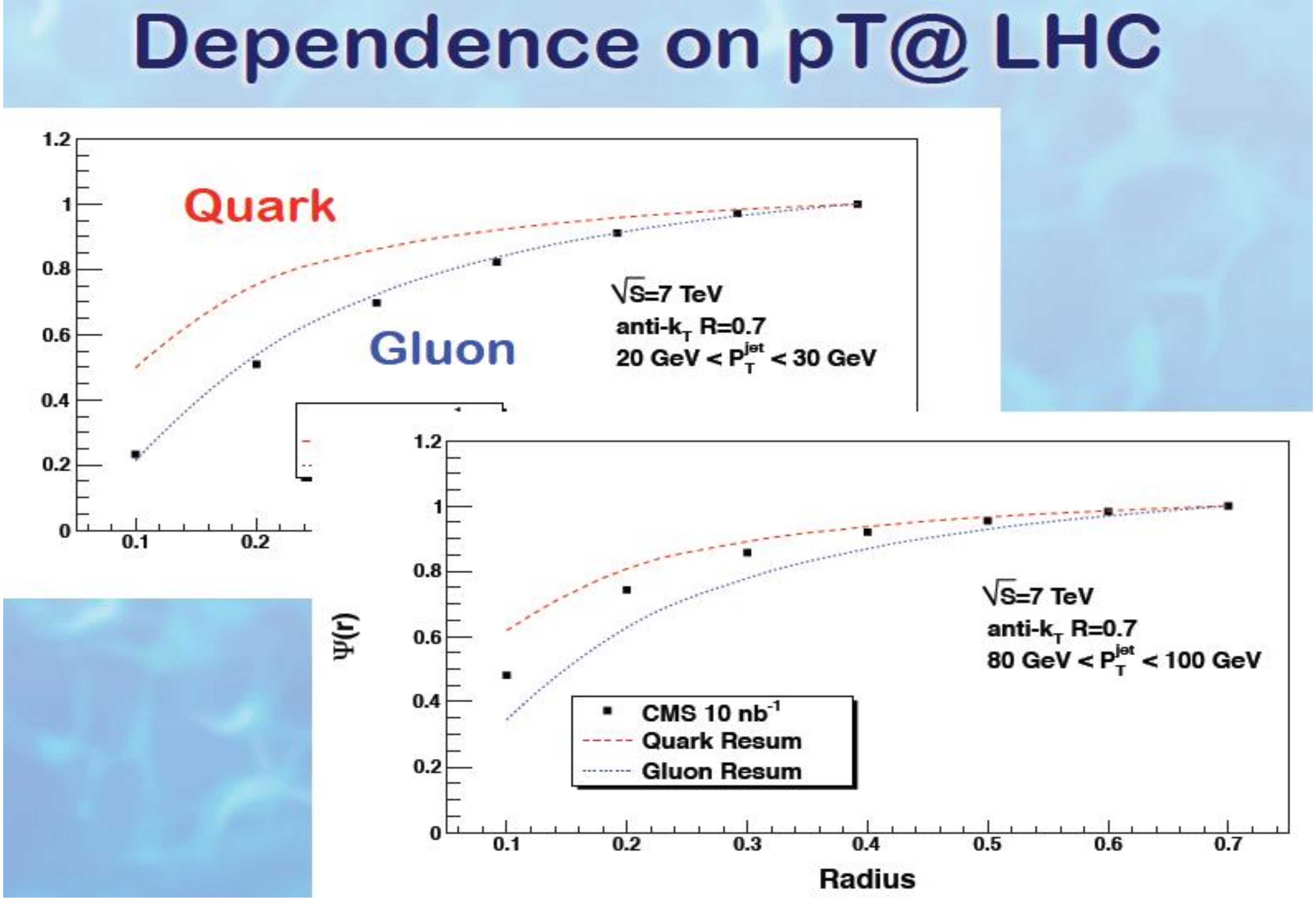

Dependence on pT@ LHC

For 125 GeV SM Higgs Boson

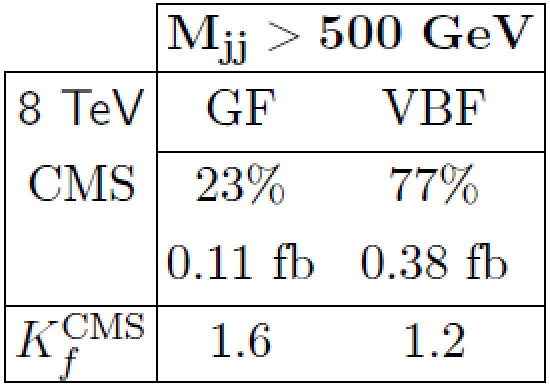

	$\mathbf{M_{jj} > 500\ GeV}$	
8 TeV	GF	VBF
CMS	23%	77%
	0.11 fb	0.38 fb
K_f^{CMS}	1.6	1.2

TABLE I: CMS cross-sections at the 8 TeV LHC using tight cuts and the corresponding compositions of VBF and GF to the total SM rate [2]. The factor, K_f^{CMS}, is the correction factor needed to rescale the MadGraph cross-sections to agree with the CMS data.

Simulate H+1,2,3 jets events with MadGraph v5

Pass them to Pythia v6.4 for showering and hadronization, and use MLM prescription for matching.

Jets are reconstructed using SpartyJet, a wrapper for FastJet, using the anti-k_t jet algorithm with $R = 0.7$

Compare Jet Energy Profiles from Pythia and pQCD

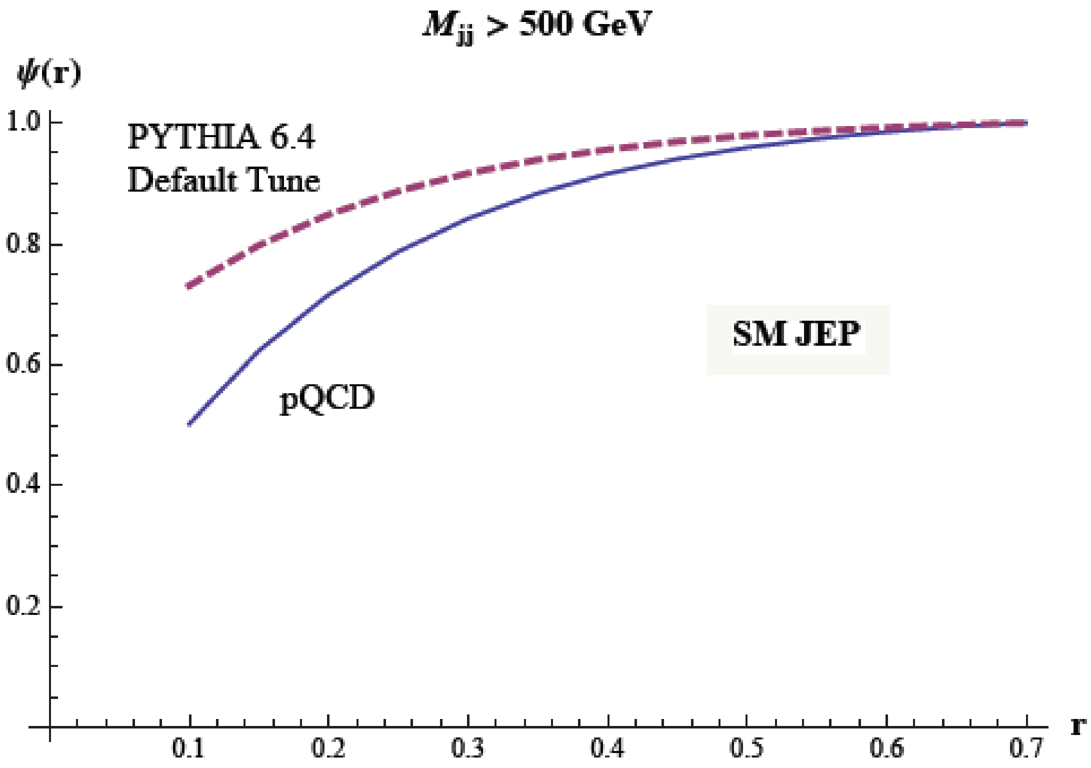

FIG. 7: Energy profile of the central jet for SM obtained by analyzing the jet substructure after Pythia v6.4 (default tune) showering, compared to the theoretical pQCD prediction using jet functions [11, 12].

$$\psi(r) = \frac{\sum_{r'<r} p_T(r')}{\sum_{r'<R} p_T(r')}.$$

The central jet is chosen, for its jet energy profile (JEP) could be better measured than a forward jet.

Our Analyses

- Pythia predictions depend on the specific tune considered (Pythia tune-A).
- pQCD resummation predictions, without including power suppressed contribution, do not depend on any non-perturbative physics.
- Hence, we use pQCD prediction to determine the central value of the JEP, and use Pythia results to estimate the error on the JEP.

Compare various model predictions in JEP

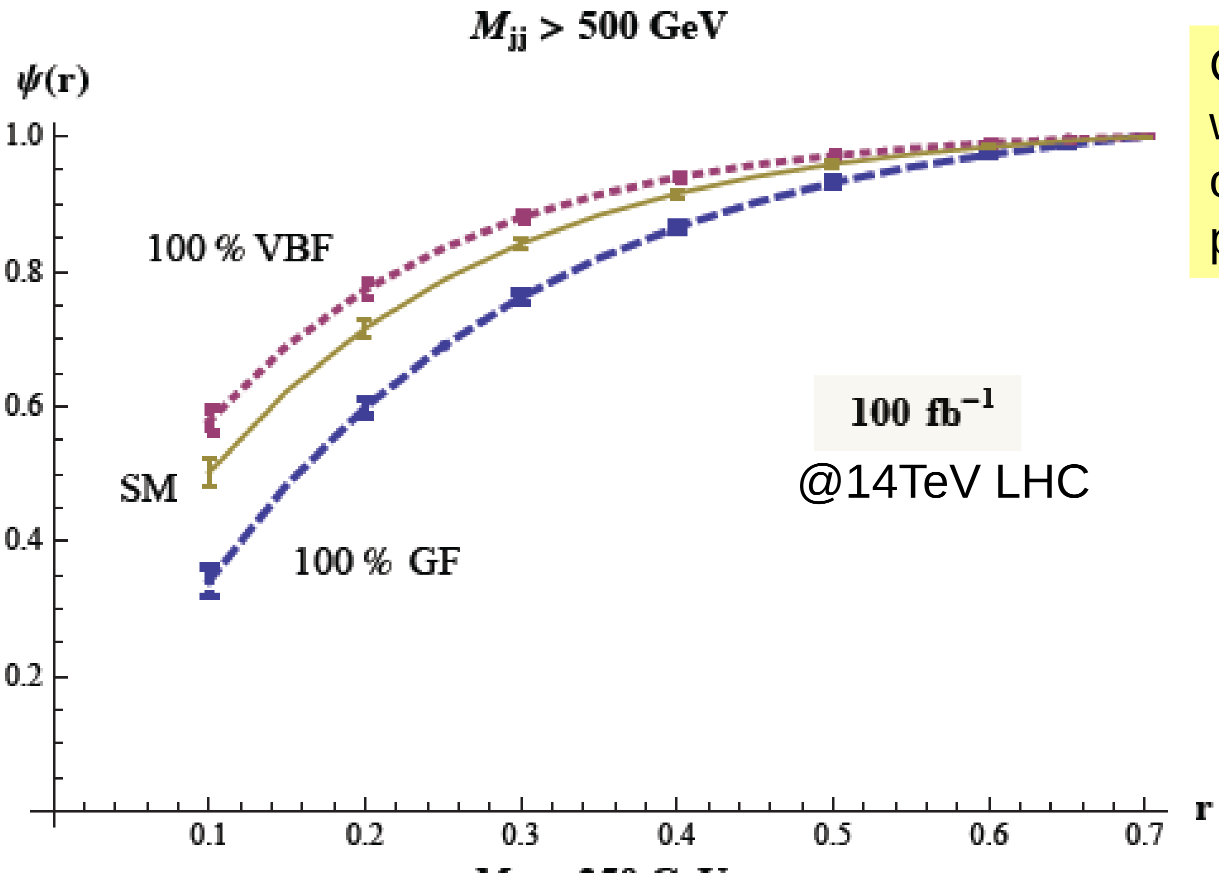

@14TeV LHC

Compare SM prediction with two hypothetical cases of a Higgs produced via pure VBF or GF.

The statistical errors are derived from Madgraph+Pythia simulation.

Event rates and f_V at 14 TeV LHC

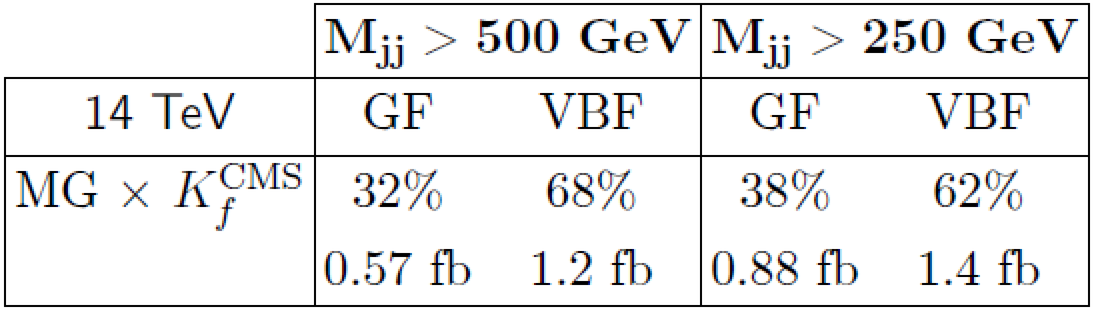

	$\mathbf{M_{jj} > 500}$ **GeV**		$\mathbf{M_{jj} > 250}$ **GeV**	
14 TeV	GF	VBF	GF	VBF
MG × K_f^{CMS}	32%	68%	38%	62%
	0.57 fb	1.2 fb	0.88 fb	1.4 fb

TABLE II: SM expected cross-sections at the 14 TeV LHC, using tight cuts with $M_{jj} > 500$ GeV and with $M_{jj} > 250$ GeV.

(with 100 1/fb)

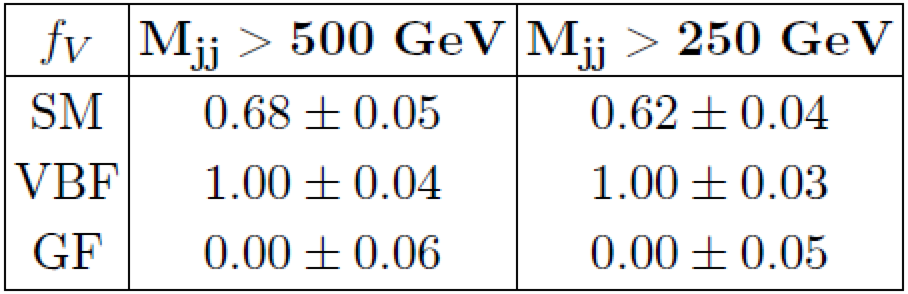

f_V	$\mathbf{M_{jj} > 500}$ **GeV**	$\mathbf{M_{jj} > 250}$ **GeV**
SM	0.68 ± 0.05	0.62 ± 0.04
VBF	1.00 ± 0.04	1.00 ± 0.03
GF	0.00 ± 0.06	0.00 ± 0.05

$$\boxed{\begin{aligned}\psi_{f_V}(r) &= f_V\, \psi_{\mathrm{VBF}}(r) \\ &\quad + (1 - f_V)\, \psi_{\,\mathrm{GF}}(r)\end{aligned}}$$

TABLE IV: Fraction of VBF-like events (f_V) for SM, pure VBF and pure GF events with error bars shown for both tight cuts with $M_{jj} > 500$ GeV and with $M_{jj} > 250$ GeV. f_V is determined

$$\psi(r) = \frac{1 - be^{-ar}}{1 - be^{-aR}},$$

Background contamination

- Assume the $(\gamma\gamma jj)$ background JEP, $\psi_B(r)$, can be measured from (side-band) data, so that the signal JEP, $\psi_s(r)$, can be obtained from the observed JEP, $\psi_{obs}(r)$.

$$\psi_S(r) = \psi_{obs}(r) + \frac{B}{S}\left(\psi_{obs}(r) - \psi_B(r)\right)$$

The errors scale by the factor

$$\sqrt{1 + 2\frac{B}{S}}$$

Background cross sections

14 TeV Background

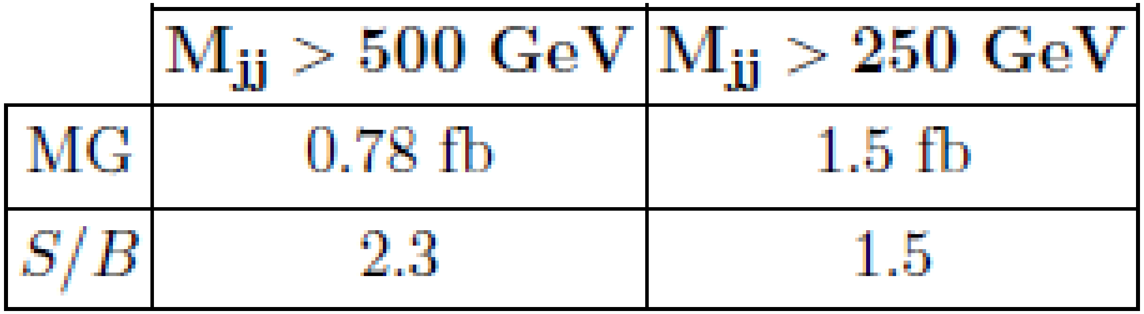

	$M_{jj} > 500$ GeV	$M_{jj} > 250$ GeV
MG	0.78 fb	1.5 fb
S/B	2.3	1.5

8 TeV Background

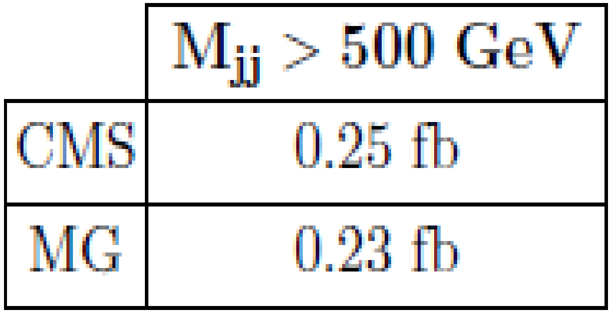

	$M_{jj} > 500$ GeV
CMS	0.25 fb
MG	0.23 fb

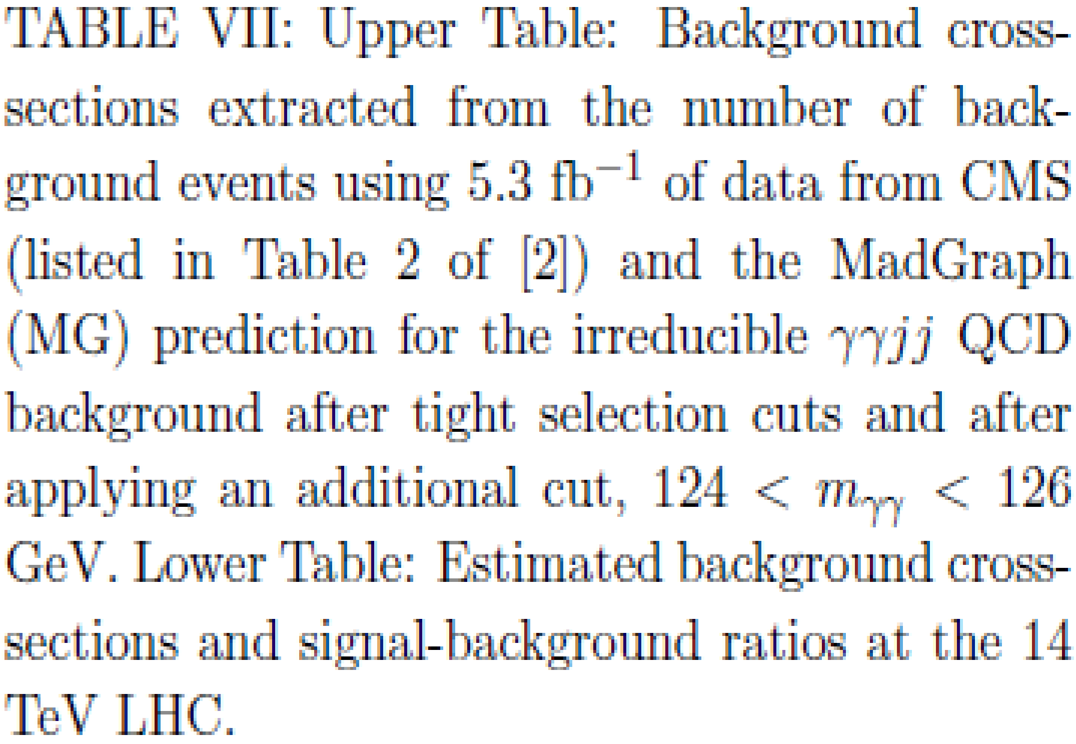

TABLE VII: Upper Table: Background cross-sections extracted from the number of background events using 5.3 fb^{-1} of data from CMS (listed in Table 2 of [2]) and the MadGraph (MG) prediction for the irreducible $\gamma\gamma jj$ QCD background after tight selection cuts and after applying an additional cut, $124 < m_{\gamma\gamma} < 126$ GeV. Lower Table: Estimated background cross-sections and signal-background ratios at the 14 TeV LHC.

Summary on JEP

- We use (quark vs. gluon) Jet Energy Profile to discriminate the production mechanism of Higgs boson, VBF vs. GF.
- Similar techniques can be applied to probe New Physics.

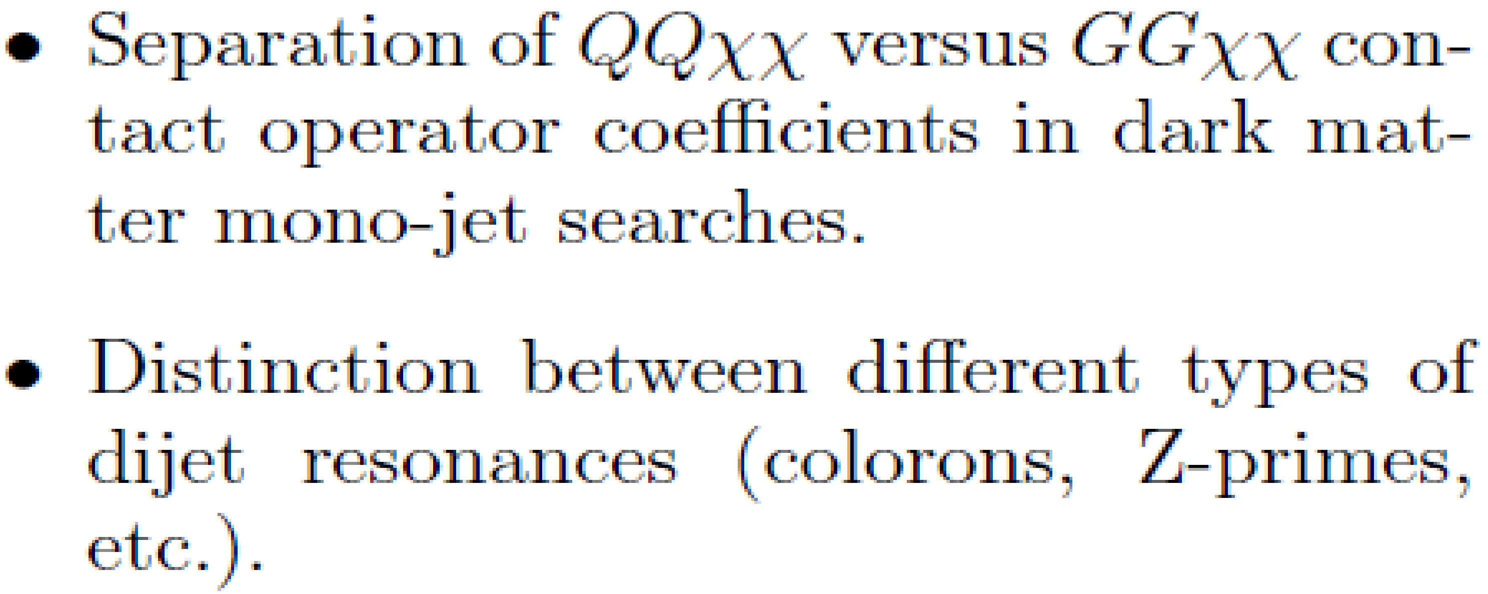

  - Separation of $QQ\chi\chi$ versus $GG\chi\chi$ contact operator coefficients in dark matter mono-jet searches.
  - Distinction between different types of dijet resonances (colorons, Z-primes, etc.).

The Big Question

- As requested by Prof. Mihoko Nojiri
- After separating weak boson fusion process from gluon fusion process, we need to study the scatterings of weak bosons in the TeV region, for the final state of weak bosons or top quark pairs.

➡

To probe electroweak symmetry breaking mechanism by studying Unitarity property of scattering amplitudes

Problems with the Higgs Model

- No (other?) fundamental scalars observed in nature

- No explanation of dynamics responsible for Electroweak Symmetry Breaking

- Hierarchy or Naturalness Problem

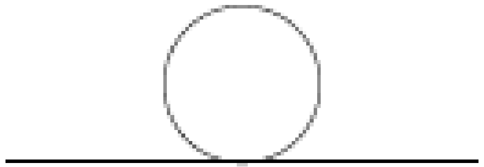

$$\Rightarrow \quad m_H^2 \propto \Lambda^2$$

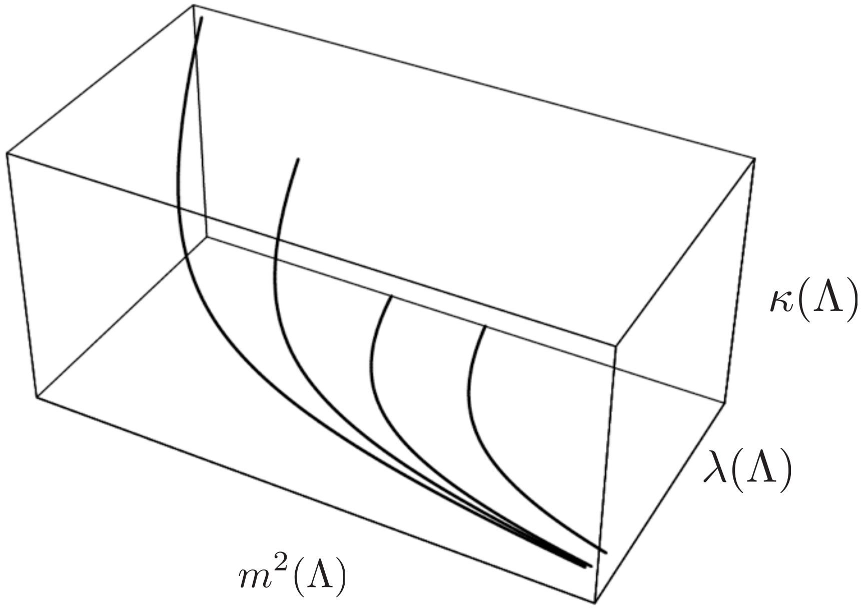

- Triviality and Vacuum Stability Problems...

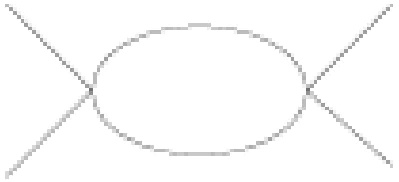

$$\Rightarrow \beta = \frac{3\lambda^2}{2\pi^2} > 0 \qquad \lambda(\mu) < \frac{3}{2\pi^2 \log\frac{\Lambda}{\mu}}$$

Triviality and Vacuum Stability

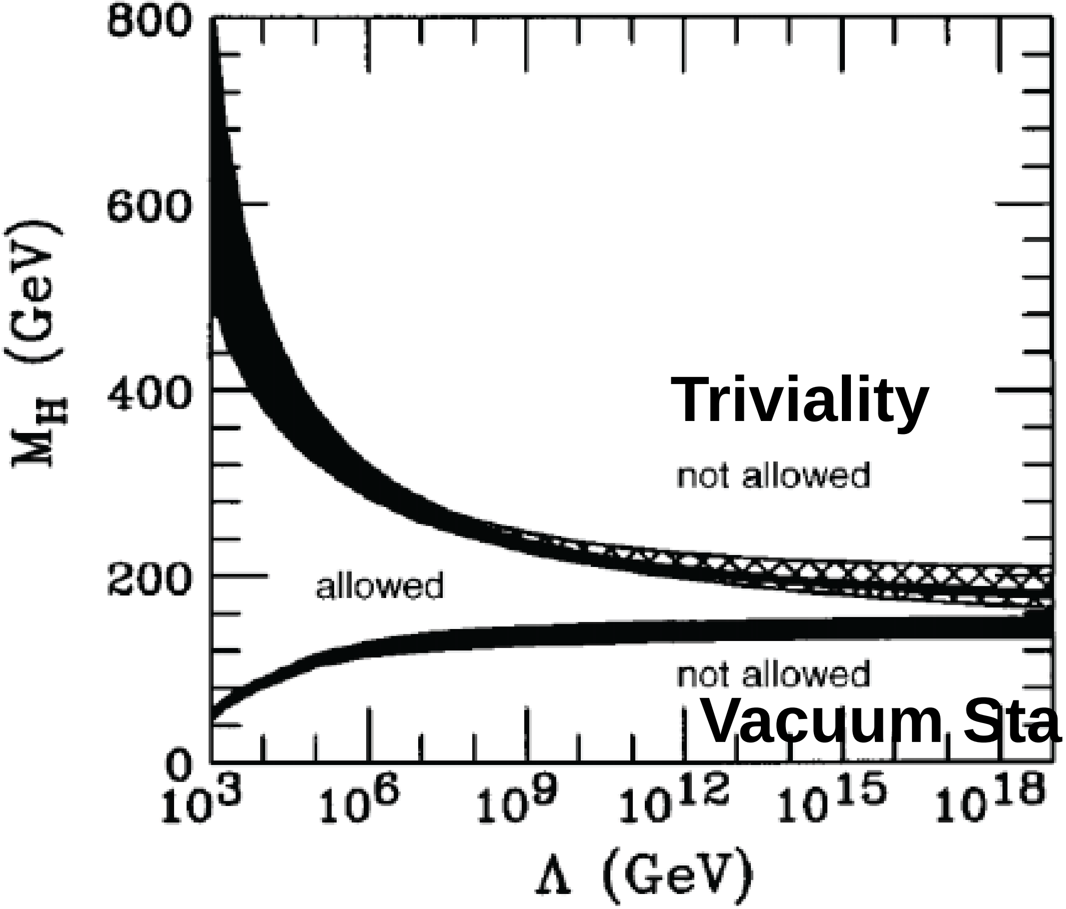

For 125 GeV Higgs,
$\Lambda \sim 10^{11} GeV$
with $m_t = 173\ GeV$

$$\frac{d\lambda}{d\log\mu} = \frac{3}{8\pi^2}\left[4\lambda^2 + 2\lambda g_t^2 - g_t^4\right]$$

T. Hambye and K. Riesselmann, Phys. Rev. D55, 7255 (1997), [hep-ph/9610272].

UPDATED

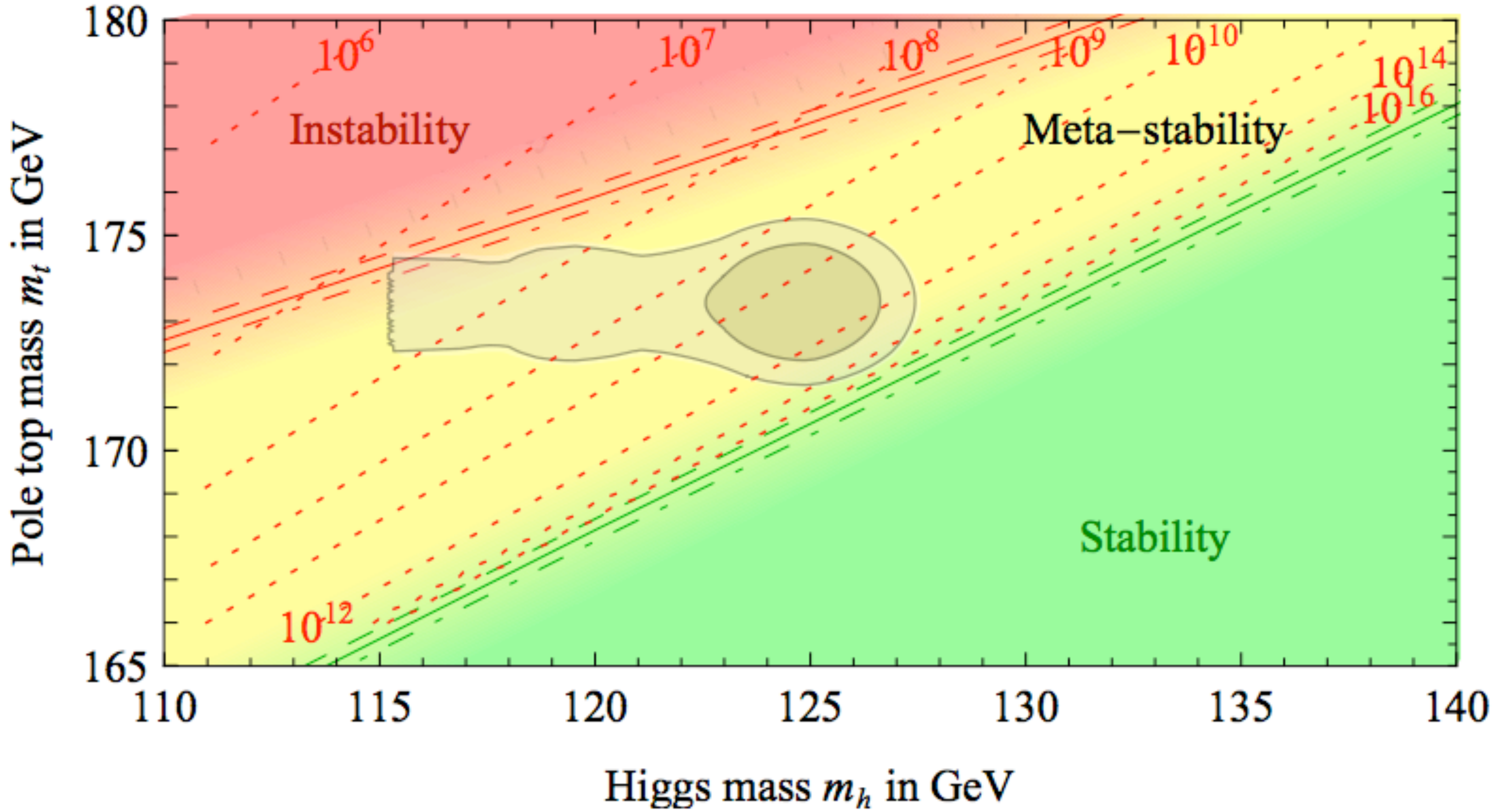

Or: other particles (e.g. superpartners) could stablize the potential...

Elias-Miro, et. al., arXiv:1112.3022

Further tests in the TeV region are absolutely needed

- Must study the longitudinally polarized vector boson scatterings in the TeV region to check the unitarity property.
- If the scattering amplitudes are shown to be unitary, then the discovered Higgs boson is responsible for the electroweak symmetry breaking. Otherwise, New Physics must exist to unitarize the longitudinal vector boson scatterings in the TeV region.

Loss of Unitarity in

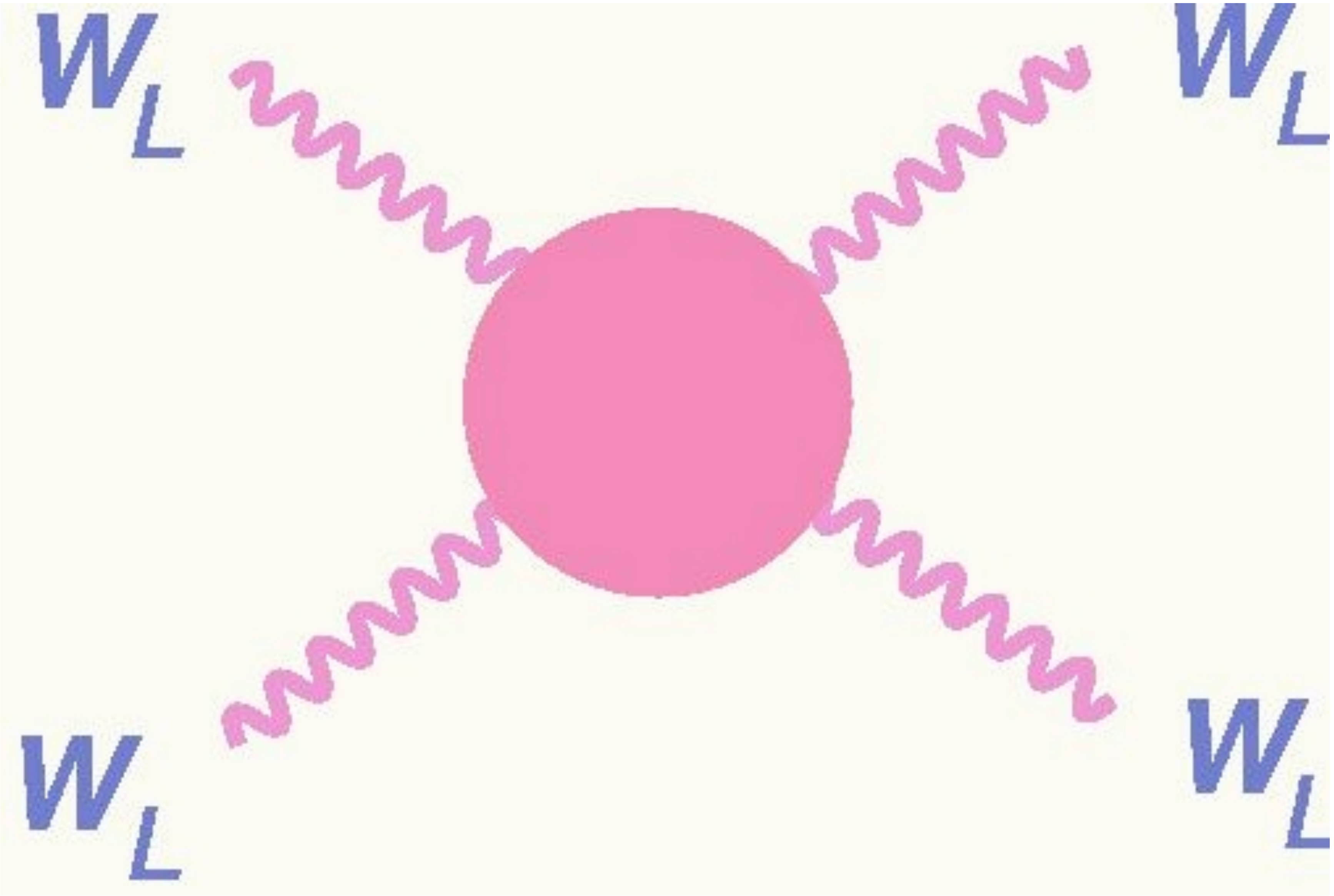

SU(2) x U(1) @ E^4

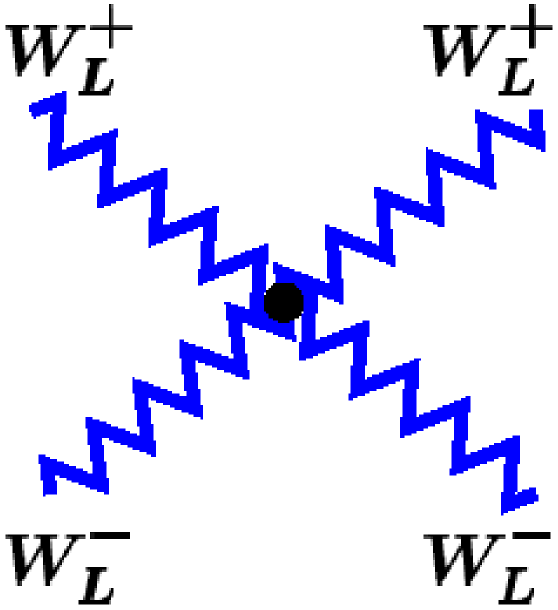

(a)

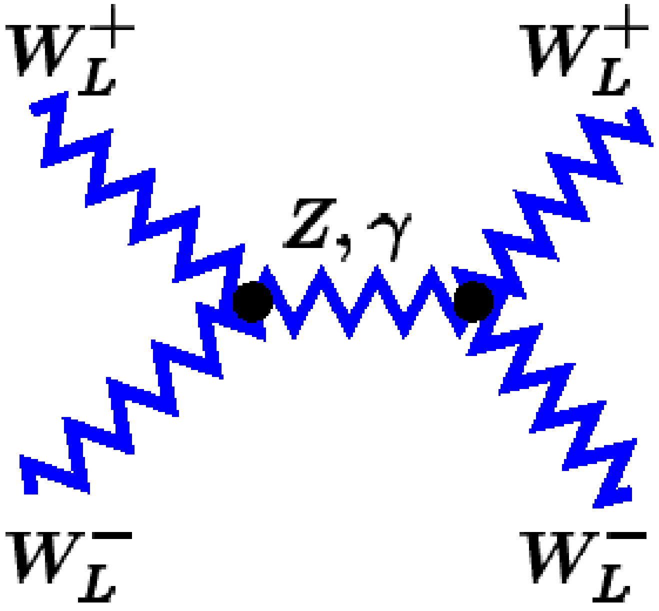

(b)

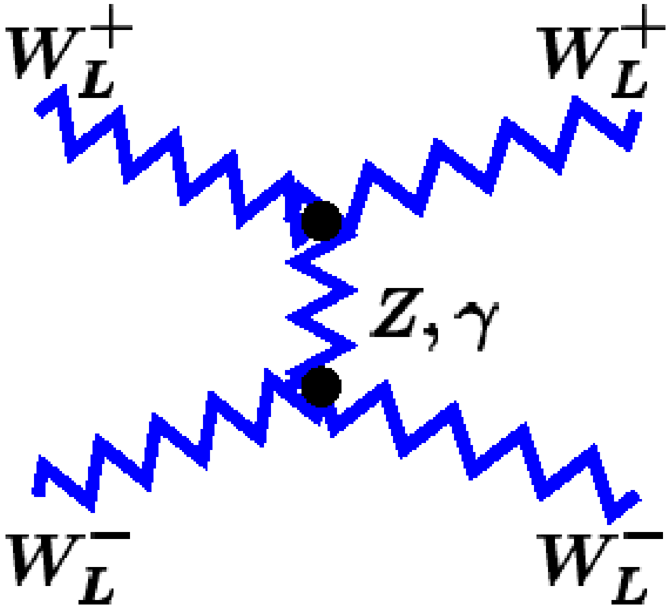

(c)

Graphs	$g^2 \frac{E^4}{m_w^4}$
(a)	$-3 + 6\cos\theta + \cos^2\theta$
(b)	$-4\cos\theta$
(c)	$+3 - 2\cos\theta - \cos^2\theta$
Sum	0

$$\epsilon_L^\mu(k) = \frac{k^\mu}{m_w} + \mathcal{O}\left(\frac{m_w}{E}\right)$$

SU(2) x U(1) @ E² & THE HIGGS

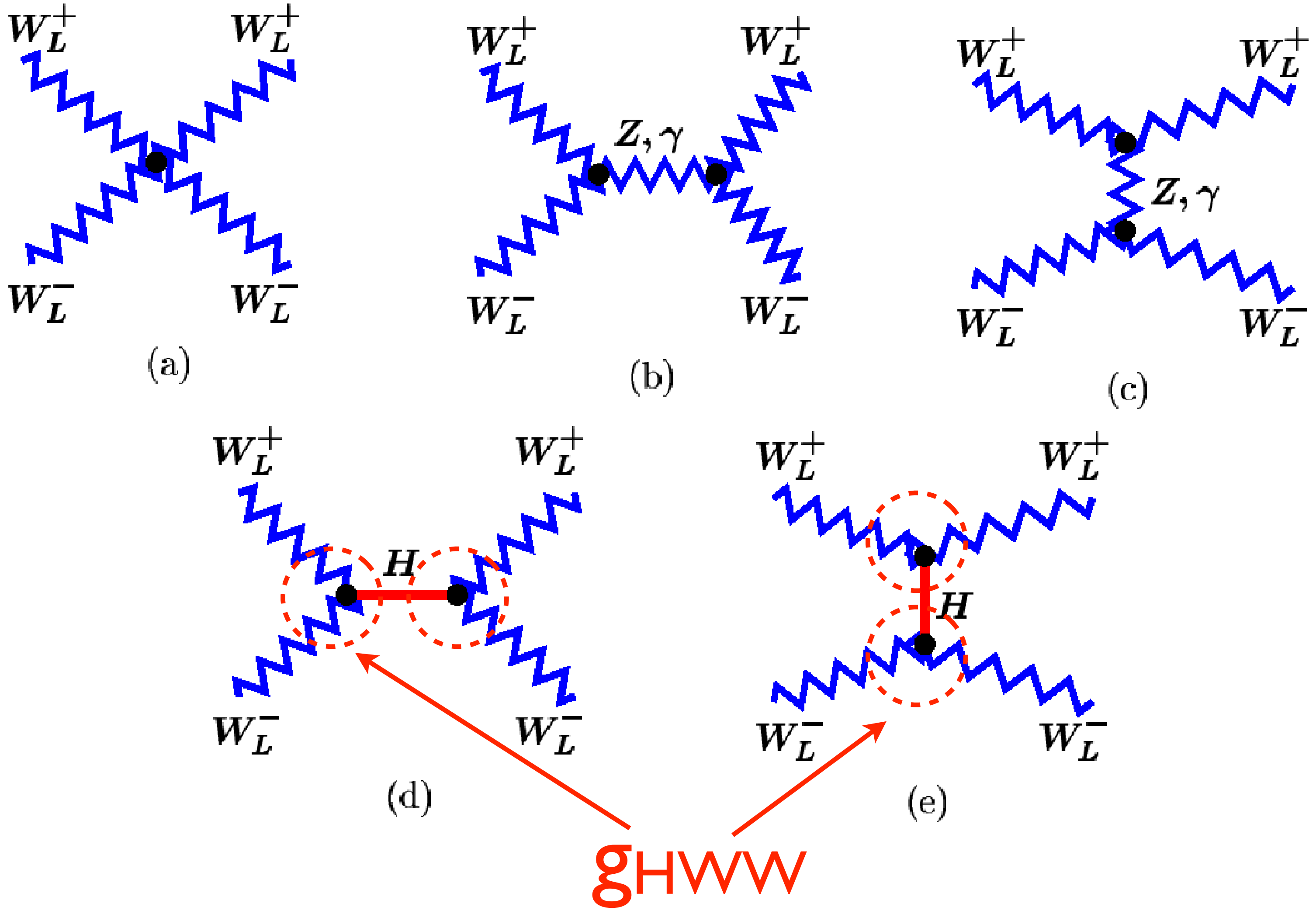

Graphs	$g^2\frac{E^2}{m_w^2}$
(a)	$+2-6\cos\theta$
(b)	$-\cos\theta$
(c)	$-\frac{3}{2}+\frac{15}{2}\cos\theta$
$(d+e)$	$-\frac{1}{2}-\frac{1}{2}\cos\theta$
Sum including (d+e)	**0**

- ▶ $\mathcal{O}(E^0) \Rightarrow$ 4d m_H bound: $m_H < \sqrt{16\pi/3}\,v \simeq 1.0$ TeV
- ▶ If no Higgs $\Rightarrow \mathcal{O}(E^2) \Rightarrow\ E < \sqrt{4\pi}\,v \simeq 0.9$ TeV

Lee, Quigg, Thacker

Weak Boson Scatterings in the TeV region

- Consider an Effective Chiral Lagrangian, with custodial symmetry (as g’ → 0):

$$\mathcal{L}_{\text{eff}}^{(d\leqslant 4)} = -\frac{1}{4}\overrightarrow{W}_{\mu\nu}\cdot\overrightarrow{W}^{\mu\nu} - \frac{1}{4}B_{\mu\nu}B^{\mu\nu} + \frac{1}{4}\left(v^2 + 2\kappa v H + \kappa' H^2\right)\mathrm{Tr}(D_\mu\Sigma^\dagger D^\mu\Sigma)$$

$$+\frac{1}{2}(\partial_\mu H)(\partial^\mu H) - \frac{m_H^2}{2}H^2 - \frac{\lambda_3 v}{3!}H^3 + \frac{\lambda_4}{4!}H^4,$$

$$\Sigma = \exp[i\overrightarrow{\tau}\cdot\overrightarrow{\omega}/v], \qquad D_\mu\Sigma = \partial_\mu\Sigma + i\frac{g}{2}\overrightarrow{\tau}\cdot\overrightarrow{W}_\mu\Sigma - i\frac{g'}{2}B_\mu\Sigma\tau_3$$

$$v \simeq 246\,\mathrm{GeV}$$

Hep-ph/0211229

Dimension-6 Operators

$$
\begin{aligned}
\mathcal{O}_{\Phi,1} &= (D_\mu \Phi)^\dagger \, \Phi^\dagger \Phi \, (D^\mu \Phi) \, , \\
\mathcal{O}_{BW} &= \Phi^\dagger \hat{B}_{\mu\nu} \hat{W}^{\mu\nu} \Phi , \\
\mathcal{O}_{DW} &= \mathrm{Tr} \left(\left[D_\mu , \hat{W}_{\nu\rho} \right] \left[D^\mu , \hat{W}^{\nu\rho} \right] \right) , \\
\mathcal{O}_{DB} &= - \frac{{g'}^2}{2} \left(\partial_\mu B_{\nu\rho} \right) \left(\partial^\mu B^{\nu\rho} \right) , \\
\mathcal{O}_{\Phi,2} &= \frac{1}{2} \partial^\mu \left(\Phi^\dagger \Phi \right) \partial_\mu \left(\Phi^\dagger \Phi \right) , \\
\mathcal{O}_{\Phi,3} &= \frac{1}{3} \left(\Phi^\dagger \Phi \right)^3 , \\
\mathcal{O}_{WWW} &= \mathrm{Tr} [\hat{W}_{\mu\nu} \hat{W}^{\nu\rho} \hat{W}_\rho^\mu] , \\
\mathcal{O}_{WW} &= \Phi^\dagger \hat{W}_{\mu\nu} \hat{W}^{\mu\nu} \Phi , \\
\mathcal{O}_{BB} &= \Phi^\dagger \hat{B}_{\mu\nu} \hat{B}^{\mu\nu} \Phi , \\
\mathcal{O}_{W} &= (D_\mu \Phi)^\dagger \hat{W}^{\mu\nu} (D_\nu \Phi) , \\
\mathcal{O}_{B} &= (D_\mu \Phi)^\dagger \hat{B}^{\mu\nu} (D_\nu \Phi) ,
\end{aligned}
$$

$$
\hat{B}_{\mu\nu} = i \frac{g'}{2} B_{\mu\nu} , \qquad \hat{W}_{\mu\nu} = i \frac{g}{2} \sigma^a W^a_{\mu\nu} ,
$$

$$
\mathcal{L}_{\mathrm{eff}} = \sum_n \frac{f_n}{\Lambda^2} \mathcal{O}_n \, ,
$$

$$
\begin{aligned}
& pp \to Z_L Z_L jj \to \ell^+ \ell^- \ell^+ \ell^- jj , \ell^+ \ell^- \nu \bar{\nu} jj , \\
& pp \to W_L^+ W_L^- jj \to \ell^+ \nu \ell^- \bar{\nu} jj , \\
& pp \to W_L^+ W_L^+ jj \to \ell^+ \nu \ell^+ \nu jj , \\
& pp \to W_L^- W_L^- jj \to \ell^- \bar{\nu} \ell^- \bar{\nu} jj , \\
& pp \to Z_L W_L^+ jj \to \ell^+ \ell^- \ell^+ \nu jj , \\
& pp \to Z_L W_L^- jj \to \ell^+ \ell^- \ell^- \bar{\nu} jj .
\end{aligned}
$$

hep-ph/0303048
B Zhang, Y.-P. Kuang, H.-J. He, CPY

SU(2) x U(1) @ E & THE HIGGS

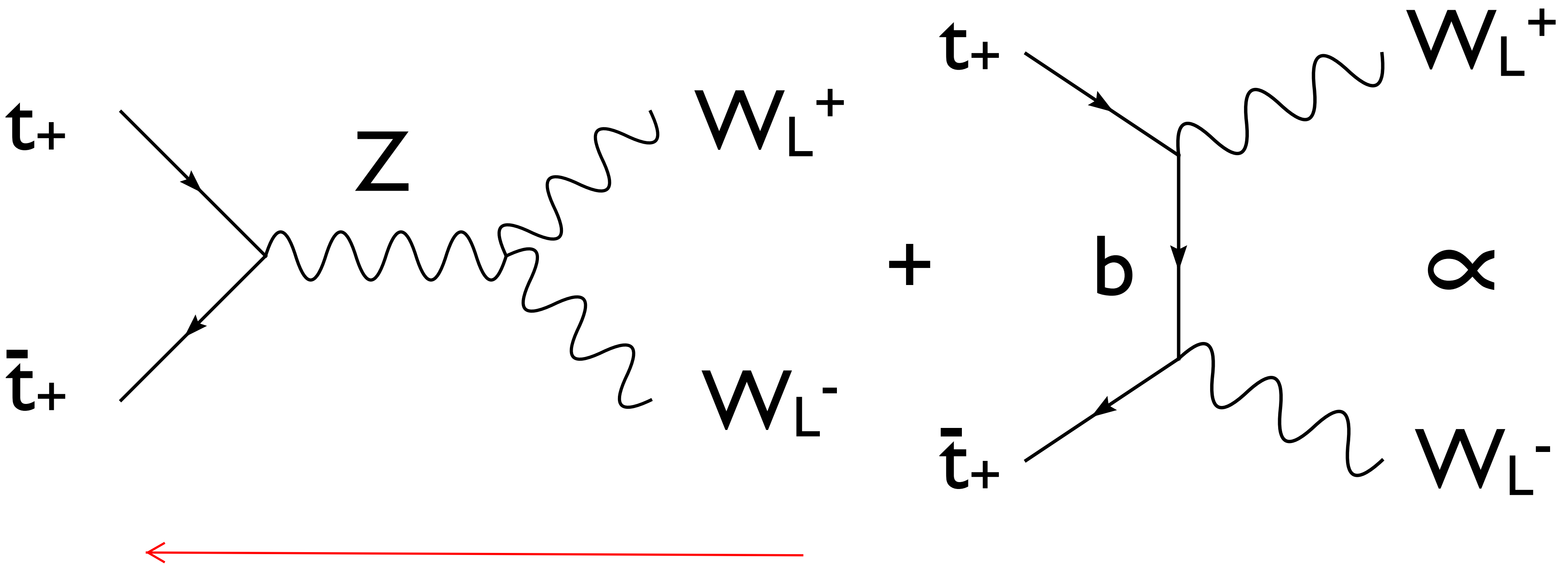

$$\propto \frac{m_t E}{v^2}$$

Bad high-energy behavior cancelled by:

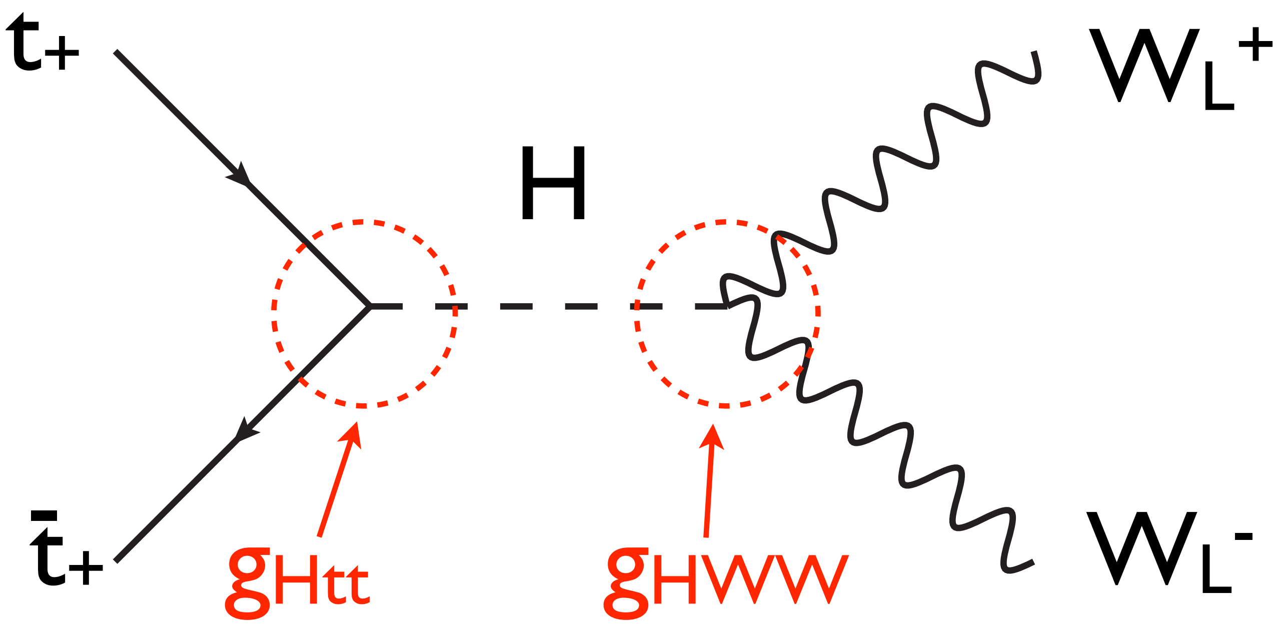

Chanowitz, Furman, Hinchliffe

Thanks for your attention!
It is a very long lecture.

Backup Slides

What accounts for Vector Boson Mass Generation?

⇒ Higgs Mechanism

Electroweak Symmetry Breaking (EWSB)

- The Standard Model Higgs Boson
- Make the Higgs Composite: Little Higgs
- Make the (Multiple) Higgs Natural: Supersymmetry

The Higgs Mechanism (EWSB)

The polarization tensor $\Pi_{\mu\nu}(p)$ is defined as:

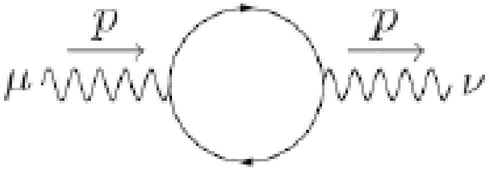

$$i\,\Pi_{\mu\nu}(p) \equiv i(p_\mu p_\nu - p^2 g_{\mu\nu})\Pi(p^2)$$

where the form of $\Pi_{\mu\nu}(p)$ is governed by gauge invariance, i.e. it satisfies $p^\mu \Pi_{\mu\nu}(p) = p^\nu \Pi_{\mu\nu}(p) = 0$.

The renormalized propagator is the sum of a geometric series

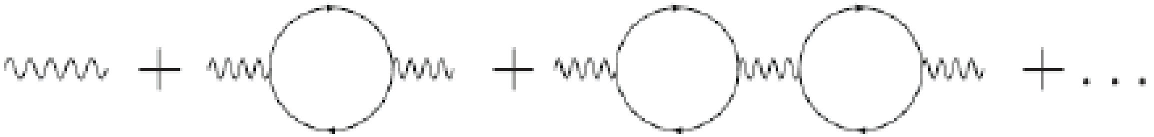

$$= \frac{-i(g_{\mu\nu} - \frac{p_\mu p_\nu}{p^2})}{p^2[1+\Pi(p^2)]}$$

The pole at $p^2 = 0$ is shifted to a non-zero value if:

$$\Pi(p^2) \underset{p^2\to 0}{\simeq} \frac{-g^2v^2}{p^2}\,.$$

Then $p^2[1+\Pi(p^2)] = p^2 - g^2v^2$, yielding a gauge boson mass of gv.

Trial answer: the SM with a Higgs

A Fundamental Scalar Doublet:

$$\phi = \begin{pmatrix} \phi^+ \\ \phi^0 \end{pmatrix} \quad ,$$

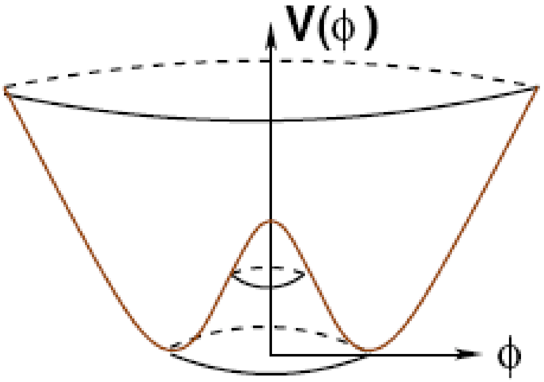

with potential:

$$V(\phi) = \lambda \left(\phi^\dagger \phi - \frac{v^2}{2} \right)^2$$

is employed both to break the electroweak symmetry and to generate masses for the fermions in the Standard Model.

Matrix Notation

Define $\tilde{\phi} = i\sigma_2\phi^*$ and

$$\Phi = \begin{pmatrix} \tilde{\phi} & \phi \end{pmatrix} \quad \Rightarrow \quad \Phi^\dagger\Phi = \Phi\Phi^\dagger = (\phi^\dagger\phi)\mathcal{I} \ .$$

Under $SU(2)_L \times U(1)_Y$, $\Phi \to L\Phi R^\dagger$,

$$L = \exp\left(\frac{iw^a(x)\sigma^a}{2}\right) \ , \ R = \exp\left(\frac{ib(x)\sigma^3}{2}\right)$$

The Higgs-sector Lagrangian becomes

$$\frac{1}{2}\mathrm{Tr}\left(D^\mu\Phi D_\mu\Phi^\dagger\right) + \frac{\lambda}{4}\left(\mathrm{Tr}\left(\Phi\Phi^\dagger\right) - v^2\right)^2 \ ,$$

$$D_\mu\Phi = \partial_\mu\Phi + \mathrm{i}g\mathbf{W}_\mu\Phi - \mathrm{i}\Phi g'\mathbf{B}_\mu \ .$$

The potential manifests the symmetry
$SU(2)_L \times SU(2)_R \to SU(2)_V$

Non-linear Representation

A "Polar decomposition" of Φ

$$\Phi(x) = \frac{1}{\sqrt{2}}(H(x) + v)\,\Sigma(x)\ ,$$

$$\Sigma(x) = \exp(i\pi^a(x)\sigma^a/v)\ .$$

neatly separates the radial "Higgs boson" from the "pion" modes (Nambu-Goldstone Bosons).

By gauge choice, $\langle\Sigma\rangle = \mathcal{I}$.

Broken Symmetries $\Rightarrow$ Nambu-Goldstone Bosons

Gauge $SU(2)_W \times U(1)_Y$ $\Rightarrow$ Higgs Mechanism

$$\pi^{\pm},\ \pi^0 \longrightarrow W_L^{\pm},\ Z_L$$

$$M_W = \frac{gv}{2} \Longleftarrow \qquad v = \sqrt{\frac{1}{\sqrt{2}G_F}} = 246GeV$$

Custodial Symmetry: SU(2)V

$$SU(2)_L \times SU(2)_R \to SU(2)_V$$

Due to residual $SU(2)_V$ "custodial symmetry" for $g' \to 0$, the $SU(2)_L$ gauge bosons are degenerate.

This, plus $m_\gamma = 0$, tells us

$$M^2 = \frac{v^2}{2} \begin{pmatrix} g^2 & & & \\ & g^2 & & \\ & & g^2 & -gg' \\ & & -gg' & g'^2 \end{pmatrix} ,$$

and hence

$$\rho \equiv \frac{M_W^2}{M_Z^2 \cos^2\theta_W} = 1 \ .$$

Violations of Custodial Symmetry

Conventionally, one speaks of $\Delta\rho \equiv \rho - 1$

Electromagnetism: $\mathcal{O}(\alpha)$ corrections to $\Delta\rho$ from

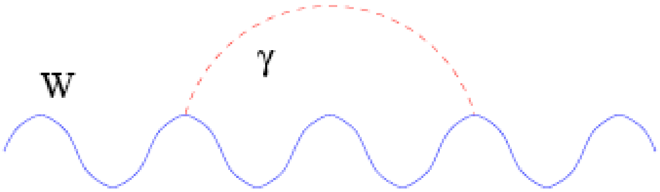

Yukawa Couplings: (i.e. mass differences) $\Delta\rho \approx \dfrac{3y_t^2}{32\pi^2}$

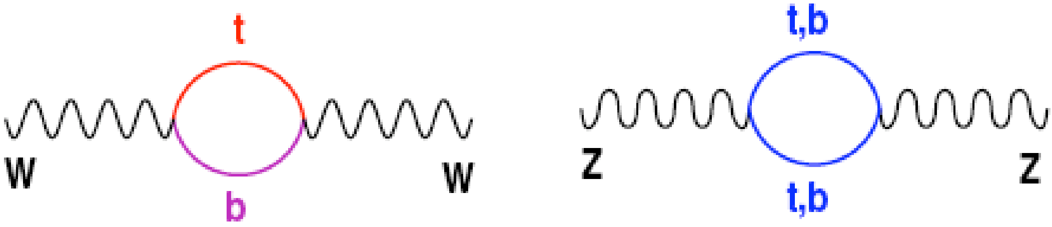

Experiment finds $|\Delta\rho| \leq 0.4\%$, which constrains physics beyond the SM.

Custodial Symmetry is an important part of any theory of EWSB!